Developing a personalized heterologous prime boost vaccination strategy for tumor therapy

Ramiro Andrei Ramirez-Valdez

Christ Church College

University of Oxford

A thesis submitted for the degree of

Doctor of Philosophy

Michaelmas Term 2021

LUDWIG CANCER RESEARCH

NIH

NIH Oxford-Cambridge Scholars Program

"Everyone has his own specific vocation or mission in life; everyone must carry out a concrete assignment that demands fulfillment. Therein he cannot be replaced, nor can his life be repeated. Thus, everyone's task is unique as is his specific opportunity to implement it."

Victor E. Frankl, *Man's Search for Meaning*

Acknowledgements

Personal

This work was conducted under the supervision of Professor Benoit van den Eynde and Dr. Carol Leung at the Ludwig Institute of Cancer Research, Oxford, and Dr. Robert Seder at the Vaccine Research Center, NIH, in Bethesda, Maryland.

I was privileged to work with many talented scientists who contributed ideas, materials, and experimental support over the course of this DPhil, for which I am very grateful. In particular, I would like to thank:

Dr. Robert Seder and Prof. Benoit van den Eynde for granting me the opportunity to work in their labs. Their tailored supervision and support has been gratefully received and has irrefutably improved my skills as a scientist.

Dr. Carol Leung, who co-supervised and encouraged me during my time at Oxford. She was always available to provide feedback and advise me on my plans for the future, which was greatly appreciated.

My VRC colleagues, in particular Kennedy Tobin, Alec Schrager, Patricia Darrah from the Seder lab for their friendship and experimental/administrative support over the years.

My Ludwig colleagues James McAuliffe and Vineeth Chandrasekar for their friendship and support during my time at Oxford.

Dr. Geoffrey Lynn from Avidea technologies for always providing materials for our studies and his eagerness to support our research in any way possible.

Dr. Faezzah Baharom, who was a steadfast colleague and friend. She was always willing to lend a hand with large experiments and routinely offered unique insights that improved the quality of the research presented herein.

Dr. Andrew Ishizuka, for his enthusiasm in discussing study designs, new data, and life beyond the lab. His advice has been invaluable over the years. He asked the difficult questions that forced me to re-think conclusions and consider alternative explanations – often at the expense of my stubbornness and pride. This emphasis on critical evaluation will undoubtedly serve me well, and for his role in developing that skill I am incredibly grateful.

My parents, Ramiro and Araceli, for their unwavering support throughout the DPhil and for providing a holistic perspective when I became too focused on the research. My brothers, Edric and Adrian, for their support and the laughs we shared that always made me smile.

Susannah Bane, for her patience, understanding, and emotional support throughout my DPhil. The joy her company has brought me has kept me sane throughout the last few years.

Institutional

This work was supported by an Intramural Research Training Award through the NIH-Oxford-Cambridge Scholars Program.

Declaration of Authentication

The work presented herein was performed by me and in no way forms part of another thesis from this or any other university. The project was conceived by Dr. Robert Seder, Prof. Benoit van den Eynde, Dr. Carol Leung, Dr. Andrew Ishizuka and I. We were all involved in the design of experiments, and I conducted the experiments with assistance from Dr. Faezzah Baharom, Kennedy Tobin, and Alec Schrager. This work was performed under the supervision of Professor Benoit van den Eynde and Dr. Carol Leung at the Ludwig Institute of Cancer Research at the University of Oxford.

Ramiro Andrei Ramirez-Valdez
University of Oxford
Michaelmas Term 2021

Developing a personalized heterologous prime boost vaccination strategy for tumor therapy

Ramiro Andrei Ramirez-Valdez, Christ Church College

Thesis submitted for the degree of Doctor of Philosophy, Michaelmas Term 2021

Abstract

The limited success of therapeutic cancer vaccines to date is likely due to sub-optimal generation of anti-tumor CD8 T cells and insufficient tumor microenvironment (TME) modulation. In this study, a novel intravenous (IV) heterologous prime-boost vaccination strategy with a self-assembling neoantigen-peptide nanoparticle TLR-7/8 agonist (SNP) vaccine platform and a chimp adenovirus (ChAdOx1) was used to elicit high magnitude neoantigen-specific CD8 T cells and modulate the TME. Mice primed with SNP encoding the neoantigen Reps1 for a colon carcinoma (MC38) and boosted with ChAdOx1 IV encoding Reps1 elicited on average ~40% Reps1-specific CD8 T cell responses, which were ~4x higher than mice boosted by the conventional IM route. These CD8 T cells were capable of mediating protection from tumor challenge in a prophylactic setting experiment. Therapeutically, heterologous prime-boost with ChAdOx1 given IV or IM enhanced protection compared to the use of ChAdOx1 alone. Remarkably, IV administration of 'empty' ChAdOx1 (not encoding Reps1) after Reps1-SNP prime also improved protection compared to Reps1-SNP prime or ChAdOx1 prime alone. Subsequently, IV vaccination with ChAdOx1 or SNP was found to induce production of IFNα and activation of cDC1s in the spleen, tumor and tumor-draining lymph node (td-LN). The activation of cDC1s was found to be dependent on functional IFNα signaling and blockade of IFNα signaling at the time of boost completely abrogated tumor regression in the therapeutic setting. Together, these data suggest that IV ChAdOx1 boosting not only increases the magnitude of antigen-specific CD8 T cells, but also modulates the TME to promote tumor regression, representing a readily translatable therapeutic paradigm to drive the Cancer Immunity Cycle.

Table of Contents

List of tables

List of figures

List of abbreviations

ABTS	2,2'-Azino-bis(3-ethylbenzothiazoline-6-sulfonic acid
ACT	Adoptive Cell Transfer
ANOVA	Analysis of Variance
APC	Antigen Presenting Cell
B-ALL	B-cell Acute Lymphoblastic Leukemia
Batf3	Basic Leucine Zipper ATF-Like Transcription Factor 3
BUV	Brilliant ultra violet
BV	Brilliant violet
CAR	Chimeric Antigen Receptor
CCL	C-C Chemokine Ligand
CCR	C-C Chemokine Receptor Type
CD	Cluster of differentiation
cDC	Conventional Dendritic Cell
ChAdOx1	Chimp Adenovirus Oxford 1
CIC	Cancer Immunity Cycle
CPI	Checkpoint Inhibitor
CRS	Cytokine Release Syndrome
CTLA-4	Cytotoxic T-lymphocyte-associated Protein 4
CXCL	C-X-C Chemokine Ligand
CXCR	C-X-C Chemokine Receptor
DAMP	Damage Associated Molecular Pattern
DC	Dendritic Cell
DLBCL	Diffuse Large B Cell Lymphoma
DMEM	Dulbecco's modified Eagle's medium
DMSO	Dimethyl sulfoxide
DNA	Deoxyribonucleic acid
Dnase I	Deoxyribonuclease I
DPEC	Double positive effector cell
EDTA	Ethylenediaminetetraacetic acid
EEC	Early effector cell
ELISA	Enzyme-linked Immunosorbent Assay
FACS	Fluorescence Activated Cell Sorting
FBS	Fetal Bovine Serum
FDA	Food and Drug Administration
FGF	Fibroblast Growth Factor
FoxP3	Forkhead box P3
GM-CSF	Granulocyte Macrophage Colony Stimulating Factor
GMP	Good Manufacturing Practice
GSK	GlaxoSmithKline
HCV	Hepatitis C Virus
HLA	Human Leukocyte Antigen
HPLC	High Performance Liquid Chromatography
HPV	Human Papilloma Virus
ICS	Intracellular cytokine stain
IFA	Incomplete Freund's Adjuvant
IFN	Interferon
Ii	Invariant chain
IL	Interleukin

IM	Intramuscular
IPEX	Immune Dysregulation, Polyendocrinopathy, Enteropathy, X-linked
IRAE	Immune Related Adverse Event
IU	Infectious units
IV	Intravenous
JAK	Janus Kinase
KLRG1	Killer Cell Lectin-like Receptor Subfamily G Member 1
KO	Knock Out
KRAS	Kirsten rat sarcoma virus
LN	Lymph Node
LPS	Lipopolysaccharide
Mac	Macrophage
MAGE	Melanoma-associated antigen
MDSC	Myeloid Derived Suppressor Cell
µg	microgram
mg	Milligram
MHC	Major histocompatibility complex
Min	Minimal Epitope
µl	microliter
ml	milliliter
MPEC	Memory Precursor Effector Cell
MVA	Modified Vaccinia Ankara
NF-κB	Nuclear Factor Kappa-light-chain-enhancer of Activated B Cells
NK	Natural Killer
NSCLC	Non-small Cell Lung Cancer
OD_{450}	Optical Density (wavelength 450)
PAMP	Pathogen associated molecular pattern
PAP	Prostatic Acid Phosphatase
PBMC	Peripheral blood mononuclear cells
PBS	Phosphate Buffered Saline
PD-1	Programmed cell death protein 1
pDC	Plasmacytoid Dendritic Cell
PD-L1	Programmed death ligand 1
PE	Phycoerythrin
PFA	Paraformaldehyde
PGE_2	Prostaglandin E2
Poly-ICLC	Polyinosinic-polycytidylic Acid with Polylysine and Carboxymethylcellulose
PRR	Pattern Recognition Receptor
PSA	Prostate Specific Antigen
rpm	Revolutions per minute
RPMI	Roswell Memorial Park Institute 1640
RNA	Ribonucleic Acid
r/r	Relapsed or Refractory
SaPE	Streptavidin Phycoerythrin
SARs-CoV-2	Severe Acute Respiratory Syndrome Coronavirus 2
SD	Standard deviation
SEM	Standard error of the mean
SLEC	Short lived effector cell
SLP	Synthetic Long Peptide
SNP	Synthetic Nanoparticle – TLR-7/8 agonist vaccine
ssRNA	Single Stranded RNA
STAT1	Signal Transducer and Activator of Transcription 1

STEAP1	Six Transmembrane Epithelial Antigen of the Prostate 1
T-bet	T-box Expressed in T Cells
TAA	Tumor Associated Antigen
TAM	Tumor Associated Macrophage
TCD	Tolerogenic Cell Death
TCF-1	Transcription Factor 7
TCGA	The Cancer Genome Atlas
TCR	T cell receptor
Tet	Tetramer
TGF-β	Transforming Growth Factor β
Th	T Helper type
Tim-3	T cell immunoglobulin and mucin domain-containing protein 3
TIL	Tumor Infiltrating Lymphocyte
TLR	Toll-like Receptor
TMB	Tumor Mutational Burden
TME	Tumor Microenvironment
TNFα	Tumor Necrosis Factor alpha
TRAIL	Tumor Necrosis Factor-related Apoptosis-inducing Ligand
Treg	Regulatory T cell
VCAM	Vascular Cell Adhesion Molecule
VEGF	Vascular Endothelial Growth Factor
VVCF	Viral Vector Core Facility
WHO	World Health Organization
WT	Wild Type
XCR1	X-C Motif Chemokine Receptor 1

Chapter 1

Introduction

1.1 Immunotherapy

1.1.1 Conventional cancer therapy

Cancer is a leading cause of death across the globe, and was responsible for ~10 million deaths in 2020 according to the World Health Organization (WHO)[1]. Cancer is a heterogeneous disease that can affect almost any tissue in the body. It arises through the acquisition of mutations that affect cell proliferation and results in uncontrolled cell division. Through sequential acquisition of mutations affecting different cellular functions a tumor can grow and spread (known as metastasis) to other parts of the body. These hyper-proliferative characteristics that cancer cells acquire as they gain mutations are described in detail by Hanahan and Weinberg in their well-known publication, "Hallmarks of Cancer" [2]. In general, metastasis is the main cause of mortality from cancer as tumors begin to grow in organs other than the primary site and lead to organ failure.

Throughout the 20th and early 21st century the main treatments available for cancer were surgery, chemotherapy, and radiotherapy. These could be used independently or in combination to improve patient outcomes. However, there are some major limitations of these treatments. Some cancers may be inoperable depending on the location of the tumor, and major surgery carries significant risks during recovery. Chemotherapy and radiotherapy are not tumor specific and can cause adverse effects (damage) to other healthy tissue in an individual.

Despite these limitations, patient survival rates have increased in recent decades due to improvements in earlier detection as well as therapeutic advances in the use of the conventional trio of interventions. In the 40 years between 1971-2011, the 5-year survival rates of adults (men and women) in the UK across all cancers increased from 30% to 54% [3]. However, this improvement was not uniform across all cancer types. For example,

tumors arising in the pancreas are only now approaching a 30% 5-year survival rate [4] and esophageal cancer has a 5-year survival rate between 15% and 25% [5].

One major factor that causes this effect is that some cancers (like pancreatic) do not present with symptoms until they are quite advanced and therefore only provide a narrow window of time during which to administer treatment. Being advanced, these tumors may have already metastasized and are usually larger and refractory to the conventional treatments that have been available thus far. For this reason, it is necessary to develop a therapeutic strategy that is capable of dealing with advanced metastatic disease and immunotherapy shows potential to achieve this goal.

1.1.2 Immunotherapy

Immunotherapy refers to interventions that function by manipulating the immune system to identify cancer cells as foreign and engage its natural functions to eradicate the cancer. The idea that the immune system can take on this role started in the 19th century with the surgeon William Coley, who noticed that patients with erysipelas (a streptococcal skin infection) displayed remission of soft-tissue sarcomas. He followed up on this observation by injecting patients with a mixture of heat-inactived *Streptococcus pyogenes* and *Bacillus prodigious*, which remarkably resulted in long-term cancer remission. Unfortunately, due to the development of radiotherapy and the lack of understanding of the mechanisms underpinning the success of Coley's toxins, it was many decades before this work was followed up on [6]. Retrospectively, it seems clear now that this cocktail was likely working through the activation of pattern recognition receptors (PRRs) that could stimulate an immune response, and help promote anti-tumor immunity indirectly.

Interferons (IFNs) were initially discovered based on their anti-viral properties in the 1950s [7]. In the 1960s, mice with tumors were treated with purified interferons (IFNs)

and it was shown that these exhibited anti-tumor effects [8]. At the time, the understanding of immunology was not sufficient to identify immune cells as the key player in mediating this anti-tumor effect and the IFNs were thought to be acting directly on the tumor cells. In a clinical trial of hairy cell leukemia, 55 patients were treated with purified IFNα2 and 40 of the patients experiences a partial response, indicating the therapeutic benefits of a specific IFNα family member [9]. In a separate clinical trial of high-risk resected cutaneous melanoma, treatment of patients with IFNα2 was associated with a statistically significant increase in survival. In this clinical trial from 1996, the authors noted that the mechanism of action for IFNα2 was still poorly understood, in particular with respect to its effects on the immune system [10]. Today, we know that IFNα has numerous effects on immune cells that promote anti-tumor immunity, but the use of IFNα2 as a therapy has been curtailed. This was due to the development of small molecules that can activate pathways down stream of IFNα selectively without the concomitant adverse effects that lead to dose-limiting toxicity with IFNα2 [7].

Separate, but contemporary with the work on IFNs, there was an improvement in the understanding of lymphocyte biology in the 1980s – particularly with respect to the role of T cells in anti-tumor immunity. The identification of IL-2 [11] and a means to mass-produce this cytokine in *E. coli* enabled its use as an immunotherapeutic agent early on [12]. Recombinant IL-2 became important because it could be used to expand tumor-infiltrating lymphocytes (TILs) derived from a tumor biopsy *in vitro* in order to re-infuse these tumor-specific T cells back into the patients at much higher numbers to promote tumor regression [13]. In addition, IL-2 could be given with the adoptive cell transfer (ACT) in order to promote T cell growth and anti-tumor immunity. This strategy has proven to be effective in treating metastatic disease, with objective tumor regression displayed by 11 of 25 patients in a clinical trial in 1985 [14].

Despite this improvement, there was only one patient that displayed complete regression of their tumors and so current efforts have focused on identifying ways to improve ACT efficacy. More recently in 2011, a clinical trial was published where 93 patients with metastatic melanoma were treated with ACT and high-dose IL-2 following a lymphodepleting regimen. The lymphodepleting regimen was either a chemotherapy or radiotherapy and the goal was to eliminate potentially immunosuppressive immune cells from the patient prior to administering the TILs. Of the 93 patients, 20 (22%) displayed complete tumor regression – of which 19 were tumor free at a 3 year follow up [15].

During the work with IL-2 and ACT, it became increasingly apparent that cytotoxic T cells were the major mediators of anti-tumor immunity [16]. However, not all patient tumors contain functional effector T cells capable of being cultured for re-infusion. To address this problem, some groups began to create new T cells with unique specificities for antigens that are uniquely or highly expressed in particular cancers across patients. These were called chimeric-antigen receptor (CAR) T cells [17].

To create a CAR T cell, T cells are isolated from the blood of a patient and then genetically modified to express the CAR receptor. The extracellular domain of the CAR is comprised of the variable region from a monoclonal antibody specific for the antigen of interest expressed by the cancer. The intracellular portion of the CAR contains the normal signaling components of a T cell receptor (TCR). The newly created CAR T cells are re-infused into the patient, typically after a lymphodepleting treatment, and then binding of the CAR to its target antigen on the tumor cell surface initiates intracellular signaling resulting in tumor cell lysis [18].

CAR T cells have been demonstrated to provide excellent anti-tumor efficacy in B cell malignancies such as B-cell acute lymphoblastic leukemia (B-ALL) and diffuse large B cell lymphoma (DLBCL). This is due to the high expression of the target antigen CD19

on tumor cells and also that CD19 expression is restricted to B cells. Relapsed or refractory (r/r) B-ALL and DLBCL have poor prognosis with standard therapies. However, by infusing CD19 specific CAR T cells, it is possible to achieve complete remission in 90% of patients with r/r B-ALL [19]. For DLBCL, the infusion of anti-CD19 CAR T cells resulted in a complete response rate (no more detectable disease) of 52% as compared to the complete response rate of 22% due to alternate therapies [20]. CAR T cells were detectable for up to 20 months after infusion, indicating that these may have durable long term effects [21]. The positive outcomes with these CAR T cell therapies resulted in food and drug administration (FDA) approval of CD19 CAR T cells for treating both B-ALL [22] and DLBCL [23].

In addition to ACT based therapies, immune checkpoint inhibitors (CPIs) have also been developed over the past decade [24]. These are typically monoclonal antibodies that block the interaction between ligands expressed on cells in the local environment and receptors on T cells that would inhibit effector function. CPIs prevent this interaction and thereby enable continued activation of T cells or re-activate T cells that were being inhibited [25].

There are three major targets of immune checkpoint inhibitors, known as programmed cell death protein 1 (PD-1), programmed death-ligand 1 (PD-L1), and cytotoxic T-lymphocyte-associated protein 4 (CTLA-4). Antibodies against PD-1 and PD-L1 are targeting the same interaction, but PD-1 is the receptor on the T cell and PD-L1 the ligand. The combination of nivolumab (PD-1 antibody) and ipilimumab (CTLA-4 antibody) has proven particularly effective in the treatment of melanoma [26], non-small cell lung cancer (NSCLC) [27], and renal cell carcinoma [28]. The response rate in melanoma has been particularly striking. During the checkmate 067 study, patients with advanced melanoma treated with this combination of checkpoint inhibitors have achieved

a 52% survival rate at 5 years. The combination was slightly more effective than nivolumab alone (44% 5-year survival) and twice as effective as ipilimumab alone (26% 5-year survival) [29]. This is compared to the historical standard 5 year survival for advanced melanoma of 10% [30]. Due to the promising outcomes from treatments with checkpoint inhibitors targeting the PD-1/PD-L1 axis and CTLA-4, the FDA has approved 7 different antibodies for multiple indications in the US [31].

1.1.3 Limitations of current immunotherapies

The major immunotherapies in use today are CAR T cells and checkpoint inhibitors. Though they have both greatly improved the survival and even cured cancer for some patients, they are not without their drawbacks. This is partly why both CPIs and CAR T cells have a limited range of cancers for which they are approved, though for different reasons.

(I) Factors affecting CPI and CAR T cell efficacy

CPIs have variable response rates depending on the tumor and the treatment regimen used, but rarely achieve a complete response rate of 40% [32]. This may be due to numerous factors including having a low number of TILs or the presence of an immunosuppressive microenvironment that is not dependent on the targeted axis for example. Behavioral and environmental factors also impact the response to checkpoint inhibitors. One recent finding is the role of the gut microbiome in promoting effective anti-tumor immunity following checkpoint blockade. In a recent phase I clinical trial, fecal microbiota transplant and renewed administration of anti-PD-1 antibody elicited clinical response in 3 out of 10 patients with refractory metastatic melanoma [33]. This finding demonstrates that factors as general as diet and microbiome might have on the response to

CPIs. A more comprehensive review discussing what is currently known about the factors affecting response to CPIs can be found in [32].

CAR T cells have been successful for B cell malignancies, but there are still patients who relapse following treatment. One mechanism that underpins this is the loss of the target antigen CD19, which can be achieved by alternative splicing of CD19 that removes the target epitope [34] or loss of CD19 trafficking to the cell surface [35]. Often, these tumors can be targeted by another CAR T cell for CD22 (another B cell expressed antigen), though the median remission time for these patients may be as little as 6 months [36].

CAR T cells have proved difficult to adapt for solid tumors. This is because solid tumors have more heterogeneous cell types and it is difficult to identify an antigen that is specifically expressed on tumor cells and not on healthy tissue. In addition, the CAR T cell must be able to function in the immunosuppressive environment that it is likely to encounter, but this environment is also likely to be different between patients, so more detailed characterizations would be required to develop tailored CAR T cells for a patient's unique tumor microenvironment (TME) [37].

(II) Toxicity

Though both CPIs and CAR T cells are considered better tolerated than conventional chemotherapeutic agents, they both induce immune related adverse events (IRAEs) in a large proportion of patients. In the case of CPIs, this is because the targets of the antibodies have regulatory functions in normal immune system homeostasis. Therefore interrupting those signals through checkpoint blockade may also activate non-tumor specific immune cell responses and result in excessive inflammation [38]. The most commonly affected organs are the skin, liver, and gastrointestinal tract, though it can

affect the heart, brain and lungs as well. Combination therapy induces greater levels of IRAEs than monotherapy alone, as evidenced by the CheckMate067 study where 59% of patients receiving both nivolumab and ipilimumab experienced IRAEs as compared to 22% for nivolumab alone or 28% for ipilimumab alone [39]. In addition, the use of checkpoint inhibitors has been shown to worsen autoimmune conditions in 50% of patients with pre-existing autoimmune disease that were treated with CPIs [40]. Though IRAEs may be mild, some will require management with additional therapeutics to limit the inflammation.

In a similar way, CAR T cells introduced into the patient may react aggressively to the cancer and release large amount of pro-inflammatory cytokines resulting in what has now been termed cytokine release syndrome (CRS). The symptoms of CRS are systemic and include fever, hypotension, and hypoxia, but may also affect neurological function and induce cerebral edema or seizures [41]. The systemic toxicity of CRS following CAR T therapy can be partially managed by infusion of an anti-IL-6 antibody (tocilizumab) or administration of corticosteroids, which will reduce inflammation [42].

(III) Cost

These novel immunotherapies are the result of decades of research and large upfront costs to demonstrate their efficacy in clinical trials. As a result of their novelty and improved therapeutic benefits the cost of treatment with CPIs or CAR T cells is substantial. For context, the cost in the UK per patient with advanced melanoma of nivolumab treatment for 4 years was £248,000 [43] or £62,000 per year. This raises cost-effectiveness concerns as it is predicted that 43% of cancer patients in the US may be eligible for CPI treatment but only 12.5% would be expected to respond [44]. In addition, the production of CAR T cells requires technical expertise and patient-specific production

of cells – which is quite costly. This underpins the estimated cost of a single round of Tisagenlecleucel (anti-CD19 CAR T cell) reaching a price of US $475,000 [45].

1.1.4 An opportunity to improve immunotherapy

This brief history of immunotherapy shows how researchers have gone from very general treatments with bacterial cocktails to the targeting of specific pathways to activate T cells in order to promote anti-tumor immunity. Despite all this progress, there are still multiple problems with modern immunotherapies that need to be addressed, and therefore space to innovate and improve patient outcomes. There are numerous opportunities that could be exploited to improve immunotherapy, from improving the understanding of inhibitory factors at the tumor site to increasing the anti-tumor T cell response through identification of novel checkpoint inhibitors or vaccination. It is clear that more precise immunotherapeutic interventions are required, and to achieve this a better understanding of the TME is needed.

1.2 Cancer Immunity

1.2.1 The cancer immunity cycle

Cancer immunotherapy relies on both innate and adaptive immune cells to mediate tumor clearance. The last decade of work has focused heavily on understanding the role of T cells in immunotherapy as CPIs have been shown to work, in large part, through the activation of CD8 T cell responses [46, 47]. However, in order to generate effective T cell responses, innate immune cells must also fulfill their natural functions.

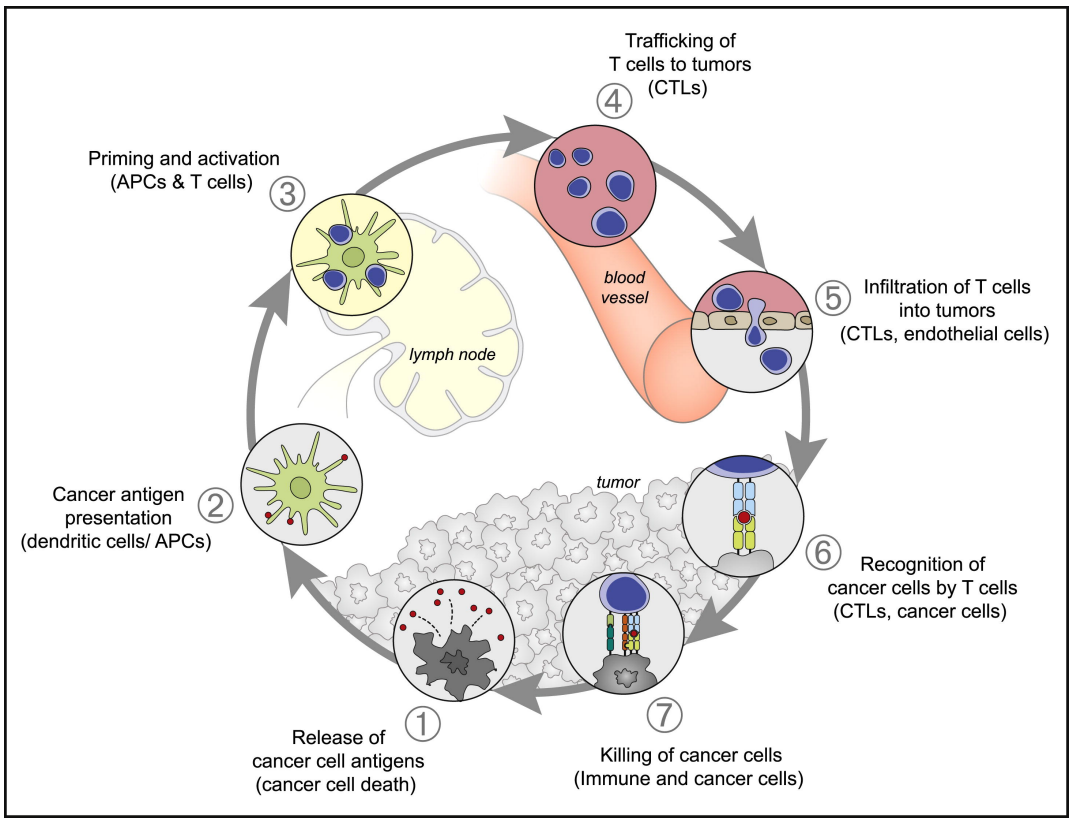

Figure 1.1 The Cancer Immunity Cycle – *Adapted from Chen and Mellman, Immunity, 2013*
The cycle begins with (1) the release of antigens from dying tumor cells that are (2) picked up by APCs and processed for presentation on MHC to (3) prime and activate T cells against the tumor specific antigens. The activated T cells (4) migrate to the tumor and (5) infiltrate the tumor. The T cells (6) recognize their cognate peptide-MHC complex on tumor cells and (7) kill the recognized cells to (1) release antigens and repeat.

In 2013, Daniel Chen and Ira Mellman published a seminal review that provides a framework for understanding cancer through an immunology-focused lens (Figure 1.1) [48]. The cancer immunity cycle (CIC) is a continuous process that is taking place during the development of a tumor and identifies key steps that are required to form a successful anti-tumor immune response. Briefly the steps are as follows:

1. Cancer cells die, either naturally or killed by innate immune cells (e.g. natural killer (NK) cells) or adaptive T cell responses, and release antigens.
2. Antigen presenting cells (APCs) acquire and process cancer antigens for presentation on major histocompatibility complex class I or class II (MHC-I, MHC-II).

3. T cells are activated by binding of the TCR to its cognate MHC-peptide complex on APCs, CD8 T cells recognize MHC-I whilst CD4 T cells bind to MHC-II.
4. Activated T cells migrate to the tumor.
5. T cells infiltrate the tumor.
6. T cells recognize cancer cells by the expression of the tumor antigen.
7. T cells kill cancer cells, which then feeds back into step 1.

By using this framework, one can understand the different bottlenecks that may be encountered in attempting to treat a patient's tumor with immunotherapies. For example, anti-PD-1/anti-PD-L1 therapy works by blocking inhibitory signals that prevent recognition and killing of cancer cells (steps 5/6). However, if a patient failed to prime T cell responses (step 3), then anti-PD-1 therapy would not be predicted to help. Similarly, if CAR T cells are introduced into a patient (aiding step 4/5) but reach the tumor and are inactivated by the immunosuppressive TME, then killing of the tumor cells will not ensue and the patient will experience progressive disease. This framework can therefore be used to understand the roles of innate and adaptive immune cells in cancer immunotherapy.

1.2.2 Innate immunity in cancer

The innate immune system is highly specialized to act as immune first-responders. Two key players for consideration are dendritic cells (DCs) and macrophages (Macs). These cells will primarily aid with the first three steps of the CIC, which involve the acquisition, processing, and presentation of tumor antigens to activate T cells. The underlying mechanism that triggers activation of these cells is similar. DCs and Macs express pattern recognition receptors (PRRs) which are specialized to recognize pathogen associated molecular patterns (PAMPs) that are conserved between different infectious agents, like single stranded RNA (ssRNA) or lipopolysaccharide (LPS). These cells can

also respond to damage associated molecular patterns (DAMPs), such as DNA, which are released by dying cells. Upon activation, the DCs and macrophages proceed to initiate an inflammatory response to limit the spread of infectious agents, recruit immune cells, promote anti-tumor immunity, and initiate an adaptive immune response [49] [50].

(I) DCs

DCs are highly specialized for stimulating naïve T cells to initiate an adaptive immune response. Conventional DCs (cDCs) can be split into two distinct subsets known as cDC1s and cDC2s, with different functions and cell surface markers [51]. In addition, plasmacytoid DCs (pDCs) are a third class of DC that is highly specialized in anti-viral immunity and capable of releasing large amounts of IFNα following activation to potentiate an immune response [52].

cDC1s have many important functions in the generation of effective anti-tumor immune responses, and can be identified by flow cytometry in mice and humans by staining for CD11c, MHC-II, and XCR1 [53]. The development of cDC1s is dependent on the transcription factor *Batf3*. Hildner and colleagues showed that *Batf3* knock-out (KO) mice lacking cDC1s were unable to reject an immunogenic fibrosarcoma, whereas wild-type (WT) mice were capable of rejection [54]. In a study using an autochthonous oncogene-driven melanoma mouse model, Spranger and colleagues demonstrated that *Batf3* KO mice did not have T cell infiltrates in developing tumors [55]. In addition, cDC1s loaded with tumor antigens *ex vivo* and then reinfused into mice have been demonstrated to reduce tumor growth [56]. Together, these data demonstrated the importance of cDC1s for generating effective anti-tumor immunity.

The specialized function of cDC1s is to take-up antigen from peripheral tissue sites (like the tumor) and process antigens to load onto MHC class I molecules to activate CD8

T cells, a process known as cross-presentation. To achieve this, cDC1s must migrate to a draining lymph node (LN) after acquiring tumor antigens to activate CD8 T cell immunity. The expression of C-C chemokine receptor type 7 (CCR7) on activated cDC1s is required for the migration to the LN. The evidenced for this was provided by a mixed bone-marrow chimera experiment where all cDC1s, and only cDC1s, were genetically manipulated to lose CCR7. The cDC1s in these mice failed to migrate to the LN and did not reject immunogenic tumors [57]. Once activated, cDC1s also upregulate co-stimulatory molecules CD80 and CD86, which aid in the activation of T cell responses [58].

In addition, cDC1s are a non-redundant source of IL-12 [59] which has multiple effects. This can help activate natural killer (NK) cells to produce IFNγ [60]. IL-12 also skews the T cell response towards a Th1 T cell response which is generally considered to be anti-tumoral (discussed further below). The production of IFNγ, first by NK cells and later by antigen-specific CD8 T cells, slows down the rate of cell division and can induce apoptosis in cancer cells that have intact IFNγ signaling pathways [61]. Furthermore, the expression of the chemokines C-X-C chemokine ligand 9 (CXCL-9) and CXCL-10 by cDC1s in the tumor is required to recruit CD8 T cells to the tumor site [62]. Collectively, these data demonstrate a key role for cDC1s in orchestrating anti-tumor immunity.

Whilst the role of cDC1s in cancer has been relatively well-studied, the role of cDC2s is less well understood. In part, this is because cDC2s represent a more heterogenous set of DCs. Generally, cDC2s are thought to be more efficient at priming CD4 T cell responses. Recent work in mouse models demonstrated that cDC2s can prime CD4 T cell responses (without inducing differentiation) to promote anti-tumor immunity [63]. The lack of CD4 T cell differentiation may enable IL-12 produced by cDC1s to skew the CD4 T cell response towards a Th1 type response. In addition, activated CD4 T cells can interact with cDC1s through the upregulation of CD40 ligand (CD40L), which

interacts with CD40 on cDC1s to enhance cross-presentation and co-stimulatory molecule expression to promote CD8 T cell responses [64].

In contrast to conventional DCs, pDCs are best known for their ability to rapidly produce and release large amount of type I IFNs (like IFNα) to activate innate immunity. However, it appears that pDCs can be induced to activate CD8 T cells upon stimulation through the toll-like receptor 7 (TLR-7) or TLR- 9 [65], but are not nearly as efficient as cDC1s. In the event that pDCs are activated and release IFNα, this will promote cross presentation of antigen by cDC1s. This was shown through the use of IFNα receptor (IFNar) KO cDC1s in a mouse tumor model. Mice with this particular genotype were unable to clear immunogenic tumors [66]. The promotion of cross-presentation is partly through the upregulation of co-stimulatory molecules (CD80/86) upon exposure of cDC1s to pDC derived IFNα [58].

Collectively, there is substantial evidence for the importance of DCs, and particularly cDC1s, in tumor immunity. These cells function primarily by collecting antigen from the tumor site and migrating to LNs to activate adaptive T cell responses, thus fulfilling their role in the initiation of the CIC.

(II) Macrophages

Macs are highly responsive to environmental stimuli and change their phenotype/function in response to perturbations of the tissue which they surveil. In the context of a healthy immune response to tissue damage or infection, macrophages play both pro-inflammatory and anti-inflammatory role depending on signals in the environment. For example, early in tissue damage or infection, macrophages adopt a pro-inflammatory role by responding to DAMPs/PAMPs and producing pro-inflammatory cytokines such as IL-6 and tumor necrosis factor (TNFα). However, during the process of

tissue repair/regeneration, the Macs alter their function to inhibit the immune response (mitigate damage) and promote tissue repair through the production of cytokines and growth factors [67].

For this reason, Macs have been observed to have both pro-tumoral and anti-tumoral roles depending on the context. In pro-inflammatory conditions, Macs can continue to produce pro-inflammatory cytokines to promote tumor response, and the presence of tumor associated macrophages (TAMs) has been associated with a positive prognosis in colon [68] and gastric [69] cancers.

However, Macs in cancer are typically associated with a poor prognosis. Their natural immunosuppressive function during wound healing and tissue repair may be aberrantly activated in certain cancers and consequently promote tumor growth. This may take the form of producing pro-angiogenic factors such as VEGF, which improves the blood supply to the tumor to promote growth [70]. TAMs may also express co-inhibitory receptors like PD-L1 to directly reduce T cell function [71]. The expression of anti-inflammatory cytokines such as transforming growth factor β (TGF-β) and IL-10 can reduce the activation of Th1 type responses [72]. In addition, the production of matrix metalloproteinases by Macs can promote tumor cell invasion and metastasis [73]. Macs have multiple functions that can inhibit progression through the CIC at many stages and this resistance must be overcome for effective immunotherapy.

1.2.3 Adaptive immunity in cancer

The innate immune cells have clear and distinct roles in the context of cancer immunotherapy, and CPI success relies on DC acquisition of tumor associated antigens (TAAs) and migration to the LN in order to prime T cells responses. However, the major

CPIs targeting the PD-1/PD-L1 axis or CTLA-4 work predominantly by enhancing the T cell response.

(I) T cell activation

T cells are lymphocytes identified by the expression of a TCR, which is comprised of CD3ε, CD3δ, CD3ζ sub-units that associate with TCR α and β chains for the most common type of T cells. The αβ T cells predominantly fall into two major categories; CD4 or CD8. Both types express unique TCRs that can recognize a peptide presented on MHC-I/II. The expression of the co-receptor CD8 stabilizes the interaction between TCR and MHC-I, whilst CD4 stabilizes the interaction between TCR and MHC-II – thereby making the co-receptor a defining characteristic and the basis for defining these cells by CD4/CD8. The interaction between the TCR and a peptide-MHC complex on professional antigen presenting cells, such as cDC1s, is one of three signals required to optimally activate T cells [74].

The co-stimulatory molecules CD80 and CD86 are members of the B7 gene family. APCs constitutively express CD86 and upregulate its expression following activation through their PRRs, whereas CD80 is not normally expressed but must be induced by APC activation [75]. These molecules bind to the co-stimulatory molecule CD28, which is constitutively expressed on the T cell surface [76]. The co-stimulatory signal amplifies the signal produced by interaction between the TCR and MHC complex, and this is known as signal 2 [77].

The final signal is provided by cytokines produced by APCs in response to the precise PRR that activated the cells. This is because not all pathogens require the same immune response. For example, a cytotoxic CD8 T cell response is desirable to target intracellular infections but extracellular pathogens are better controlled by an antibody

response. This dichotomy is demonstrated in the polarization of T cell response by exposure to IL-12, which skews CD4 T cells towards a Th1 fate and CD8 T cells acquire cytolytic functions [78], whereas exposure to IL-4 will skew CD4 T cells towards a Th2 response to promote B cell activation [79]. For cancer immunotherapy, a Th1 response is preferred as studies inhibiting IL-12 have demonstrated the CD8 T cells can proliferate following signals 1 and 2 but fail to develop cytolytic functions in the absence of IL-12 [80] [81].

Upon receiving all three signals, a naïve T cell will become activated and begin to divide, and develop specialized effector functions. The transcription factor T-bet is induced by IL-12 and is required for the development of Th1 functions, particularly IFNγ production [82] [83]. Following activation T cells begin to produce IL-2, which will aid in the survival and proliferation of the response [11]. In addition, other co-stimulatory signals may be provided by APCs to promote survival and proliferation. One example is the interaction between OX40 (T cell side) and OX40-L (APC side), which induces CD4 T cells to increase production of IL-2 and promotes proliferation [84]. The OX40/OX40L interaction increases production of Th subset specific cytokines regardless of polarization. i.e. IFNγ in the case of Th1 and IL-4 in the case of Th2 response [85]. The successful activation of tumor antigen-specific T cell responses represents progression through step 3 of the CIC and provides a reservoir of tumor antigen-specific CD8 T cells that can migrate to the tumor to mediate anti-tumor immunity.

In addition to Th1 and Th2 CD4 T cell subsets, there is one further CD4 T cell subset that plays a critical role in cancer immunity. This is the T regulatory (Treg) cell, which functions to dampen anti-tumor T cell responses through its immunosuppressive functions [86]. In the course of fighting a normal infection, Tregs help Macs to restrain over-active immune responses to prevent excessive damage. Tregs require the

transcription factor forkhead box P3 (FoxP3) and loss-of-function mutations in humans are associated with an auto-immune condition known as immune dysregulation, polyendocrinopathy, enteropathy, X-linked (IPEX) syndrome [87].

(II) T cell trafficking to the tumor site

Once activated, the tumor specific T cell responses must migrate to the tumor in order to mediate anti-tumor functions. Naïve T cells express CCR7 which enables them to home to LNs where they can be activated [88]. Effector T cells upregulate the chemokine receptor CXCR-3 upon activation [89] and is non-redundant for migration to the tumor site [90]. CXCR-3 enables T cell migration to the tumor in response to CXCL-9 and CXCL-10 [91]. Expression of CXCL-9/CXCL-10 by APCs, in particular cDC1s, has been shown to be required for effective T cell migration to the tumor site [62]. The importance of this interaction is supported by the high expression of CXCL-9 and CXCL-10 correlating with positive outcomes following anti-PD-1 therapy in mouse models [92]. This trend is also seen in human cancers, such as skin cutaneous melanoma [93], colorectal cancer [94], and esophageal squamous cell carcinoma [95].

In cancer, tumors that display high levels of T cell infiltration are referred to as ‘hot’ tumors, whereas those without T cell infiltrates are referred to as ‘cold’. As ‘hot’ tumors have high levels of TILs, it is likely that a lack of response in these tumors is due to interactions with co-inhibitory receptors (checkpoints) at the tumor site. This is supported by the correlation between anti-PD-1 blockade efficacy in melanoma patients and TIL infiltration/PD-1 expression status [96]. In contrast, cold tumors can be further subdivided into two categories, known as immune-ignorant or immune excluded. In the case of immune ignorant, there is no evidence of activation and recruitment of T cells to the tumor site indicating a problem with priming of T cell responses. For immune-

excluded tumors, TILs can be identified at the periphery of the tumor but fail to penetrate and therefore have limited anti-tumor functions [97].

(III) T cell effector function at the tumor site

Once T cells have reached the tumor (completed step 4 of the CIC), they must recognize the tumor cells and engage in tumor-cell killing. It is generally accepted that CD8 cytotoxic T cells are the key mediators of anti-tumor immunity. CD8 T cells require the interaction of the TCR with its cognate peptide-MHC complex to identify target cells for killing. All nucleated cells express MHC-I and continuously present peptide which can be 'scanned' by CD8 T cells in the vicinity. Auto-reactive T cells – those that would recognize normal self-peptides – are screened out during T cell development in a process known as negative selection. Cytotoxic T cells can mediate anti-tumor immunity through 3 mechanisms:

- Production of IFNγ and TNFα
- Perforin and granzyme introduction into cancer cells
- Interaction with cell death ligands like TRAIL [98].

The initial evidence for the role of IFNγ in anti-tumor immunity came from KO studies where tumor-antigen-specific CD8 T cells from IFNγ KO mice were transferred into WT mice with tumors and shown to be unable to mediate anti-tumor effects [99]. The production of IFNγ has pleiotropic anti-tumor effects. IFNγ can directly promote apoptosis in tumor cells by inducing caspase-1 [100] and -8 [101] through signal transducer and activator of transcription 1 (STAT1) signaling. Furthermore, IFNγ induces the production of CXCL-9 [102] and CXCL-10, which functions in a positive feedback loop to continue to attract effector cells that can produce more IFNγ. The expression of MHC-I is upregulated by exposure to IFNγ and can enhance the immunogenicity of cancer cells

[103]. In addition, IFNγ can cause the upregulation of tumor necrosis factor-related apoptosis-inducing ligand (TRAIL) and it's receptor, which is a membrane protein that can induce cell death, on tumor cells [104]. TNFα also has pleiotropic effects on tumor cells and can induce cellular apoptosis, activate effector T cells, and influence Macs to take on a more pro-inflammatory, anti-tumor phenotype [105].

In addition to the effects of cytokines, and the TRAIL death ligand, cytotoxic T cells can also induce cell death in tumor cells by directly introducing granzymes, serine protease enzymes, into the cytosol of the tumor cells. The formation of the TCR-MHC-I synapse polarizes the cytoskeleton of the T cell. Granules containing perforin and granzymes translocate to the immunological synapse and are released into the synaptic cleft. The perforin integrates into the tumor cell membrane and forms pores allowing the granules with granzymes to pass into the cytosol. The granzymes degrade substrates required for normal cell function and cause apoptosis [106]. Perforin is required for this process as evidence by the lack of efficacy of perforin KO mice in clearing tumors [107].

Together these mechanisms underpin much of the success of immunotherapeutic interventions. However, as tumors evolve, they also develop resistance mechanisms.

1.2.4 Tumor immune evasion

Tumor immune evasion can take many forms, but can all be linked back to inhibiting progression through the CIC. The three major areas that will be covered are:

1. Inhibition of T cell priming (CIC steps 1-3)
2. Inhibition of T cell migration and infiltration of the tumor (CIC Step 4/5)
3. Immunosuppression of T cell functions at the tumor site (CIC step 5/6)

Understanding the mechanisms that underpin cancer immune evasion will enable the development of effective immunotherapeutics.

(I) Inhibiting priming of T cell responses

In order for T cell responses to develop, antigen must first be released from dying cells along with DAMPs that can activate APCs to migrate to the LN for T cell priming. However, not all cell death is immunogenic and some cancers are capable of undergoing physiological apoptosis, which does not elicit an immune response and is referred to as tolerogenic cell death (TCD) for cancer cells [108]. To achieve TCD, cancer cells may down-regulate the expression of "don't eat me" signals such as CD47 [109], and upregulate "eat me" signals like phosphatidylserine which signals for phagocytes to engulf the cell [110]. When macrophages engulf a cell undergoing physiological apoptosis, DAMPs are not released and a proinflammatory response is not initiated. The importance of phosphatidylserine was demonstrated in a study of mouse lymphoma. Mice were vaccinated with irradiated lymphoma cells that had masked phosphatidylserine with Annexin V and resulted in better tumor clearance than irradiated cells with unmasked phosphatidylserine. This was associated with increased release of proinflammatory cytokines in the masked vs unmasked group [111]. Co-opting physiological apoptosis is one of the ways cancer cells avoid inducing an immune response to TAAs.

In addition, tumors may inhibit the activation and maturation of cDC1s through the production of inhibitory cytokines and down-regulation of cytokines required to attract cDC1s to the tumor. For example, production of β-catenin in the tumor is associated with a reduction in cDC1s in the tumor, T cell exclusion, and lack of responsiveness to CPI in melanoma. This is a result of β-catenin signaling reducing CCL4 expression, which is the chemokine that mediates recruitment of cDC1s to the tumor [55]. Alternatively, tumor infiltrating NK cells may produce CCL5 to promote cDC1 migration into the tumor. However, NK cells may be inhibited by the production of prostaglandin E_2 (PGE_2), thereby also reducing cDC1 infiltration and survival [112]. Vascular endothelial growth

factor (VEGF) inhibits the activity of the transcription factor NF-κB, which is required for complete cDC development [113]. Finally, IL-10 produced by Macs at the tumor site can inhibit IL-12 production by cDC1s, thereby abrogating induction of CD8 T cell responses [114]. This is a non-exhaustive list of the potential roadblocks cDC1s must overcome in order to gather TAAs, migrate to the LN, and prime anti-tumor CD8 T cell responses.

(II) Inhibiting T cell migration to the tumor

Many of the immunosuppressive functions described for inhibiting T cell priming also negatively impact recruitment of effector T cells to the tumor site. Additional mechanisms can take the form of attracting immunosuppressive cells or misdirecting effector T cells so they do not co-localize with tumor cells. Stromal cells in the tumor have been shown to produce CXCL12, which can attract effector T cells and segregate them away from tumor cells and within the stromal compartment of a tumor. In a mouse model of pancreatic cancer, treating mice with both a CXCL12 inhibitor and anti-PD-1 improved efficacy of checkpoint blockade [115]. In addition, the chemokine CCL2 has also been associated with increased tumor infiltration. However, it is not specific for effector T cells and can recruit myeloid derived suppressor cells (MDSCs) and Tregs, which can mediate immunosuppressive effects on effector T cells [116]. In addition, the nitrosylation of CCL2 produced in the tumor environment can inhibit its ability to recruit T cells, but enables it to retain its MDSC recruitment functions, thereby providing an asymmetric signal to increase suppressor cell recruitment [117].

In addition to the chemokine signals, T cell require signals like E-selectin and vascular cell adhesion molecule 1 (VCAM-1) in order to translocate from the bloodstream into tissue. During angiogenesis in the tumor, the expression of VEGF and fibroblast growth factor (FGF) downregulates the expression of these adhesion molecules on

endothelial cells and prevents T cells from attaching to the vasculature and entering the tissue [118]. The vasculature associated with tumors therefore provides a barrier to extravasation of T cells into the tumor site. These inhibitory features represent some of the factors that cause a "cold" tumor phenotype, with low TIL infiltration and low probability of response to CPIs.

(III) Immunosuppression at the tumor site

The final stages of the CIC occur when effector CD8 T cells have successfully managed to infiltrate the tumor. However, the tumor cells and TME still employ numerous inhibitory mechanisms to hinder tumor cell killing. These involve:

1. Co-inhibitory receptors to suppress T cell function
2. Loss of MHC-I or signaling components to respond to IFNγ
3. Selection over time for tumor cells without T cell recognized antigens

The best studied and most clinically relevant of these is the use of co-inhibitory receptor antibodies, though the others have interesting ramifications for T cell therapeutics.

The natural function of co-inhibitory receptors in immunity is to prevent auto-immunity and enable the immune response to be reined in once it has fulfilled its role in clearing an infection or cancer. The expression of PD-1 is induced upon activation of T cells, and if these cells are continuously exposed to antigen they will upregulate other co-inhibitory receptors like T cell immunoglobulin-3 (Tim-3). These co-inhibitory receptors enable activated T cells to respond to different environmental cues so they can efficiently mediate their function without causing damage [119].

PD-1 can interact with either PD-L1 or PD-L2, and interaction between receptor and ligand can induce a more exhausted phenotype in effector T cells. Exhaustion in this context refers to a reduction in ability to produce IFNγ as well as reduced proliferation.

This can be reduced/reversed by treating with a blocking antibody, as demonstrated initially in mouse studies of chronic viral infection [120]. The expression of PD-L1 is induced on tumor cells by exposure to IFNγ [121]. The efficacy of blockade has been exploited to develop CPIs in humans that have improved outcomes for cancer patients across a wide variety of cancer types, as previously discussed. Recently, multiple groups reported that the CD8 T cells that respond to anti-PD-1 blockade could be identified by the co-expression of transcription factor 7 (TCF-7) and PD-1 [46] [122]. These represent a reservoir of 'stem-like' cells that can proliferate after CPI in both mice and humans [47].

Tim-3 was originally identified on Th1 CD4 T cells and cytotoxic CD8 T cells [123], though is now known to be expressed on Tregs and multiple innate immune cells such as cDC1s. Knowledge of its role as an inhibitor of the immune response came from Tim-3 deficient mouse studies that developed spontaneous auto-immune conditions [124]. Co-expression of Tim-3 and PD-1 on CD8 T cells is associated with severe exhaustion, and these cells were capable of producing IL-10 (immunosuppressive) and could not clear chronic viral infection [125]. Moreover, a similar exhaustion phenotype was described in a mouse model of acute myelogenous leukemia, and tumor regression could in part be restored by combined blockade of both receptors [126]. PD-1+ Tim-3+ CD8 T cells have been identified in patients with melanoma and respond to co-blockade of PD-1/Tim-3 by increasing production of cytokines and proliferation relative to unblocked cells. Co-blockade was shown to be synergistic in culture and provides a basis for testing this in humans [127]. For this reason, Tim-3 blockade, in combination with PD-L1 or PD-1 blockade is being pursued in multiple trials [128].

In addition to co-inhibitory receptors, cancer cells have also been observed to lose expression of MHC-I. This can occur through loss of the β2m sub-unit of MHC-I, which prevents the cell from presenting any peptides to T cells. In humans, this was first

identified as a possible mechanism of immunoresistance in 1996 in a series of metastatic melanoma patients [129]. Additionally, cancer cells may acquire mutations that affect signaling through the janus kinase (JAK) STAT pathway downstream of IFNγ signaling. This would make the cells refractory to T cell produced IFNγ. Mutations in Jak1/Jak2 that inhibit functional IFNγ signaling have been observed in melanoma patients who developed resistance to PD-1 blockade [130]. Finally, if effector T cells manage to avoid these immunosuppressive mechanisms they will kill the tumor cells that they are capable of recognizing. Over time, this may lead to the selection of tumor cell clones that are less immunogenic, or have acquired some of the resistances mentioned here.

The myriad factors that impede effective cancer immunotherapy are unlikely to be addressed by a single therapeutic and are likely to require multiple interventions to target the different resistance mechanisms. Overall, one of the major resistance mechanisms is the lack of CD8 T cell responses primed in many patients, thereby precluding them from benefiting from any intervention that targets the later stages of the CIC. Vaccination is one intervention that can be developed to address this issue.

1.3 Therapeutic Cancer Vaccination

1.3.1 Rationale for cancer vaccination

To address some of the limitations of current immunotherapies it is necessary to develop complementary interventions that can enhance the effect of current treatments. In the case of CPIs, these require a pre-existing T cell response which not all patients are capable of generating. Vaccination has historically been an excellent strategy to induce immunity against infectious diseases, though this has always been a prophylactic intervention. In the context of cancer, vaccination would be a therapeutic strategy to

induce *de novo* or boost pre-existing T cell responses against tumor antigens [131]. Generating T cell responses through vaccination could be synergistic with CPI use.

The idea of cancer vaccination is not novel and has been tested historically in a number of different ways, with limited clinical success thus far. The earliest vaccination strategies were comprised of patient tumor cells, which would be irradiated and then admixed with an immunostimulatory agonist to be readministered to the patients. These autologous cell vaccination strategies were tested in patients with lung cancer [132], colorectal cancer [133], and renal cell cancer [134], but had limited therapeutic efficacy. One further problem with autologous cell vaccination is that it may require tumors to be advanced enough in size to be able to surgically resect the cells needed to make the vaccine, and so may be limited to late-stage cancer patients who are less likely to respond to intervention.

A different form of autologous cell vaccination involves isolating peripheral blood mononuclear cells (PBMCs), or even more specifically DCs and loading them with patient TAAs to then re-infuse these loaded cells into the patient to generate an adaptive immune response. The only FDA approved therapeutic cancer vaccine (Sipuleucel-T) to date is an autologous cell vaccine used in the treatment of prostate cancer that is based on this strategy. To generate Sipuleucel-T, PBMCs are isolated from patients and incubated *in vitro* with a recombinant fusion protein made by fusing prostatic acid phosphatase (PAP) to granulocyte-macrophage colony-stimulating factor (GM-CSF). The purpose of GM-CSF is to activate DCs to promote maturation and adaptive immune response initiation. These cells are then re-infused into the patient to generate a T cell response against PAP. In patients with castration resistant prostate cancer, this resulted in a median increase of 4.1 months in the treated vs untreated groups in terms of survival [135]. Subsequent work on cancer vaccines has aimed to build on this initial success and improve upon it.

Improving the efficacy of cancer vaccines requires understanding the shortcomings of current technologies. There are three major factors that have likely limited the efficacy of cancer vaccines thus far. The first is the selection of the target TAA, as not all TAAs share the same features and this can present challenges in targeting tumor cells effectively and specifically [136]. The second is the technology used for eliciting CD8 T cell responses. Historically, vaccination has been used to elicit potent responses against infections which relies heavily on an antibody response rather than a CD8 T cell response. Many vaccine technologies were thus designed to achieve high titers of neutralizing antibodies, without necessarily ensuring effective CD8 T cell response priming [137]. Finally, the TME is highly immunosuppressive and to address this, it is likely that a vaccination strategy would have to be paired with a CPI intervention to ensure maximal efficacy.

1.3.2 Types of antigen to target

Tumors can present a variety of different types of antigen for recognition by cytotoxic T cells. Mutations, aberrant transcription/translation, or viral transformation can all result in cancer cells producing peptide fragments that could be recognized by CD8 T cells if presented on MHC-I. As a result, there are 4 main types of TAA, namely neoantigens, melanoma antigen family (MAGE) -type antigens, viral antigens and over-expressed antigens or tissue-specific antigens [136]. These antigens differ in many regards, which makes some more suitable for cancer vaccination than others.

(I) Over-expressed or tissue specific antigens

Over-expressed antigens are usually tissue-specific antigens that are expressed at higher levels on tumor cells than on healthy tissue. These are not tumor-specific, and so T

cell responses that recognize these will also recognize the same antigens on healthy tissue, which can result in auto-immune activity [136]. Additionally, T cells clones that would naturally recognize many of these self-antigens would be selected out during development through central tolerance to limit the possibility of auto-immunity. This may limit the ability to induce effective CD8 T cell responses against these self-antigens through vaccination.

There are however some antigens against which central tolerance does not appear to remove possible T cell clones. In melanoma patients, spontaneous T cell responses can be primed against melanocyte specific antigens such as Melan-A [138] and tyrosinase [139]. This will enable the T cells to recognize both the melanoma cells and melanocytes as non-self. This likely underpins the correlation between spontaneous melanoma clearance and the development of vitiligo, which is an auto-immune condition responsible for loss of pigmentation in regions of the skin, in some patients [140].

Similarly, the restricted expression of prostate-specific antigen (PSA) and PAP to prostate tissue enables vaccine design to elicit anti-PSA and anti-PAP T cell responses to promote anti-prostate cancer immunity. Sipuleucel-T was designed to prime T cell responses against PAP, and a different vaccine (PROSTVAC) was designed to target PSA. PROSTVAC is a viral vector vaccine, consisting of a combination approach using a recombinant vaccinia virus prime followed by fowlpox vector boosts. The viruses encode three co-stimulatory molecules and the PSA protein as an antigen [141]. PROSTVAC showed promising results in a phase II trial [142], but eventually failed in phase III as patients in the treated group did not display significantly improved survival rates as compared to controls [143]. Overall, these tissue-specific over-expressed antigens may not be particularly suitable for cancer vaccination strategies due to the potential for off-target

effects and the possible limitations that central tolerance may impose on the development of T cell responses.

(II) MAGE-type antigens

MAGE-type antigens are encoded in genes known as cancer germline genes, many of which are X-chromosome linked. The expression of these genes is tightly controlled and they are usually only expressed on male germline cells, the placenta, and cells in the developing trophoblast. During cancer development, cancer germline genes may be expressed by tumor cells. The cells in which cancer germline genes would be normally expressed are considered 'immune-privileged', which means that the cells of those tissue do not express MHC-I and therefore can't present peptide for recognition by CD8 T cells. This makes aberrantly expressed MAGE-type antigens a suitable target for vaccination as anti-MAGE-type antigen T cell responses should specifically target tumor cells [144]. In humans, cytotoxic CD8 T cell responses against MAGE-type antigens have been detected in patients with melanoma [145]. Additionally, cancer germline genes have been shown to be expressed by multiple different cancer types including lung carcinoma and colorectal cancer, thus demonstrating the breadth of tumor types that could potentially be targeted by MAGE-type antigen vaccination [146].

Despite the tumor specificity and array of tumors that have been shown to express MAGE-type antigens, an effective T cell vaccine has not yet been developed. Two recent phase III clinical trial undertaken by GSK aimed to induce immunity against MAGE-A3 in melanoma [147] and lung [148] cancer patients. Patients had been pre-screened for tumor expression of MAGE-A3 to ensure the target was present in patient tumors. The vaccine was made of recombinant MAGE-A3 protein admixed with the adjuvant AS015. Both clinical trials failed to show an increase in progression free survival compared to

control groups. Despite these failures, MAGE-type antigens continue to be pursued as a clinical target for cancer vaccination due to their desirable characteristics.

(III) Viral antigens

The most well studied viral antigens in cancer immunotherapy are E6 and E7, which are expressed by human papilloma virus (HPV) and promote tumorigenesis [149]. The benefit of viral antigens is that they are uniquely expressed in the tumor and are entirely non-self, therefore carry a much lower risk of generating cross-reactive T cell responses against normal tissue peptides. Two prophylactic vaccines against HPV have been approved by the FDA to combat the incidence of HPV-related cancer, and they achieve this by eliciting an antibody response against HPV and preventing infection [150]. However, vaccines to target E6 and E7 by inducing a CD8 T cell responses in patients who already have HPV+ tumors are being developed. They have been reasonably successful across trials in eliciting CD8 T cell responses against E6 and/or E7 and providing modest improvements in outcomes, though none are yet FDA approved [151]. The downside for viral antigens is that not all tumors are the result of viral transformation and so these vaccines have a restricted utility to those patients who have tested positive for virally induced malignancies. One major benefit for the field is that these trials provide proof-of-concept evidence for different types of cancer vaccine platforms to elicit effective immune responses.

(IV) Neoantigens

Neoantigens are perhaps the most novel TAAs recognized to date. They are the result of mutations altering the amino acid sequence of proteins produced in the cell, and as a result are exclusively expressed in tumor cells. The tumor specific expression of

neoantigens means that central tolerance would not have removed potential CD8 T cell clones that could recognize these from the T cell pool. Neoantigens can arise through point mutations at the gene level that lead to a single amino acid change in a peptide sequence. This may alter the way in which the peptide is presented on MHC-I relative to the normal sequence or may enable a peptide sequence that wouldn't have been presented normally to bind to the MHC-I groove [152]. Alternatively, frame-shift mutations (insertions or deletions) can cause the production of entire amino acid sequences that are unique, and therefore could have numerous epitopes not present in any normal tissue [153]. Lastly, gene-fusions can result in unique amino acid sequences that may contain a T cell epitope capable of being presented on MHC-I [154].

Evidence for the importance of neoantigens comes from multiple sources. Analysis of two independent cohorts of NSCLC patients treated with anti-PD-1 therapy found that a higher tumor mutational burden (TMB) was positively correlated with increased progression free survival and improved objective response rate following treatment [155]. A high TMB is hypothesized to result in a higher number of neoantigens that could be recognized by T cells, and underpins the improved efficacy of CPIs in tumor with high TMB. This may explain why tumors that have low TMB are typically less responsive to CPIs.

In addition, a clinical trial tested pembrolizumab (anti-PD-1) in metastatic colorectal cancer patients, whose tumors could be segregated by mismatch repair proficiency or deficiency. Mismatch repair deficiency in colorectal cancer is associated with a 10-100 times higher rate of somatic mutations than mismatch repair proficient tumors. Pembrolizumab treatment resulted in progression free survival for 78% of patients with mismatch repair deficient carcinomas as compared to 11% in patients with mismatch repair proficient cancers [156]. In a follow up study, the observation that mismatch repair

deficient tumors are sensitive to PD-1 blockade was expanded to 12 different cancer types. The objective response rate was 53% of patients, with a complete response observed in 21%. Furthermore, tumor antigen-specific clones were identified in a responding patient that were shown to recognize neoantigens expressed by their tumor. This supports the idea that mutations can result in highly tumor specific CD8 T cell responses that expand after PD-1 blockade [157].

The association between TMB and cancer response to CPI has been expanded in a meta-analysis of multiple tumor types and their response to PD-1 blockade. These analyses have shown a strong positive correlation across tumor types between TMB and PD-1 blockade efficacy [158] [159]. Interestingly, in patients that are not treated with CPIs there is no correlation between TMB and survival when averaged across different tumor types, and even a negative correlation between TMB and progression free survival in some tumor subtypes [160]. The prognostic value of high TMB has reached a point where some groups are developing blood-based assays to assess TMB. This has been shown in a proof-of-concept retrospective analysis of two large randomized trials to reliably identify patients that are likely to respond to the anti-PD-L1 inhibitor atezolizumab [161]. This removes a significant barrier to patient stratification for treatment as it can often be difficult to biopsy sufficient tissue to assess prognostic markers to support a particular intervention.

Supporting evidence for the correlation between high TMB and increased T cell presence came from assessing 515 patients from six tumor sites that had RNA-sequencing data available on the cancer genome atlas (TCGA). A positive correlation between the TMB and expression of *CD8A,* as well as T cell exhaustion markers such as *PDCD1* and *CTLA4*, was identified through this analysis. Tumors with low TMB were also associated with reduced T cell infiltration, suggested again by RNA-sequencing [162]. A follow up

study found that the number of predicted MHC-I neoantigens across 18 tumor types positively correlated with cytolytic activity, which was approximated by the expression of granzyme A (*GZMA)* and perforin (*PRF1)* [163]. This correlation was lower than expected for some cancer types, such as colorectal cancer, and the authors hypothesized that this was due to effective immune mediated killing of neoantigen containing tumor cells. This process is known as immunoediting, whereby the tumor evolves in response to the immune selection pressure to become less immunogenic [164].

Thus far the evidence for neoantigens as suitable targets of anti-tumor immunity have been correlational. In recent years, two small trials with human patients using adoptively transferred neoantigen-specific T cells have also demonstrated an ability to promote tumor regression [165] [166] . In both cases, neoantigen-specific T cells were isolated from patients, expanded *ex vivo* and re-infused into patients to mediate anti-tumor immunity. One patient had metastatic colorectal cancer, with 7 concomitant metastases in the lungs. The tumor harbored a specific constitutive activation mutation in KRAS (G12D) that promotes proliferation and could be presented on HLA-C*08-02 (human leukocyte antigen, humanized nomenclature for MHC-I). This neoantigen could be recognized by 4 distinct T cell clones derived from the patient, and regression was observed in all 7 lung metastases following infusion. One lesion progressed after 9 months and was found to have lost the chromosome encoding HLA-C*08-02, meaning it could no longer present this neoantigen to T cells. This is an example of immunoediting and results in effective tumor immune evasion against this particular intervention [165]. In a separate human trial, a patient with metastatic cholangiocarcinoma was infused with a >95% pure preparation of patient derived CD4 T cells that could recognize a mutated form of *ERBB2IP* expressed by the tumor and experienced tumor regression [166]. This highlights the under-appreciated role that neoantigen-specific CD4 T cells may play in anti-tumor

immunity. Collectively, these two trials provide direct evidence for the potential of neoantigen-specific T cell responses to mediate anti-tumor immunity.

Finally, in mouse tumor models, vaccination against neoantigens expressed by either the B16F10 mouse melanoma model [167] or the MC38 colorectal cancer model [168] have been shown to elicit efficacious anti-tumor T cell responses. In addition, neoantigens that induce a CD4 T cell response were also found to be able to mediate tumor regression in B16F10 [169]. Collectively, the data from mouse and human cancers has revealed neoantigens to be an excellent target for therapeutic vaccination.

1.3.3 Vaccine platforms

Once an antigenic target has been selected, it is important to develop a vaccination platform that is well suited to eliciting T cell responses, particularly in humans. Most vaccine platforms developed for infectious diseases have been developed to induce neutralizing antibody responses and so may not be the most effective vectors for inducing T cell immunity [137]. There are three major classes of vaccine platform in development for tumor therapy (not including cell based vaccines) and these are:

1. genetic vaccines (based on RNA/DNA, focus will be on RNA)
2. viral vectors (e.g. adenoviruses, vaccinia virus, fowlpox, etc.)
3. protein/peptide and adjuvant vaccines (e.g. PROSTVAC, focus will be on peptide).

These platforms are not equally well-suited to elicit CD8 T cell responses or for use in targeting all antigen types, so a better understanding of these platforms is required.

(I) RNA vaccines

There is currently a lot of enthusiasm surrounding RNA vaccines due to the successes of the Pfizer and Moderna vaccines in combating the SARs-CoV-2 pandemic. These were the first RNA vaccines developed and deployed at scale, which demonstrated 2 major benefits of this type of vaccine platform – they can be rapidly developed and manufactured at scale, and they can safely induce protective immune responses in humans.

For cancer, RNA vaccines have been tested in mouse models and more recently in a human trial. The RNA is typically delivered within a lipoplex nanoparticle as the RNA functions as the adjuvant for this vaccine. In order to generate neoantigens the RNA must be translated and so therefore relies on being taken up by APCs. The proof of concept was demonstrated by Kreiter and colleagues who vaccinated mice with B16F10 tumors with a single CD4 neoantigen mRNA vaccine and were able to show tumor control [169].

This was followed up with the first RNA based personalized cancer vaccine clinical trial [170]. The good manufacturing practice (GMP) production of personalized RNA vaccines ranged from 49 to 102 days, demonstrating the speed with which this platform can be adapted to produce unique vaccines. For each patient, 10 neoantigens were selected for use in the vaccine design. These vaccines were injected directly into inguinal lymph nodes to maximize the probability that they would be picked up by DCs. All patients were shown to develop T cell responses against multiple antigens encoded in the RNA vaccine. Of the 5 patients, 3 displayed an objective response and 1 of those was a complete response after receiving anti-PD-1 blocking antibody [170]. This trial was the first glimpse that neoantigen vaccination may be able to induce meaningful anti-tumor T cell responses in humans, and development of these platforms is currently underway.

(II) Viral vectors

Viruses are naturally immunogenic and as such are some of the most potent CD8 T cell inducing vectors in existence. This is likely due to the natural function of CD8 T cells, as they specialize in the destruction of cells infected by intracellular pathogens. With the current understanding of molecular biology, it is possible to create recombinant viral vectors that encode antigens and/or co-stimulatory molecules to elicit potent immune responses, such as PROSTVAC [171].

One major family of viruses that is being investigated for eliciting CD8 T cell responses following vaccination is adenoviruses. Adenoviruses are double stranded DNA viruses that were originally being developed for gene therapy due to the sustained transgene expression they exhibited [172]. This sustained expression, along with the broad tissue tropism they display, and the potent immune responses they can elicit suggested adenoviruses might be better suited to a role as a vaccination platform.

However, not all adenoviruses are suitable for use as a vaccine. Human adenoviruses naturally infect people and generate neutralizing antibodies against the virus. If these are naturally present in a large proportion of the population, it limits the utility of that virus (and similar vectors) as the neutralizing antibodies are likely to negatively affect the viral vector's ability to infect cells and produce transgene products to elicit immunity against the antigen of interest. To avoid this, recent efforts have focused on developing viral vaccines that are derived from viruses with low human seroprevalence – for example chimp adenoviruses.

A further limitation of using viruses is that patients may develop anti-vector neutralizing antibodies post vaccination. This may limit the number of times a vaccine may be administered to a patient to effectively boost immune responses. One method to deal with vaccine induced anti-vector immunity is to use a heterologous prime boost

vaccination strategy, where one viral vector is used to prime responses and a different vector is used to boost. The combination of adenoviral vector prime and modified vaccinia Ankara (MVA) boost has been shown to elicit higher magnitude CD8 T cell responses than homologous vaccination against hepatitis C virus (HCV) [173], HPV [174], and malaria [175] antigens.

The chimp adenovirus oxford 1 (ChAdOx1) virus was derived from a chimp adenovirus isolate Y25 [176]. It has been successfully tested in a mouse model of prostate cancer and shown to elicit T cell responses against six transmembrane epithelial antigen of the prostate 1 (STEAP1) when used in combination with MVA. When this heterologous prime boost approach was combined with PD-1 blockade, this improved survival and resulted in a 80% of mice achieving tumor-free status [177]. A similar second study targeting the oncofetal glycoprotein 5T4 was also undertaken and shown to achieve similar results, demonstrating the utility of heterologous prime boost when using ChAdOx1 and MVA [178]. These results led to a phase I clinical trial involving 40 patients with prostate cancer who were vaccinated with 5T4 encoding ChAdOx1 followed by MVA. Most patients developed T cell responses against 5T4 and the vaccination strategy was well tolerated. Effects on tumor regression and survival are pending, and will be expanded upon in a follow up phase I/II trial known as ADVANCE [179].

The combination of ChAdOx1/MVA has also recently been tested in a mouse mastocytoma model that expresses the antigen P1A – a mouse MAGE-type antigen. In this model, heterologous prime boost was shown to synergize with anti-PD-1 blockade and enabled tumor control. The heterologous prime boost approach also promoted CD8 T cell infiltration into the tumor and was associated with a reduced expression of PD-1 on P1A-specific CD8 T cells in the tumor [180].

In pre-clinical models, ChAdOx1 has often been given in combination with MVA as a boost to elicit potent anti-tumor immunity. The results support the use of these vectors in combination for cancer vaccination in patients. Thus far, there has been no publication utilizing these viral vectors to target neoantigens.

(III) Peptide and adjuvant vaccines

Peptide adjuvant vaccines were initially developed to induce CD8 T cell immunity by using the minimal epitope (peptide fragment presented on MHC-I) and admixing this with an adjuvant. The theory was that the minimal epitope peptide would be easily loaded on to MHC-I and this would elicit potent CD8 T cell responses. However, it was quickly found that this was sub-optimal for two reasons. First, the peptide could be presented on MHC-I by cells other than APCs in the absence of appropriate co-stimulation and this could result in tolerized CD8 T cell responses. A second observation associated in particular with vaccination with short minimal epitopes formulated with incomplete Freund's adjuvant (IFA) is that T cells may accumulate at the vaccine site and appear to die due to a lack of co-stimulation and CD4 T cell help [181].

To address these problems, the field of peptide based vaccination for T cells has moved towards using the synthetic long peptide (SLP). These peptides are usually 25-35 amino acids long, and the minimal epitope is placed in the middle of the sequence. This helps restrict presentation to professional APCs that are able to process the peptides and load them onto MHC-I [182]. In addition, the use of longer peptides allows for the possibility of a CD4 T cell epitope to also be present in the vaccine, which may be beneficial to inducing CD8 T cell immunity or have complimentary anti-tumor functions [183] [184].

In 2014, one group adapted this approach to target neoantigens expressed by the mouse colorectal cancer model MC38. To achieve this, it was important to develop a strategy for identifying neoantigens for vaccination. This process was comprised of multiple steps:

1. Whole exome and RNA sequencing
2. Mutation identification
3. *In silico* translation of mutated gene sequences to generate neoantigen peptide sequence
4. MHC-I binding prediction and rank ordering by predicted binding affinity
5. Neoantigen selection and SLP production for vaccination

In this study, the MC38 cancer line started with 1,290 possible transcript coding variations, which culminated in the identification of 7 neoantigens. These were validated by mass-spectrometry to bind to MHC-I. However, upon vaccination of mice with SLP and poly-ICLC (a commonly used TLR-3 agonist), only 3 neoantigens were validated as being immunogenic. Vaccination with these peptides was still able to delay tumor growth in a prophylactic study using MC38 [168].

This work was foundational for a phase I clinical trial in melanoma patients that targeted neoantigens by using SLP with poly-ICLC. The process of identifying patient neoantigens contained the same steps as in the mouse study and the RNA neoantigen vaccine trial [170]. In another study, the SLP and poly-ICLC vaccine was able to induce better CD4 T cell responses (58/90, 60%) than CD8 T cell responses (15/90, 16%) in human patients [185]. There were no therapeutic outcomes in this trial, it was just to assess safety and immunogenicity. The neoantigen vaccine studies illustrate the difficulty in targeting neoantigens for vaccination, as a patient has limited time to wait for the production of personalized vaccines and the process is complex.

One recently developed vaccine platform based on SLP and adjuvant is the self-assembling nanoparticle-TLR7/8 agonist (SNP-7/8a or SNP) vaccine, which is formed by conjugating a modified SLP to a hydrophobic block covalently linked to the TLR agonist [186]. The rationale for using a TLR-7/8 agonist was because of the wide-spread expression of TLR7/8 across multiple APC subsets in both mice and humans. TLR-7/8 activation is associated with a strong type I IFN response and production of IL-12 which favors induction of cytotoxic CD8 T cells and Th1 CD4 T cell responses [187]. The SNP vaccine can deliver almost any SLP antigen as a 20-50 nm nanoparticle in solution. In addition, because the peptide is directly conjugated to the hydrophobic block containing the TLR-7/8 agonist, peptide will always be taken up with the appropriate stimulant. This formulation has been shown to prime superior CD8 T cell responses against neoantigens as compared to SLP given with poly-ICLC. SNP not only stimulated a higher magnitude response, but also elicited CD8 T cell responses against all 7 mass spectrometry validated neoantigens, including those that did not elicit a response when given as SLP and poly-ICLC [186].

One further interesting finding with the SNP vaccine was the importance of route of vaccination for CD8 T cell quality and efficacy in clearing MC38 tumors in mice. Mice that were vaccinated subcutaneously (SC) achieved approximately ~10 fold higher magnitude antigen-specific CD8 T cell responses in the blood as compared to mice that were vaccinated intravenously (IV). However, IV SNP elicited CD8 T cell responses had a greater frequency of ‘stem-like’ cells than SC. Moreover, in the therapeutic setting SC vaccination was unable to elicit any tumor regression in the MC38 model, whereas IV vaccination routinely cleared ~40-50% of tumors [188]. This suggested that the route of vaccination may be an important factor to consider when eliciting CD8 T cell responses.

1.4 Specific Aims

Previous members of the Seder lab developed the novel SNP vaccine platform. SNP effectively induces neoantigen-specific anti-tumor CD8 T cell responses against MC38 in mice. However, upon testing SNP for immunogenicity in non-human primates, the magnitude of elicited CD8 T cell responses was found to be very low [186]. In contrast, ChAdOx1 can induce high magnitude CD8 T cell responses in mice and humans. However, due to anti-vector immunity, ChAdOx1 may be more limited in the number of times it can be given. Additionally, production time for personalized viruses is likely to be longer than peptides, time which may be critical for effective intervention for a patient. My DPhil project therefore sought to combine SNP and ChAdOx1 to determine if heterologous prime boost using these platforms could elicit more potent anti-tumor immunity than either platform alone. Neoantigens were selected as the target because they are the most tumor specific antigens and should be applicable to almost any tumor type. The specific aims were:

1. To determine if heterologous prime boost using SNP and ChAdOx1 increases magnitude of antigen-specific CD8 T cell responses relative to either platform alone, and characterize the effect on T cell quality
2. To understand the effect of route of vaccination and interval between prime and boost on antigen-specific CD8 T cell responses
3. To determine if heterologous prime boost elicited CD8 T cell responses are capable of mediating tumor control in the prophylactic and therapeutic setting
4. To determine what role, if any, activation of innate immunity following IV vaccination has in mediating anti-tumor immunity

Chapter 2

Materials and Methods

2.1 Materials

2.1.1 Reagents and kits

Table 2.1 List of reagents and kits

Reagent	Supplier	Catalogue No.
ABTS (2,2'-Azino-bis(3-ethylbenzothiazoline-6-sulfonic acid))	Sigma	A3219
ACK (Ammonium-Chloride-Potassium) lysing buffer	Quality Biological	118-156-101
Anti-CD16/CD32 (Mouse BD Fc Block)	BD Biosciences	553142
Anti-mouse CD28 (37.51 clone)	BD Biosciences	553294
ArC Reactive amine Beads	BD	
BD Cytofix/Cytoperm™	BD Biosciences	554714
BD Golgiplug	BD Biosciences	555029
BD Horizon Brilliant Stain Buffer	BD Biosciences	566385
Dasatinib	Selleckchem	S1021
DH5α competent cells	Thermofisher Scientific	18258012
Dimethyl sulfoxide (DMSO)	Sigma-Aldrich	276855-100mL
eBioscience™ Foxp3 / Transcription Factor Staining Buffer Set	Invitrogen, Thermofisher Scientific	00-5523-00
Heparin	Fresenius Kabi	NDC 63323-540-05
IFNα ELISA Kit	Pbl Assay Science	42115-1
Isoflurane, USP	Baxter Healthcare Corp.	NDC 10019-360-60
KpnI Restriction Enzyme	New England BioLabs	R0142S
LIVE/DEAD™ Fixable Blue Dead Cell Stain Kit	ThermoFisher Scientific	L34962
Murine IL-12 ABTS ELISA Kit	Peprotech	900-K97
Murine IP-10 ABTS ELISA Kit	Peprotech	900-K153
NotI Restriction Enzyme	New England BioLabs	R0189S
Plasmid MIDI kit	Qiagen	12143
PmeI Restriction Enzyme	New England BioLabs	R0560S
Milliplex MAP mouse cytokine/chemokine Magnetic Kit	Millipore Sigma	MCYTMAG-70K-PX32
Paraformaldehyde (PFA, 16%)	Electron Microscopy Sciences	15710
Phosphate buffered saline (PBS)	Gibco	10010-023
Streptavidin PE (SaPE)	BD Biosciences	S866
Trypsin-EDTA (0.25%)	Gibco, Life Tech	25200-056
Tween-20	Sigma	P-7949
ViaStain AOPI Staining Solution	Nexcelom Bioscience	CS2-0106

2.1.2 Buffers and media

(I) Table 2.2 Complete RPMI

Reagent	Conc.	Supplier	Catalogue
RPMI 1640	-	Cytiva, HyClone Labs	SH30027.02
FBS	10%	Gibco	10438-026
Penicillin/Streptomycin/Glutamine (100X)	1%	Gibco, Life Tech	10378-016
Non-essential Amino Acids (100X)	1%	Cytiva, HyClone Labs	SH30238.01
Sodium Pyruvate (100mM)	1 mM	Cytiva, HyClone Labs	SH30239.01
Hepes Buffer (1M)		Gibco, Life Tech	15630-080
2-mercaptoethanol (1000X)	0.1%	Gibco, Life Tech	21985-023

(II) Table 2.3 MC38 media

Reagent	Conc.	Supplier	Catalogue No.
RPMI 1640	-	Cytiva, HyClone	SH30027.02
FBS	10%	Gibco	10438-026
Penicillin/Streptomycin/Glutamine (100X)	1%	Gibco, Life Tech	10378-016
Non-essential Amino Acids	1%	Cytiva, HyClone Labs	SH30238.01
Sodium Pyruvate	1 mM	Cytiva, HyClone Labs	SH30239.01

(III) Table 2.4 B16F10/TC-1 media

Reagent	Conc.	Supplier	Catalogue No.
DMEM	-	Gibco, Life Tech	11965-092
FBS	10%	Gibco	10438-026
Penicillin/Streptomycin/Glutamine (100X)	1%	Gibco, Life Tech	10378-016
Non-essential Amino Acids	1%	Cytiva, HyClone Labs	SH30238.01
Sodium Pyruvate	1 mM	Cytiva, HyClone Labs	SH30239.01

(IV) Table 2.5 Tumor digestion and dissociation buffer

Reagent	Conc.	Supplier	Catalogue No.
RPMI 1640	-	Cytiva, HyClone	SH30027.02
FBS	10%	Gibco	10438-026
Collagenase D	0.2 mg/ml	Roche	11088882001
DNase I	50 U/ml	Roche	04536282001

(V) Table 2.6 FACS buffer

Reagent	Conc.	Supplier	Catalogue No.
PBS	-	Gibco, Life Tech	10010-023
FBS	2%	Gibco	10438-026

2.1.3 Mice

Table 2.7 Mouse strains

Strain	Supplier	Catalogue No.
C57Bl6	Jackson Laboratories	000664
IL-12 KO		002693
IFNar KO		028288
Sting KO		025805

2.1.4 Tumor cell lines

Table 2.8 Mouse tumor cell lines

Cell line	Supplier	Catalogue No.
MC38	Gift from Lelia Delamarre, Genentech	-
B16F10	ATCC	CRL-6475
TC-1	Gift from Dr. T.C. Wu, John's Hopkins	-

2.1.5 ChAdOx1 vaccines

Table 2.9 ChAdOx1 antigen amino acid insert sequences

Antigen	Amino acid sequence encoded
Reps1	GRVLELFRA**AQLANDVVL**QIMELCGATR
Adpgk	GIPVHLEL**ASMTNMELM**SSIVHQQVFPT
E6	CKQQLLRR**EVYDFAFRDL**CIVYRDG
E7	GQAEPD**RAHYNIVTF**CCKCD
Trp1	VTNTEMFV**TAPDNLGYM**YEVQWPGQE

*Bold and underlined identifies the minimal epitope for immunodominant CD8 T cell response in each antigen, red letter identifies amino acid that results from point mutation in neoantigen sequence, different to wild-type sequence.

2.1.6 Peptides

Table 2.10 Peptide sequences used for stimulation and SNP vaccinations

Peptide	Amino Acid Sequence	Used For
Reps1 min	AQLANDVVL	Peptide stim
Reps1 SLP	GRVLELFRAAQLANDVVLQIMELCGATR	Peptide stim
Reps1 SNP	KKKKKKVRGRVLELFRAAQLANDVVLQIMELCGATRSPVZX	SNP vaccine
Adpgk min	ASMTNMELM	Peptide stim
Adpgk SLP	GIPVHLELASMTNMELMSSIVHQQVFPT	Peptide stim
Adpgk SNP	KKKKKKKKKVRGIPVHLELASMTNMELMSSIVHQQVFPTSPVZX	SNP vaccine
E6 min	REVYDFAFRDL	Peptide stim
E6 SLP	CKQQLLRREVYDFAFRDLCIVYRDG	Peptide stim
E6 SNP	KKKKKVRCKQQLLRREVYDFAFRDLCIVYRDGSPVZX	SNP vaccine
E7 min	RAHYNIVTFS	Peptide stim
E7 SLP	GQAEPDRAHYNIVTFCCKCD	Peptide stim
E7 SNP	KKKKKKKVRGQAEPDRAHYNIVTFCCKCDSPVZX	SNP vaccine
Trp1 min	TAPDNLGYM	Peptide stim
Trp1 SLP	VTNTEMFVTAPDNLGYMYEVQWPGQ	Peptide stim
Trp1 SNP	KKKKKKKKKKVRVTNTEMFVTAPDNLGYMYEVQWPGQESPVZX	SNP vaccine

*Red letter identifies amino acid resulting from point mutation in neoantigen sequence,

X is azidolysine.

2.1.7 Monoclonal antibodies

Table 2.11 Monoclonal antibodies for *in vivo* use

Target	Clone	Supplier	Catalogue No.
PD-L1	10F.9G2	BioXcell	BE0101
IFNα receptor	MAR1-5A3	BioXcell	BE0241
CD8β	Lyt3.2	BioXcell	BE0223

2.1.8 Tetramers

Table 2.12 Tetramer information

Antigen	Minimal Epitope	MHC-I Restriction	Supplier
Reps1	AQLANDVVL	H-2D^{b}	Gift from John Finnigan
Adpgk	ASMTNMELM	H-2D^{b}	Gift from John Finnigan
Trp1	TAPDNLGYM	H-2D^{b}	Gift from John Finnigan

2.1.9 Flow cytometry panels

(I) Table 2.13 Tetramer panel

Channel	Marker	Fluorophore	Clone	Cat. No.	Supplier
U395	CD4	BUV395	RM4-4	740209	BD
U450	Live/Dead Blue	--	--	L34962	ThermoFisher Scientific
U740	CD44	BUV737	IM7	564392	BD
V450	PD-1	BV421	29F.A12	135218	Biolegend
V605	Tim-3	BV605	RMT3-23	119721	Biolegend
V785	KLRG1	BV785	2F1	565477	BD
B710	Eomes	PerCPeFluor 710	Dan11mag	46-4875-82	Invitrogen
G575	Tetramer	PE	--	--	--
G610	CD39	PE-Dazzle594	Duha59	143812	Biolegend
G660	CD127	PE-Cy5	A7R34	135016	Biolegend
G780	FoxP3	PE-Cy7	FJK-16S	25-5773-82	Invitrogen
R660	TCF-1	Alexa647	C63D9	6709S	Cell Signaling
R710	CD3	Alexa700	17A2	100216	Biolegend
R780	CD8	APCeF780	53-6.7	47-0081-82	eBioscience

(II) Table 2.14 Peptide stimulation panel

Channel	Marker	Fluorophore	Clone	Cat. No.	Supplier
U395	CD4	BUV395	RM4-4	740209	BD
U450	Live/Dead Blue	--	--	L34962	ThermoFisher Scientific
U785	CD8	BUV805	53-6.7	612898	BD
V450	PD-1	BV421	29F.A12	135218	Biolegend
V605	Tim-3	BV605	RMT3-23	119721	Biolegend
V655	TNFα	BV650	MP6-XT22	506333	Biolegend
V785	KLRG1	BV785	2F1	565477	BD
G660	CD127	PE-Cy5	A7R34	135016	Biolegend
R660	IFNγ	APC	XMG1.2	554413	BD
R710	CD3	Alexa700	17A2	100216	Biolegend

(III) Table 2.15 Mononuclear phagocyte (MNP) panel

Channel	Marker	Fluorophore	Clone	Cat. No.	Supplier
U395	NK1.1	BUV395	PK136	564144	BD
U395	CD19	BUV395	1D3	563557	BD
U395	CD3	BUV395	145-2C11	563565	BD
U450	Live/Dead Blue	--	--	L34962	ThermoFisher Scientific
U570	Ly6G	BUV563	1A8	565707	BD
U660	CD45	BUV661	30-F11	565079	BD
U785	SiglecH	BUV805	440C	748291	BD
V450	CCR7	BV421	4B12	120120	Biolegend
V650	XCR1	BV650	ZET	148220	Biolegend
V710	CD86	BV711	GL1	740688	BD
V785	CD64	BV785	X54-5/7.1	741024	BD
B515	IA/IE	Alexa488	M5/114.15.2	107616	Biolegend
B710	CD172α	PerCP-eF710	P84	46-1721-82	Life Tech
G575	CD11c	PE	HL3	553802	BD
G610	CD80	PE-Dazzle594	16-10A1	562504	BD
G660	F4/80	PE-Cy5	BM8	15-4801-82	eBioscience
G780	B220	PE-Cy7	RA3-6B2	552772	BD
R660	CD40	Alexa647	3/23	123613	Biolegend
R710	CD11b	Alexa700	MI/70	557960	BD
R780	Ly6C	APC-eF780	AL-21	560596	BD

2.1.10 Instruments

Table 2.16 List of instruments used

Instrument	Manufacturer
BD LSR Fortessa X-50	BD Biosciences
Cellometer Auto 2000	Nexcelom Bioscience
gentleMACS OctoDissociator	Miltenyi Biotec
Infinity II (HPLC)	Agilent Technologies
MAGPIX System	Luminex
SpectraMax i3x	Molecular Devices

2.1.11 Software

Table 2.17 List of software used

Program	Supplier
Flowjo v10	Tree Star
GraphPad Prism v8	GraphPad software
Pestle v1.8	National Institutes of Health, Bethesda, MD, USA
Simplified Presentation of Incredibly Complex Evaluations (SPICE) v6	National Institutes of Health, Bethesda, MD, USA
xPONENT software	Luminex

2.1.12 Plasticware

Table 2.18 List of plasticware

Reagent	Supplier	Catalogue No.
1.5mL Starstedt tube	Starstedt AG and Co	72.692.005
15mL Falcon tube	Corning	352097
50mL Falcon tube	Corning	352070
70µm Cell strainer	Corning	431751
96 well 40µm filter plate	Millipore	MANMN4010
96 well V-bottom plate	Corning	3894
BioMasher pestle/mortar tubes	Funakoshi	320103
gentleMACS C-tubes	Miltenyi Biotec	130096334
Insulin Syringe (30G, 0.3mL)	BD Biosciences	328431
Microvette 500 Z-gel	Sarstedt AG and Co	20.1344
Nunc MaxiSorp 96 Well ELISA plate	Thermo Scientific	439454

2.2 Methods

2.2.1 SNP vaccine preparations

SNP vaccines were produced as published by Lynn and colleagues [186]. Briefly, the hydrophobic block (H-block) containing a TLR-7/8 agonist (based on Imidazoquinoline) was produced by Avidea Technologies. Peptide antigens for vaccine production were provided by Genscript. SNP vaccine peptides were conjugated with H-block through a azide-alkyne cycloaddition click chemistry reaction that was performed at room temperature. SNP vaccine peptides and H-block were mixed at ratio of 1 to 1.1 to ensure an excess of H-block and that no peptide could be delivered without agonist. Ratio was calculated by high performance liquid chromatography (HPLC). Final vaccine concentration was calculated based on the nmol of H-block used for each reaction.

2.2.2 ChAdOx1 vector construction

(I) Transgene construction

The neoantigens (Adpgk and Reps1), or the self-antigen Trp1, or the viral antigens from E6/E7 (Table 2.9) were used to create a transgene to be inserted into ChAdOx1. The constructs consisted of a fragment of the murine invariant chain (CD74, denoted mIi), which has been previously shown to increase the magnitude of CD8 T cell responses elicited against an encoded antigen [109]. The mIi was followed by a spacer sequence (GGGPGGG) and the mouse codon optimized sequence for one of the target antigen sequences. The spacer sequence should prevent formation of chimeric antigens that could have been formed by directly fusing antigen repeats together. The spacer-antigen fragment was repeated a total of 5 times to complete the transgene insert, resulting in a pentamer repeat. Stop codons were added at the end of the pentamer repeat sequence. This resulted in the creation of 4 unique ChAdOx1 vectors, 1 encoding each of Reps1, Adpgk and Trp1

and one that encodes both the E6 and E7 target sequence. The transgenes were produced as plasmids by Geneart, and were flanked by NotI and KpnI restriction enzyme sites – these leave overhangs.

(II) Transgene cloning

Transgenes were excised by NotI and KpnI restriction enzymes and cloned into a shuttle vector that contained gateway recombination sites. Gateway recombination was performed to introduce the transgenes into the ChAdOx1 bacterial artificial chromosome (BAC). Successful recombination was confirmed by sequencing the insert within the ChAdOx1 BAC. Positive clones were grown in *E. coli* (DH5α) cells for MIDI prep.

(III) ChAdOx1 vector production

Purified ChAdOx1 BAC sequences isolated through the MIDI prep were linearized by incubating with restriction enzyme PmeI. Linearized BACs were sent to the Jenner Institute Viral Vector Core Facility (VVCF) for ChAdOx1 production.

2.2.3 Cell culture

Cell banks of each cell line were established upon receipt of the cells from their different sources. Aliquots of 1 x 10^7 cells were banked at -80ºC for routine use. A selection of aliquots were tested for *Mycoplasma* and were negative.

For tumor studies, 1 x 10^7 cells were thawed into their appropriate media (see tables 2.3 and 2.4) and cultured at 37ºC with 5% CO_2. Cell were allowed to grow for 2 days before being passaged once for a further 2 days of culture prior to implantation. To passage the cells, adherent cell lines were first gently washed with PBS to remove residual cell culture media and then incubated with Trypsin-EDTA (0.25%) for 60-90 seconds in

the incubator. The activity of the trypsin was quenched by adding cell culture media, which contained FBS. At time of passage, the flasks were usually between 80-90% confluent.

2.2.4 Mouse sample collection and processing

(I) Blood

Blood was collected from mice by animal care staff through either tail vein bleed or mandibular puncture, as outlined in their standard operating procedures (SOPs). Blood was collected into a 1.5mL eppendorf tube containing ~200 units of heparin to prevent coagulation of blood. Between 100-200µl of blood was collected at any given time, in accordance with the animal protocol VRC-19-794. For serum, blood samples were collected into special serum collection tubes and centrifuged at 10,000 g for 5 minutes to separate serum from cells.

PBMCs were isolated from blood by performing two rounds of ACK lysis. To enrich the PBMC fraction, 1 mL of ACK lysis buffer (Table 2.1) was mixed with the blood samples in eppendorf tubes and then centrifuged at 600g for 10 minutes. After pelleting the PBMCs, the supernatant was aspirated off and another mL of ACK lysis buffer was added. The PBMCs were centrifuged again and supernatant aspirated. PBMCs were resuspended in 100µl of sterile PBS and then filtered through a 96-well 40µm filter plate. PBMCs were then split for peptide restimulation or tetramer staining in 96 well V-bottom plates.

(II) Spleens

To collect spleens, mice were euthanized and spleens removed by surgical excision. Spleens were placed in 1.5 mL of sterile PBS in a 24-well plate on ice, until all

spleens had been collected. Spleens were mechanically dissociated by mashing them through a 70µm filter into a 50 mL falcon tube. Single cell suspensions were centrifuged and the supernatant decanted. The samples were then incubated in 3 mL of ACK lysis buffer for 3 minutes, and then diluted by adding PBS to prevent continued cell lysis. Single cell suspensions were centrifuged, then resuspended in 5 mL of sterile PBS, and finally filtered once more through a 70µm filter. For all assays, 200µl of splenocytes were plated in 96 well V-bottom plates for antibody staining for flow cytometry.

(III) Tumor draining lymph nodes (td-LNs)

Special pestle and mortar tubes were ordered for collecting and processing tumor-draining lymph nodes (td-LNs). 150µl of sterile PBS were aliquoted into each tube. The inguinal LN (closest to the tumor) was collected by surgical excision and placed in PBS. The td-LNs were processed by mechanical dissociation using the pestle and mortar feature of the tubes. Single cell suspensions were filtered through a 96 well 40µm filter plate and centrifuged. Samples were resuspended in 200µl of PBS and 100µl of sample were transferred to 96 well V-bottom plates for antibody staining for flow cytometry.

(IV) Tumors

Miltenyi C tubes for gentlemacs cell dissociation were prepared by adding 5mL of tumor dissociation media (Table 2.5), with the exception of the collagenase. The tubes were weighed to determine their mass prior to adding tumor samples. MC38 tumors were harvested from mice and placed into the C tubes on ice. Once all tumors had been collected, the C tubes were weighed again to determine the mass of tumor for each sample. Collagenase was then added to each sample, and then the tumors mechanically dissociated by using the m_impTumor_01 program on the gentleMACS dissociator

machine. The samples were incubated in a shaking incubator for 45 minutes at 37ºC. After incubation, the samples were again run through the m_impTumor_01 program. Cell suspensions were filtered through a 70µm filter into a 50 mL falcon tube and centrifuged to remove fat and debris. The cell pellets were resuspended in 1 mL of sterile PBS, and a volume corresponding to ~30-50 mg of tumor were then transferred to a 96 well V-bottom plate for antibody staining for flow cytometry.

2.2.5 Peptide restimulation assay

To quantify the vaccine elicited CD8 T cell responses by cytokine production, isolated PBMCs or splenocytes were cultured *in vitro* with 4 µg/mL of the corresponding minimal peptide and synthetic long peptide (SLP) (Table 2.10) and 2 µg/mL of anti-CD28 (Table 2.1). Cultures were in 200µl of complete RPMI (Table 2.2) at 37ºC and 5% CO_2 for 5 hours in total. After 1 hour, 10 µg/ml of brefeldin A (Golgistop, BD, Table 2.1) was added to prevent release of cytokines from activated cells during the final 4 hours of the stimulation.

2.2.6 Serum cytokine profiling

Serum was collected from mice by tail-vein bleeding into special serum collection tubes (Microvette, Table 2.18). Once isolated, serum was frozen at -20ºC to collect all relevant sera for a given experiment prior to running ELISAs and/or a multiplexed cell bead assay (Luminex).

For IL-12 and IP-10 ELISAs, MaxiSorp ELISA plates were coated over night with 100µl of 0.50µg/mL capture antibody for desired cytokine. The next day, the capture antibody was aspirated and plates washed 4 times with 300µl of wash buffer (0.05% Tween-20 in PBS). Plates were incubated with 300µl of block buffer (1% FBS in PBS)for

1 hour. Plates were washed 4 times with 300µl of wash buffer. Serum was diluted 1:10 in diluent buffer (0.05% Tween-20, 0.1% FBS in PBS), and cytokine standards prepared according to Peprotech's protocol in diluent buffer. After washes, 100µl of standards were plated in duplicate and 100µl of samples were plated immediately after. Plates were incubated at room temperature for 2 hours. Plates were washed 4 times and then incubated with 100µl of 0.50µg/mL detection antibody in diluent for 2 hours at room temperature. Plates were washed 4 times and then incubated with Avidin-HRP conjugate for 30 minutes per Peprotech's instructions. Plates were washed 4 times and 100µl of ABTS substrate solution was added to each well. Plates were incubated at room temperature for color development and recorded on an ELISA plate reader at 405nm with correction set at 650nm.

For IFNα ELISA, plates provided in the kit were pre-coated with capture antibody. Plates were incubated with 100µl of standard, blank or sample for 1 hour at room temperature on a plate shaker (shaking at 650 rpm). Plates were washed 3 times with wash buffer (provided in the kit). Then 50µl of diluted antibody solution was added to each well for 30 minutes, again at room temperature and shaking at 650 rpm. Plates were washed 3 times with wash buffer and then incubated at room temperature for 4 minutes with 50µl of diluted HRP solution while shaking at 650 rpm. Plates were washed 5 times and then incubated for 20 minutes at room temperature in the dark with 100µl of 3,3′,5,5′-Tetramethylbenzidine (TMB) substrate. After 20 minutes, 100µl of stop solution was added to stop the reaction. Plates were read on an ELISA plate reader set to 405nm within 2 minutes of addition of stop solution.

From all ELISAs, data was exported as optical density values (OD_{450}). Empty wells were used to approximate background signal. Standards were used to calculate a standard curve and concentration of sample cytokines was calculated by interpolating the

OD_{450} values into the standard curve and then multiplying by dilution factors applied in sample preparation.

For Luminex, plates were provided in the milliplex kit (Table 2.1). Plates were first incubated with wash buffer for 10 minutes at room temperature on a plate shaker. Wash buffer was decanted and 25µl of standards or assay buffer were added to the plate. Then 25µl of appropriate matrix solution was added to each well (one specifically for each of background, standards, control, and serum sample wells). Then, 25 µl of samples were added to each sample well, followed by addition of 25µl of magnetic beads to all wells. Plate was sealed with plate sealer and incubated overnight on a plate shaker at 2-8^{o}C. Plate was then washed twice by using a plate magnet to keep beads in wells and remove supernatant. Then 25µl of detection antibody was added to each well and incubated for 1 hour at room temperature. 25µl of streptavidin-phycoerythrin was then added to each well. The plates were then sealed and incubated on a plate shaker at room temperature for 30 minutes. The plate was then washed twice by using the plate magnet to keep beads in wells and enable removal of supernatant. Beads were resuspended in 150µl of sheath fluid and run on MAGPIx instrument. Median fluorescent intensity (MFI) was recorded and xPONENT software used to calculate concentration of cytokine in original samples.

2.2.7 In vivo mouse studies

(I) Vaccinations

IM ChAdOx1 vaccinations were administered into the gastrocnemius of the right hind leg. IM SNP vaccinations were administered in the gastrocnemius of both legs. IV vaccinations were administered by heating the mice under a heat lamp for 2 minutes prior to administering the vaccine into the tail vein.

ChAdOx1 virus preparations were thawed once on ice to aliquot 1mL preparations into 100µl aliquots for routine use. The newly formed aliquots were thawed only once for use in experiments, and any excess discarded to avoid repeated freeze-thaw cycles affecting results. To prepare vaccinations, thawed ChAdOx1 was diluted in sterile PBS to reach a desired concentration, 10^8 IU per 50µl for IM vaccinations or 10^8 IU per 100µl for IV vaccinations.

SNP conjugate vaccines were prepared in sterile PBS. Concentration was adjusted to reach 32 nmol of vaccine in 100µl for IV vaccination and 8 nmol of vaccine in 100µl for IM vaccinations.

(II) Monoclonal antibodies

Mouse CD8 T cells were depleted by administering 300µg of anti-CD8 antibody (Lyt3.2) intraperitoneally (IP) 3 days and 1 day prior to tumor implantation. Mice were treated with 200µg of anti-PD-L1 (10F.9G2) given IP during tumor studies. The IFNα receptor antibody (MAR1-5A3) was administered IP at a dose of 500µg per mouse. All IP injections were 100µl.

(III) Tumor implantations and monitoring

Mice were shaved on the right flank at least 24 hours prior to implantation with tumor cells. At the end of the 4 days in culture, the cells were trypsinized and then quenched as previously described. Following quenching, the cells were washed 3 times in sterile PBS. Cells were resuspended in a known volume of PBS and counted, then adjusted such that the concentration of cells was 1 x 10^6 mL^{-1}. Mice were then anesthetized using Isoflurane and implanted subcutaneously with 10^5 cells in the right flank. Tumors were measured twice per week using digital calipers starting on day 7, which is when tumors

typically became palpable across tumor cell lines. Tumor volume was estimated by using the formula: Tumor volume = (short measurement x short measurement x long measurement)/2. Mice were euthanized when tumors reached their humane endpoints, either tumor volume exceeding 1,000 mm^3 or ulceration of the tumor.

2.2.8 Flow Cytometry staining and analysis

(I) Tetramer Stain

Single cell suspensions were prepared as described in section 2.2.4. Samples were stained in 96 well V-bottom plates beginning with 100µl of LIVE/DEAD Fixable Blue Dead Cell Stain Kit (Table 2.1) in PBS containing 50nM dasatinib for 30 minutes at room temperature to assess viability. Dasatinib enhances tetramer staining of antigen-specific CD8 T cells. Excess live/dead stain was quenched by adding 100µl of FACS buffer (Table 2.1.2V) containing 50nM dasatinib. Samples were centrifuged and supernatants flicked out of the plate. A surface stain mastermix was then prepared consisting of:

1. Anti-CD16/CD32 Fc Block (Table 2.1)
2. Brilliant stain buffer plus (Table 2.1)
3. PE conjugated tetramer
4. Fluorescently labelled antibodies (Table 2.13)
5. FACS buffer with 50nM dasatinib

Samples were stained with 100µl of the surface stain master mix for 1 hour at 4°C in the dark.

After surface stain, cells were washed in FACS buffer with 50nM dasatinib twice. Cells were fixed and permeabilized (eBioscience FoxP3 transcription factor kit (Table 2.1)) by incubating the cells in 200µl of fix/perm buffer for 20 minutes at 4°C in the dark. Following fixation and permeabilization, cells were washed once with 200µl of perm-

wash buffer. The intracellular stain master mix was prepared in perm-wash buffer and 100µl of this was used to stain the samples following the wash step. The intracellular stain was left overnight at 4^{o}C for ~12-16 hours. The intracellular stain was washed off the cells by performing 2 washes of 200µl of perm-wash buffer. The samples were resuspended in 200µl of perm-wash buffer and were ready for acquisition on the flow cytometer. After acquisition, flow data were analyzed using FlowJo v10 (Figure 2.1).

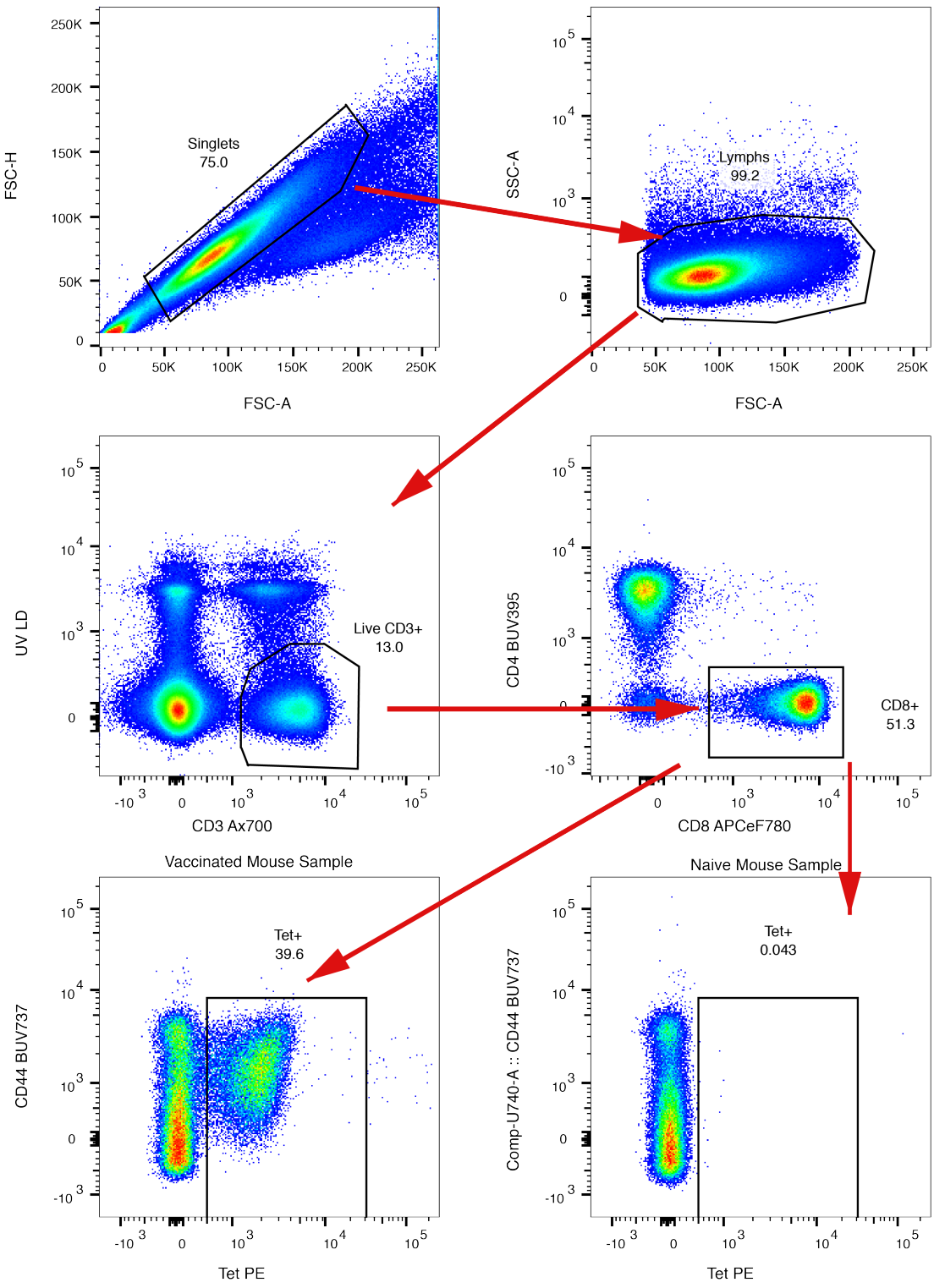

Figure 2.1 Tetramer staining example in blood. Samples are stained and gated by first identifying singlets (FSC-A against FSC-H). A lymphocytes gate removes debris and larger granulocytes that were contaminating the singlets. Then isolate the live T cells (UV LD against CD3). Subdivide the T cells into the CD4 or CD8s. Gate on the tetramer positive CD8 T cells by drawing a gate on the naïve mouse sample (bottom right panel).

(II) Cytokine Stain

Samples in a 96 well V-bottom plate are stained with 100µl of LIVE/DEAD Fixable Blue Dead Cell Stain Kit (Table 2.1) in PBS for 10 minutes at room temperature. Live/dead stain is quenched by adding 100µl FACS buffer. Samples are stained with 100µl of surface stain antibody mix containing Fc block, brilliant stain buffer, FACS buffer and fluorescently labelled antibodies (Table 2. 14) for 20 minutes at room temperature. Surface stain is washed off with FACS buffer and cells are fixed and permeabilized using 100µl of BD Cytofix/Cytoperm for 20 minutes at 4^{o}C in the dark. Samples were washed with BD perm-wash buffer and then stained with intracellular cytokine stain (ICS) antibodies in perm-wash buffer for 30 minutes at 4^{o}C in the dark. Samples were washed twice with perm-wash buffer and resuspended in 200µl of perm-wash buffer for acquisition on the flow cytometer. Example of gating is provided in Figure 2.2.

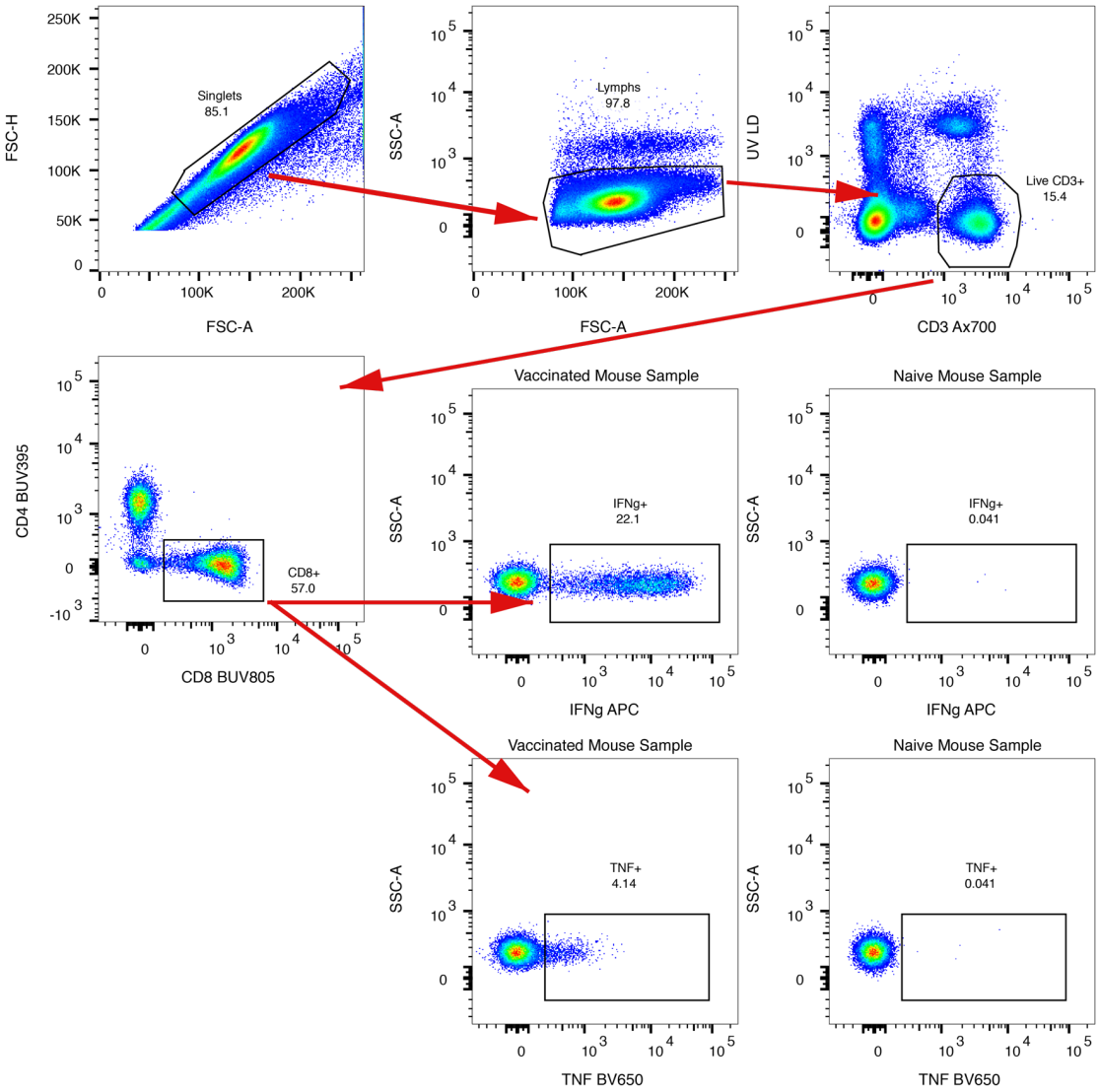

Figure 2.2 Peptide restimulation staining example in blood. Samples are stained and gated by first identifying singlets (FSC-A against FSC-H). A lymphocytes gate removes debris and larger granulocytes that were contaminating the singlets. Then isolate the live T cells (UV LD against CD3). Subdivide the T cells into the CD4 or CD8s. Gate IFNγ and TNFα producing cells by using the naïve mouse samples to determine where the positive signal begins.

(III) Mononuclear Phagocyte (MNP) stain

Samples in a 96 well V-bottom plate are stained with 100µl of LIVE/DEAD Fixable Blue Dead Cell Stain Kit (Table 2.1) in PBS for 10 minutes at room temperature. Live/dead stain is quenched by adding 100µl FACS buffer. Samples are stained with 100µl of surface stain antibody mix containing Fc block, brilliant stain buffer, FACS buffer and fluorescently labelled MNP antibodies (Table 2.15) for 20 minutes at room

temperature. Surface stain is washed off with FACS buffer and cells are washed twice with 200µl of FACS buffer. Samples are resuspended in 200µl of 0.5% paraformaldehyde (PFA) in PBS and are ready to acquire on the cytometer. Panel adapted from Baharom et al., 2021 [188].

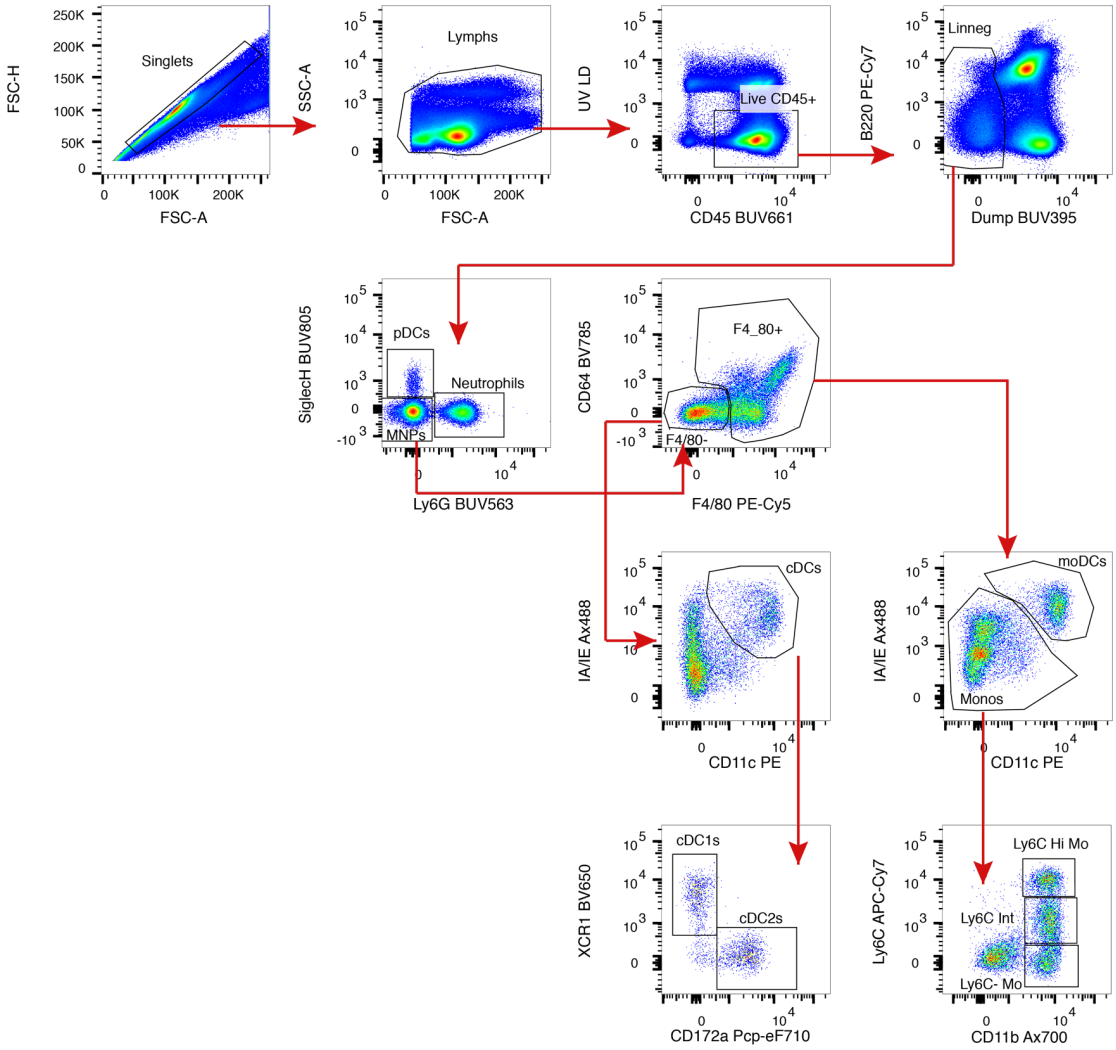

Figure 2.3 Example of MNP staining of splenocytes. Samples are stained and gated by first identifying singlets (FSC-A against FSC-H). The lymphocyte gate is used to remove debris with high SSC. Live CD45+ cells are gated. Cells expression CD3, NK1.1 and CD19 are removed through the dump channel staining. B220 cells that do not express markers in the dump channel are kept as these likely represent pDCs. The pDCs and neutrophils are separated by SiglecH and Ly6G respectively. The remaining cells are split into F4/80 positive and negative. The F4/80$^-$ fraction contains cDCs, identified by CD11c and expression of MHC II (IA/IE). The cDCs are further subdivided into cDC1s and cDC2s by XCR1 and CD172α expression respectively. The F4/80+ fraction contains monocytes and monocyte derived DCs (moDCs). The moDCs are identified by expression of CD11c and MHCII (IA/IE). The monocytes (Monos) are separated by their expression of CD11b and Ly6C.

2.2.9 Statistical analyses

Statistical analysis and visualization of data was performed using Prism v8.0 software. For comparisons of immunogenicity or frequency of response that falls into a category, two different tests were used. If the comparisons were between two groups alone, then the test was the Mann-Whitney non-parametric T test. If there were more than two groups being compared, the test used was Kruskal-Wallis with Dunn's correction for multiple comparisons. For correlations, a spearman's rank test was performed, and a line of best fit was plotted. Tumor growth curves were assessed by two-way ANOVA with Bonferroni correction for multiple comparisons. Kaplan-Meier curves were used to represent survival and statistical differences between groups were calculated by the Mantel-Cox log-rank test. All p-values are reported as exact values.

Chapter 3

Understanding the effect of route and interval on heterologous prime boosted CD8 T cell responses

3.1 Introduction

Understanding correlates of protection has always been of critical importance in screening prospective therapies for clinical use. Over the last decade, a number of immunological correlates with positive outcomes in cancer have been described, typically in the context of checkpoint inhibitors like anti-PD-1 therapy [189]. One of the reasons that patients do not respond to checkpoint inhibitors is due to a lack of tumor antigen-specific CD8 T cell responses. Vaccination has historically been a reliable method for inducing immunity against infectious diseases [137], but is in its infancy as a therapeutic intervention for cancer [190].

One of the potential targets for cancer vaccination are neoantigens. These are tumor specific and unique to each patient, and therefore would require the use of vaccine platforms that could be rapidly developed on a personalized basis. The synthetic nanoparticle peptide-TLR7/8 agonist vaccine platform (SNP) developed in the Seder lab can be rapidly developed to deliver almost any peptide as a 20-50nm nanoparticle [186]. For this reason it is well positioned to be given as a vaccine to induce T cell responses to target neoantigens. However, as it is a peptide-adjuvant vaccine, it is likely to induce low magnitude CD8 T cell responses in humans, as seen with SLP and poly-ICLC [185].

ChAdOx1 is a more potent T cell-inducing vaccine than SNP in humans, but takes longer to create personalized viral vector vaccines. For this reason, a heterologous prime boost approach may be preferred when vaccinating with these platforms if attempting to target neoantigens. This would enable a pool of neoantigen-specific CD8 T cells to be primed by SNP and ideally boosted by ChAdOx1 to a magnitude higher than would be achieved by ChAdOx1 alone.

In order to test this strategy, the neoantigen Reps1 has been created as a SNP vaccine and encoded into the ChAdOx1 vector backbone. This neoantigen is protective

against the MC38 mouse colorectal cancer cell model in both prophylactic and therapeutic settings [188]. Initial studies will focus on determining the effects of route and interval, on the resulting Reps1-specific CD8 T cell response elicited by heterologous prime boost vaccination performed with SNP and ChAdOx1.

The route of vaccination has been shown to be critical to elicit protective immune responses in TB [191] and cancer [188]. To date, ChAdOx1 has primarily been given as an intramuscular vaccine to generate adaptive immune responses against cancer by targeting prostate cancer antigens [177] and MAGE-type antigens [180]. It is possible that the IV vaccination might improve protection over the IM route as seen in other indications. If the IV route of vaccination appears promising, then the IM and IV route will be used for all studies as the IM route is the standard. If, however, the IV route is less immunogenic than IM, then the IV groups will be dropped in follow up studies.

Initially, screening will be done by assessing immunological markers of T cell responses. These include the magnitude of the CD8 T cell response, the quality of the response and the cytokine production ability of the elicited cells. These will be described in greater detail in the results chapter.

3.2 Chapter Aims

1. To evaluate the effect of vaccination route on magnitude and quality of antigen-specific CD8 T cells elicited by ChAdOx1 vaccination, either alone or as a boost.
2. To evaluate the effect of interval between prime and boost on CD8 T cell responses following heterologous prime boost vaccination with SNP and ChAdOx1.
3. To determine the efficacy of T cell responses generated by heterologous prime boost and compare these against either platform alone.

3.3 Results

3.3.1 IV ChAdOx1 primes higher magnitude CD8 T cell responses with a more terminal effector phenotype than IM vaccination 14 days after vaccination

Mice were vaccinated either IM or IV with 10^8 infectious units (IU) of ChAdOx1 encoding the neoantigen Reps1. Blood was sampled from these mice 2 weeks and 16 weeks post vaccination to assess T cell responses at a predicted peak and memory time point (Figure 3.1A). Reps1-specific CD8 T cells were identified by tetramer staining or cytokine staining for IFNγ and TNFα following peptide restimulation with the Reps1 long peptide and predicted minimal epitope (Figures 3.1B, 3.1C). Blood sampling enables the tracking of CD8 T cell responses over time as it is non-lethal, however does not provide any tissue level information. To assess tissue presence of antigen-specific CD8 T cells, a subset of mice were sacrificed at both time points to assess responses in spleen using the same assays.

In both blood and spleens sampled 2 weeks after vaccination, the IV route of vaccination elicited a higher magnitude CD8 T cell response based on tetramer staining (Figure 3.1D). In addition to the higher magnitude, IV ChAdOx1 elicited CD8 T cells appear to express higher levels of eomesodermin (Eomes) and PD-1 as shown in the overlaid histograms (Figure 3.1E). One way to quantify this is by plotting the median fluorescence intensity (MFI) of these markers on the Reps1-tetramer specific CD8 T cells for each sample. There is a significantly higher expression of PD-1 and Eomes on IV elicited CD8 T cells in both blood (p-values <0.001) and spleen (p-values = 0.0011 and 0.0148, respectively) (Figure 3.1F). Higher expression of Eomes and PD-1 is associated with a more terminally differentiated T cell phenotype [192].

Another feature of more terminally differentiated CD8 T cell responses is a lower frequency of polyfunctional cells. Polyfunctionality is the production of multiple

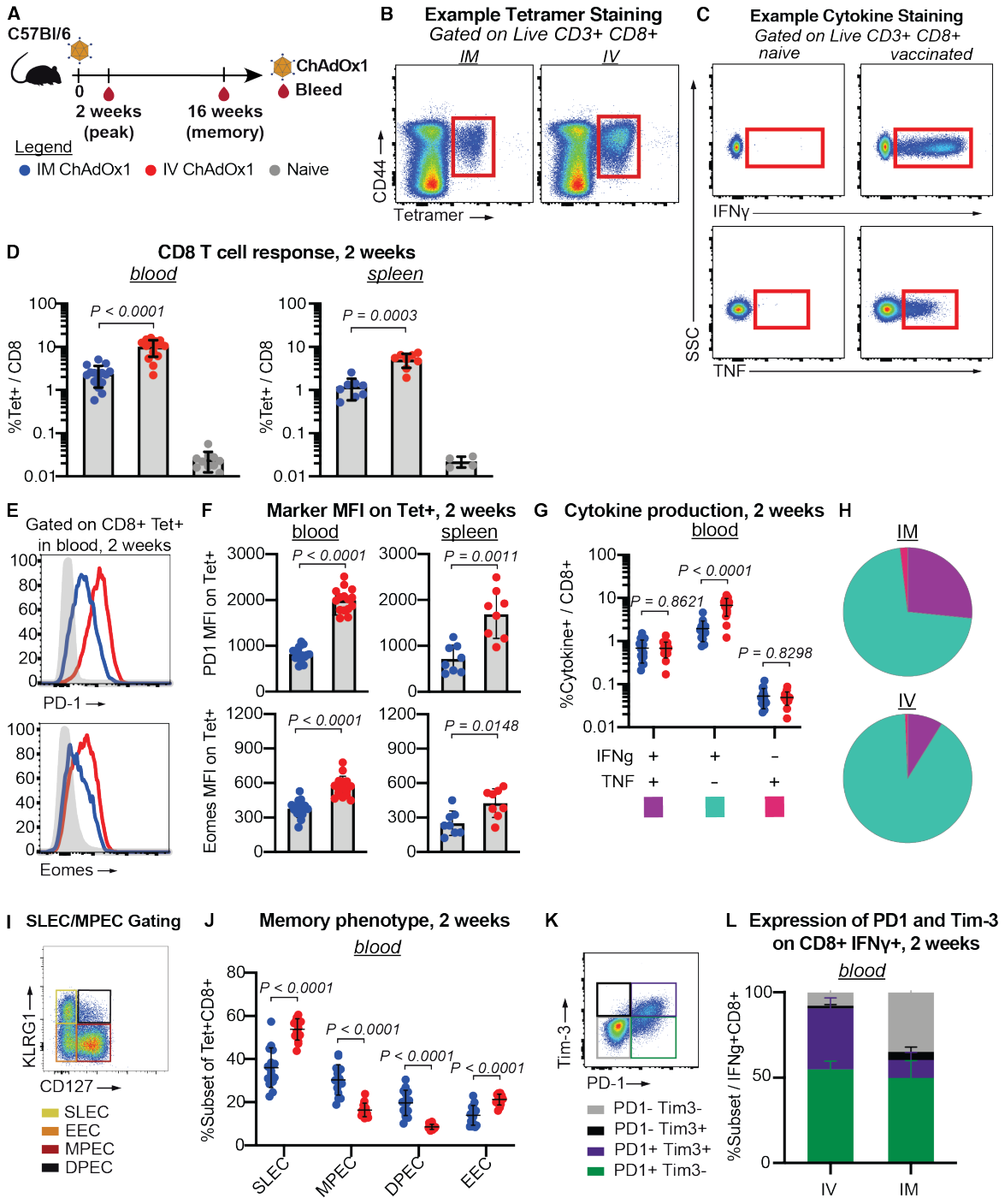

Figure 3.1 IV ChAdOx1 induces a higher magnitude neoantigen-specific CD8 T cell response with a more terminal effector phenotype than IM vaccination. (**A**) Immunogenicity study vaccination and sampling schedules, legend for entire figure. (**B**) Example Reps1 tetramer staining on CD8 T cells. (**C**) Example of IFNγ and TNFα staining of peptide restimulated PBMCs. (**D**) Immunogenicity 2 weeks after either IV or IM ChAdOx1 vaccination, measured by tetramer staining. (**E**) Histograms of the expression of PD-1 and Eomes on tetramer positive cells, overlaid with naïve CD8 T cells in gray. (**F**) MFI of PD-1 and Eomes on Reps1-tetramer positive cells in blood and spleen. (**G**) Frequency of IFNγ and TNFα co-producers following peptide restimulation detected by flow cytometry. (**H**) Pie charts showing proportion of response corresponding to cytokine production groups. (**I**) Gating strategy for SLECs/MPECs. (**J**) Frequency of tetramer positive cells that falls into each of the SLEC/MPEC categories. (**K**) Gating strategy on representative flow plot of Tim-3/PD-1 on stimulated CD8 T cells. (**L**) Proportion of IFNγ+ cells in each co-inhibitory receptor subset. **Stats: (D, F, G, J)** Data represented as mean ± SD, Mann-Whitney test.

cytokines by T cells following peptide restimulation. It is possible to assess route based differences in polyfunctionality by comparing the frequency of IFNγ and TNFα co-producers between the IV and IM vaccinated groups. In this case, there is a similar frequency of IFNγ and TNFα co-producers (polyfunctional cells) between the IV and IM vaccinated groups ($p = 0.8621$). However, there is a much higher frequency of IFNγ single producers in the IV vaccinated group as compared to the IM group in blood and spleen ($p < 0.0001$) (Figure 3.1G). When the data is shown as a pie chart, it is clear that a much smaller percentage of the response elicited by the IV route is polyfunctional relative to the total response generated (Figure 3.1H). This indicates a more terminally differentiated T cell response and is concordant with the increased Eomes and PD-1 expression. There was a very low frequency of TNFα single producers and it was equivalent between vaccine groups.

CD8 T cell responses have also been characterized by their expression of CD127 and KLRG1 (Figure 3.1I). The two most well studied subsets of antigen-specific CD8 T cells based on CD127 and KLRG1 are the memory precursor effector cells (MPECs, $CD127^+$ $KLRG1^-$) and the short-lived effector cells (SLECs, $CD127^-$ $KLRG1^+$) [193]. These were originally described in models of acute and chronic infection as having distinct memory forming capacities. The SLECs are thought to be too differentiated to become memory T cells, and MPECs represent a reservoir of effector cells with some capacity to become memory. Follow-up experiments have characterized the double negative population ($CD127^-$ $KLRG1^-$) as a transitory state between the MPEC and SLEC phenotypes known as early effector cells [194]. The double positive (CD127+ KLRG1+) cells have not been well studied and have been designated as double positive effector cells (DPECs). In comparing the IV and IM elicited CD8 T cell responses, the largest difference is in the proportion of SLECs and MPECs, though there are statistically significant

differences across all 4 subsets ($p < 0.0001$). IV vaccination elicits a greater frequency of SLECs as compared to IM, and the opposite pattern is true of MPECs (Figure 3.1J). This further supports the idea that the IV route elicits a more terminally differentiated CD8 T cell response than the IM route of vaccination when using ChAdOx1.

More recently, it has been suggested to look at the co-expression of co-inhibitory markers on T cells activated by peptide restimulation. The theory is that upregulation of multiple co-inhibitory receptors may indicate that these cells are more differentiated or exhausted. To this end, the co-expression of Tim-3 and PD-1 was assessed on IFNγ producing cells following peptide re-stimulation (Figure 3.1K). The IFNγ producing CD8 T cells elicited by the IV route had higher co-expression of these markers as compared to the IM elicited cells (Figure 3.1L). In addition, the IM elicited cells had a greater frequency of IFNγ producers that expressed neither Tim-3 nor PD-1, which may indicate they are less exhausted.

Given that the Reps1 peptide encoded in ChAdOx1 was 25 amino acids long, it is possible that it contained an MHC II epitope and could generate CD4 T cell responses. Peptide restimulation of PBMCs would cause these antigen-specific CD4 T cells produce IFNγ. Based on the flow cytometry data, there were no CD4 T cell responses detected after vaccination with ChAdOx1 by either route (data not shown).

3.3.2 IV elicited CD8 T cell responses are more stable over time, despite having a more terminally differentiated phenotype.

Characterizing the magnitude and phenotype of CD8 T cell responses elicited by IV or IM ChAdOx1 over time may provide insights into the longevity of the T cell response and memory formation. Mice were kept for 16 weeks, then bled and sacrificed for T cell analysis as described previously (Figure 3.2A). Interestingly, the magnitude of

the CD8 T cell response remained remarkably high in the blood and spleen over the 16 week period in the IV vaccinated group (Figure 3.2B). The average response in blood (frequency of CD8 that are Reps1-tetramer positive) at 2 weeks and 16 weeks for the IV group was 10.11% and 6.34%, respectively. This is a drop of ~37%. By comparison, the IM group dropped from an average of 2.37% to 0.47%, indicating a drop of ~80%. This indicates that the IV response may be more stable over time, despite having a more terminally differentiated phenotype as previously described. It is also striking that after 16 weeks, the magnitude of the response by the IV route is on average higher than the peak magnitude achieved by the IM route.

As the frequency of antigen-specific CD8 T cell responses was so low in the blood in the IM group, it was difficult to capture sufficient events to make meaningful phenotypic comparisons between both routes. For this reason, downstream analyses focus on the response in the spleen, where though the frequency is still low, there were ~10-fold more cells per sample than in the blood.

The Reps1-specific CD8 T cells elicited by the IV route maintain a higher expression of Eomes and PD-1 at the 16 week time point (p-value = 0.0064 and < 0.0002, respectively) as seen previously at the peak magnitude (Figure 3.2C). In contrast to the 2 week time point, there is now a higher magnitude of polyfunctional cells in the IV group as compared to the IM group (Figure 3.2D, p = 0.0019). As before, there is a higher magnitude of IFNγ single producers in the IV group compared to the IM group (p = 0.0002). When displayed as a proportion of the response, the breakdown is more similar to the 2-week time point, whereby a smaller proportion of the total response in the IV vaccinated group is polyfunctional as compared to the IM (Figure 3.2E). In addition, the TNFα single producers appear to be a higher percentage of the IM vaccinated response. This is likely an artefact of higher background TNFα staining, as evidenced by the

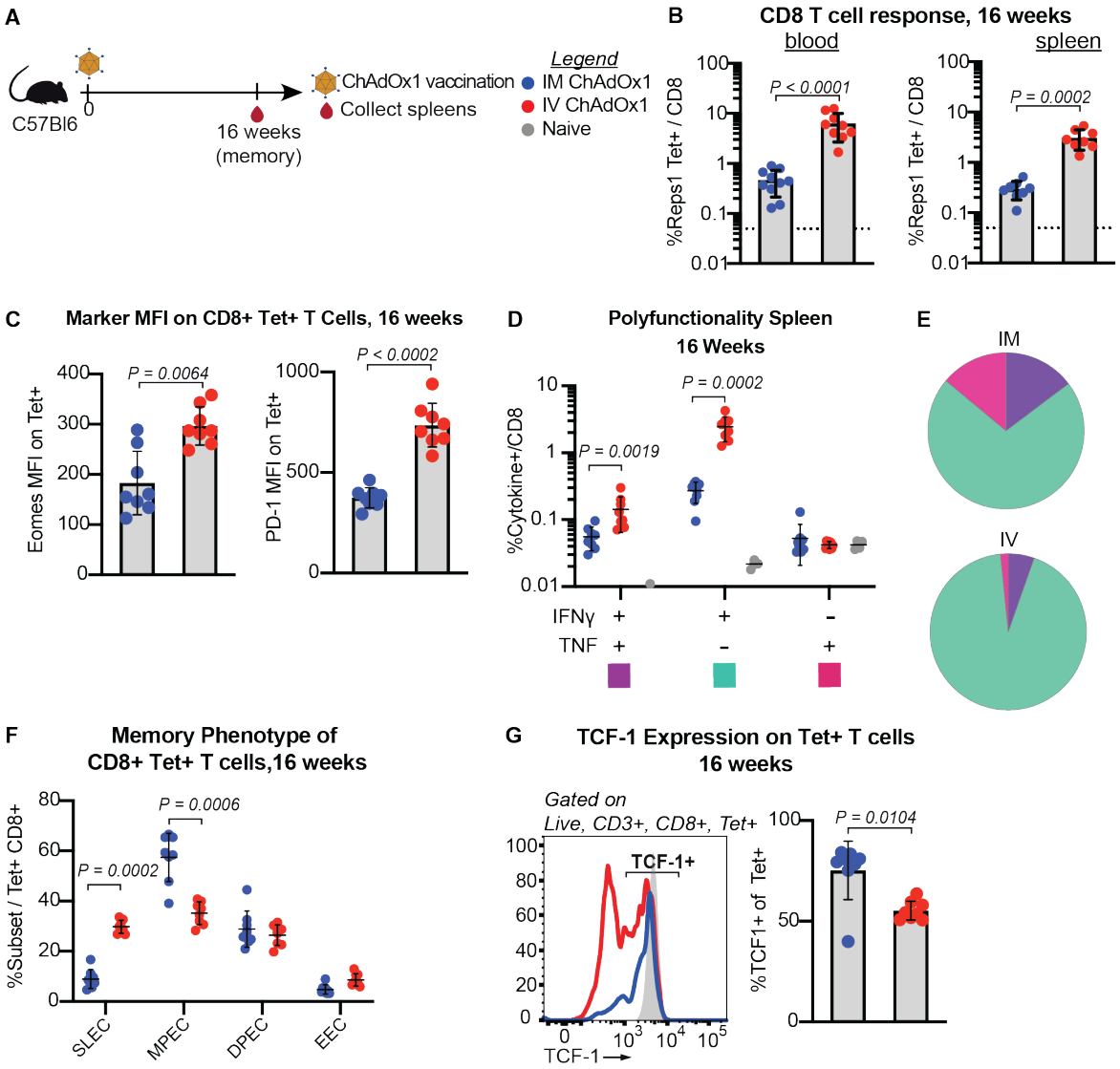

Figure 3.2 IV ChAdOx1 elicited CD8 T cell responses are more stable over time, despite having a more terminally differentiated phenotype. (**A**) Immunogenicity study vaccination and sampling schedule, legend for entire figure. (**B**) Immunogenicity 2 weeks after either IV or IM ChAdOx1 vaccination, measured by tetramer staining in blood and spleen. (**C**) MFI of PD-1 and Eomes on Reps1-tetramer positive cells in spleen. (**D**) Frequency of IFNγ and TNFα co-producers following peptide restimulation of splenocytes detected by flow cytometry. (**E**) Pie charts showing proportion of response corresponding to cytokine production groups. (**F**) Frequency of tetramer positive cells that falls into each of the SLEC/MPEC categories. (**G**) **Stats: (B, C, D, F, G)** Data represented as mean ± SD, Mann-Whitney test.

frequency of TNFα single producers in the naïve group (Figure 3.2D). As the total frequency of cells is lower in the IM group, then the background staining makes up a greater proportion of cytokine producing cells in the IM pie chart. However, this does not affect the overall trend observed.

In addition to the stable magnitude and more terminally differentiated phenotype, the IV elicited cells maintained a more SLEC-like phenotype as compared to the IM elicited cells ($p = 0.0002$) (Figure 3.2F). The opposite trend was seen with MPECs and in concordance with the observations at 2 weeks ($p = 0.0006$). There were no statistically significant differences between the EECs and DPECs between the two routes tested at 16 weeks.

As antigen-specific CD8 T cells begin to transition towards a memory phenotype, they upregulate TCF-1 [195]. IV elicited antigen-specific CD8 T cells appear to have a bimodal peak of TCF-1 expression as seen in the histogram (Figure 3.2G). By comparison, the IM elicited CD8 T cells appear to have a single peak with a tail skew that represents a minority of cells that have not re-expressed TCF-1 at this time point. For reference, a naïve CD8 T cell population ($CD62L^+$ $CD44^-$) is used to provide an example of 100% TCF1+ cells in the grey filled peak on the histogram. The bar graph quantifies the percentage of Reps1-specific CD8 T cells that express TCF-1 in the spleen, and there is a significant difference between the IV and IM route of vaccination ($p = 0.0104$).

The long-term expression of PD-1 and Eomes, the high proportion of IFNγ single producers, the stability of the SLEC-like phenotype, and the existence of a distinct TCF-1 negative population that makes up ~50% of the response 16 weeks after vaccination all suggest that the response following IV ChAdOx1 vaccination may be more akin to one elicited by chronic infection. It is possible that systemic infection of cells that are long lived enabled by IV administration of ChAdOx1 leads to prolonged production and

presentation of the antigens and provides the chronic antigen stimulation that may be required to produce these qualities in T cell responses.

3.3.3 The route of SNP priming does not affect magnitude or quality of CD8 T cells after ChAdOx1 boost by either IM or IV route.

The effect of ChAdOx1 vaccination route on the magnitude and quality of CD8 T cell responses has been clearly demonstrated when used as a stand-alone vaccine. Given the dramatic effect of route, it was important to assess how route of prime and boost vaccinations impacts the magnitude and quality of the CD8 T cell response elicited by heterologous prime boost. To this end, mice were primed with SNP providing the Reps1 antigen either IM or IV. The IM SNP vaccinations provided 8 nmol of antigen, whereas the IV vaccination was dosed at 32 nmol. This was based on previous data demonstrating that SC vaccination with SNP using 8 nmol yielded approximately similar magnitude CD8 T cell responses as 32 nmol IV, though it is not currently understood why a higher dose is required for the IV route [188]. These mice were sampled 7 days post vaccination to compare CD8 T cell responses. ChAdOx1 was used either IV or IM to boost mice 14 days after the SNP prime. These mice were then sampled 14 days after boost to determine the effect of ChAdOx1 route on boosting of responses (Figure 3.3A).

The effect of route of vaccination on SNP primed responses has been previously described by Baharom and colleagues (Nat. Immunology, 2021). However, they only compared the subcutaneous (SC) route and the IV route, but did not test the IM route of vaccination with SNP. In this study, responses were primed with SNP IM or IV. With SNP vaccination, the IM route of vaccination elicited a higher magnitude CD8 T cell response as compared to the IV route ($p < 0.0001$) (Figure 3.3B). In addition, the expression of Eomes was higher on cells elicited by IM SNP as compared to IV SNP ($p <$

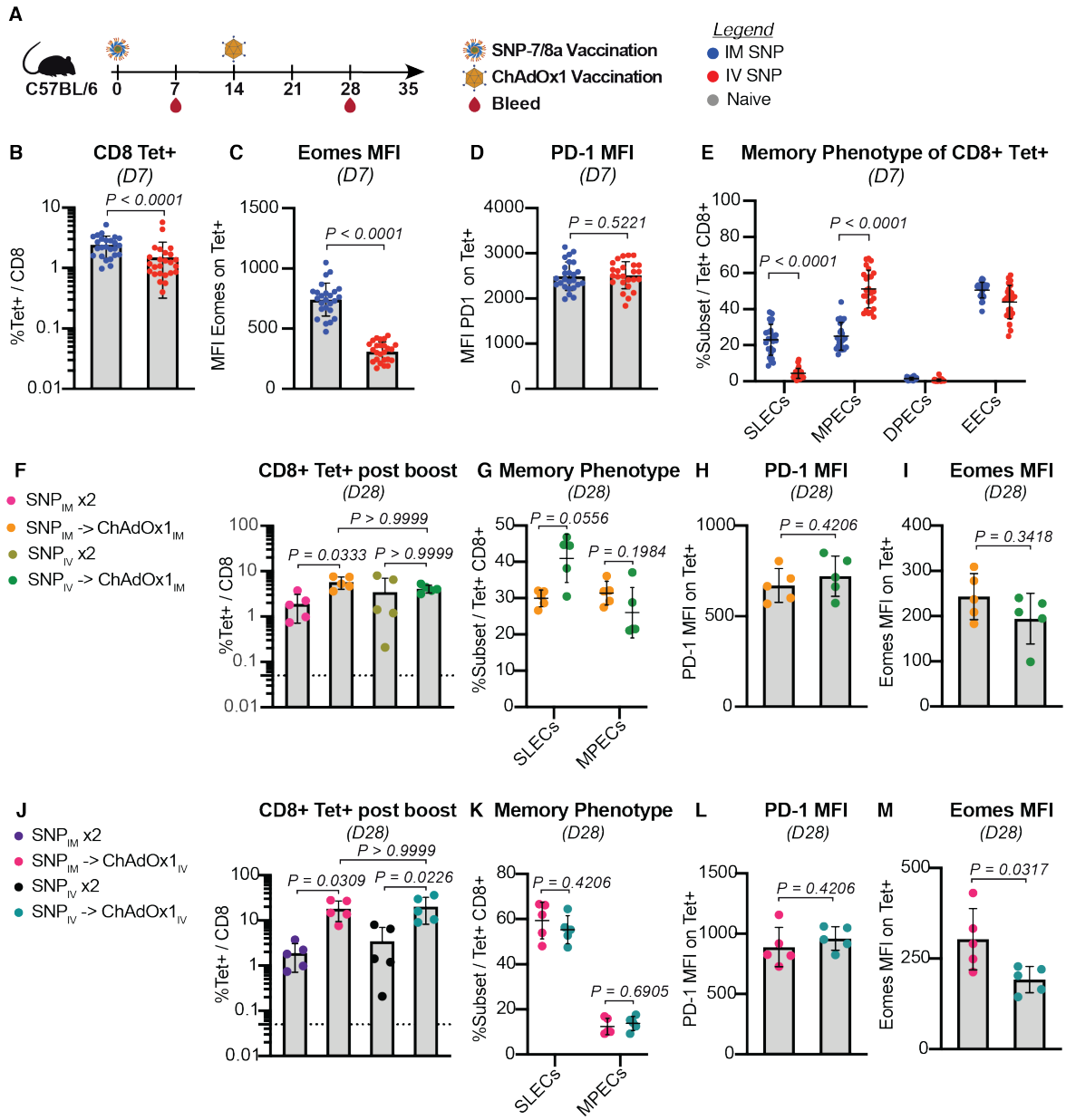

Figure 3.3 Route of SNP priming does not affect magnitude or quality of CD8 T cells after ChAdOx1 boost by either IM or IV route. (**A**) Immunogenicity study vaccination and sampling schedule, legend for panels (**B-E**). (**B**) Immunogenicity 1 week after either IV or IM SNP vaccination, measured by tetramer staining. (**C,D**) MFI of (**C**) Eomes and (**D**) PD-1 on Reps1-tetramer positive cells in blood 7 days after SNP prime. (**E**) Frequency of tetramer positive cells that falls into each of the SLEC/MPEC categories 7 days after SNP prime. (**F**) Legend for panels **F-I** and Reps1-tetramer magnitude 2 weeks post IM ChAdOx1 boost. (**G**) SLEC/MPEC frequency of heterologous prime boost group elicited Reps1-specific CD8 T cells. (**H,I**) MFI of (**H**) PD-1 and (**I**) Eomes on Reps1-tetramer positive cells in blood. (**J**) Legend for panels **J-M** and Reps1-tetramer magnitude 2 weeks post IV ChAdOx1 boost. (**K**) SLEC/MPEC frequency of heterologous prime boost group elicited Reps1-specific CD8 T cells. (**L,M**) MFI of (**L**) PD-1 and (**M**) Eomes on Reps1-tetramer positive cells in blood. **Stats: (B-E, G-I, K-M)** Data represented as mean ± SD, Mann-Whitney test. **(F,J)** Data represented as mean ± SD, Kruskal-Wallis test with Dunn's correction for multiple comparisons.

0.0001) (Figure 3.3C). These trends are the exact opposite of what was seen with ChAdOx1 vaccination in figure 3.2, but are very similar to the differences seen between SC and IV SNP vaccination [188]. However, there was no difference in the expression of PD-1 at this time point (p-value = 0.5221) (Figure 3.3D). In addition, the distribution of SLECs and MPECs in the IM/IV SNP groups was similar to the published SC/IV distributions, with IM eliciting more SLEC-like cells and IV eliciting more MPECs ($p < 0.0001$) (Figure 3.3E). Again, this trend is the opposite of that seen with ChAdOx1. Overall, there are clear differences in both quality and magnitude when CD8 T cells are primed by IV or IM SNP, and this may affect boosting with ChAdOx1.

Reps1-specific CD8 T cells elicited by SNP given IM or IV were boosted with ChAdOx1 given IM. There was no difference in the magnitude achieved 2 weeks post boost based on the route of SNP prime ($p > 0.9999$) (Figure 3.3F). IM ChAdOx1 boosting only increased magnitude as compared to IM SNP given twice ($p = 0.0333$), but not compared to IV SNP given twice ($p >0.9999$). There were no statistically significant differences in any of the qualitative markers (SLECs/MPECs, eomes expression, PD-1 expression) used to compare responses following IM ChAdOx1 boost of IM or IV SNP primed responses (Figure 3.3G-I). Overall these data suggest that the route of SNP priming may not significantly affect the magnitude or phenotype of antigen-specific cells following IM ChAdOx1 boost, or perhaps better stated, the route of the boost vaccination is the determining factor of magnitude and quality.

The same analysis was done to assess magnitude and quality of IV ChAdOx1 boosted cells. Heterologous prime boost using IV ChAdOx1 elicited higher magnitude responses than IM SNP or IV SNP given twice ($p = 0.0309$ and 0.0226, respectively) (Figure 3.3J). However, the route of prime did not affect the magnitude achieved following IV ChAdOx1 boost ($p > 0.9999$). Similarly to the IM ChAdOx1 boosted cells,

the IV boosted cells showed no qualitative difference in the proportion of cells classified as SLECs/MPECs or in their expression of PD-1 (Figure 3.3K-L). IM SNP primed responses had a slightly higher level of expression of eomes as compared to IV SNP primed responses following IV ChAdOx1 boost ($p = 0.0317$) (Figure 3.3M).

Collectively, these data suggest that the route of SNP priming has a very minimal impact on the magnitude and quality of antigen-specific CD8 T cell response elicited by heterologous prime boost.

3.3.4 Interval between prime and boost does not affect peak magnitude, but heterologous prime boost improves polyfunctionality for IV ChAdOx1 boosted cells.

The interval between prime and boost vaccinations has been shown to significantly impact the immune response generated against infectious diseases [196]. In order to determine the effect of interval on CD8 T cell responses elicited by SNP-ChAdOx1 heterologous prime boost, mice were primed with SNP in a staggered manner either 4-, 2- or 1- week(s) prior to boosting with ChAdOx1. Given that the route of priming did not have a significant impact on magnitude and quality of the antigen-specific CD8 T cell responses following ChAdOx1 boost (Figure 3.3), and that the IV route of administration is preferred for SNP, all mice received IV SNP vaccinations. Mice were bled at the time of boost in order to determine differences in magnitude of SNP primed responses based on time elapsed from vaccination. The mice were bled 1, 2, 4, 8, and 16 weeks after ChAdOx1 boost. ChAdOx1 was administered both IM and IV to understand the effect of interval and route on antigen-specific CD8 T cell responses (Figures 3.4A and 3.5A).

The complete kinetic of the Reps1-specific CD8 T cell response following heterologous prime boost using IM ChAdOx1 is displayed in figure 3.4B. Surprisingly, at the time of boost, the magnitude of the Reps1-specific CD8 T cell responses were

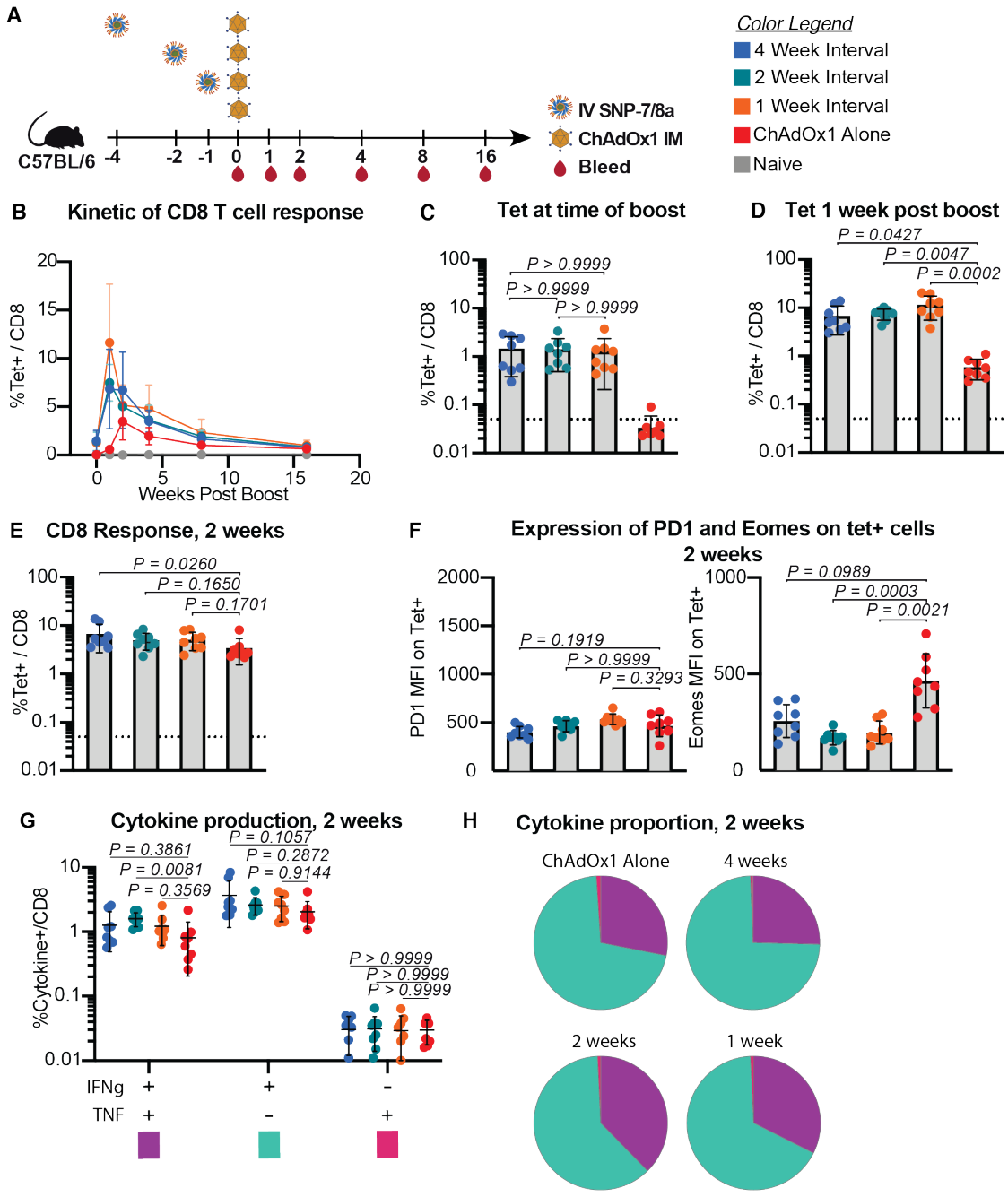

Figure 3.4 Interval between prime and IM ChAdOx1 boost does not affect magnitude or quality of CD8 T cell response. (**A**) Immunogenicity study vaccination and sampling schedule, legend for entire figure. (**B**) Kinetic of CD8 T cell response over 16 weeks starting at time of boost, measured by tetramer staining. (**C**) Reps1-tetramer response after priming, at time of boost. (**D**) Reps1-tetramer response 1 week post boost. (**E**) Reps1-tetramer response 2 weeks post boost. (**F**) MFI of PD-1 and Eomes on Reps1-tetramer positive cells in blood 2 weeks post boost. (**G**) Frequency of IFNγ and TNFα co-producers following peptide restimulation of PBMCs 2 weeks post boost detected by flow cytometry. (**H**) Pie charts showing proportion of response corresponding to cytokine production groups. **Stats: (C-G)** Data represented as mean ± SD, Kruskal-Wallis test with Dunn's correction for multiple comparisons.

equivalent between all groups that received an IV SNP prime ($p > 0.9999$), regardless of how much time had elapsed between the vaccination and sampling (Figure 3.4C). The only time point at which SNP prime appears to increase magnitude of the Reps1-specific CD8 T cell response relative to no-prime IM ChAdOx1 vaccination is 7 days post boost. At this time point, there is no difference in the peak magnitude between the different interval SNP prime groups, but all heterologous prime boost groups are significantly different to IM ChAdOx1 alone (Figure 3.4D). By 14 days post boost, the heterologous prime boost groups are not significantly different to the magnitude achieved by IM ChAdOx1 alone, except for the 4-week interval ($p = 0.0260$) (Figure 3.4E). At all time points after 2 weeks post boost, there are no statistically significant differences between the heterologous prime boost groups and IM ChAdOx1 alone.

In addition to understanding the effect of interval on magnitude, it was important to determine if there were any qualitative differences in the Reps1-specific CD8 T cell response following heterologous prime boost as compared to using IM ChAdOx1 alone. The frequency of Reps1-specific CD8 T cells 7 days post IM ChAdOx1 alone was very low and not suitable for comparison. There were no significant differences in the expression of PD-1 between heterologous prime boost groups and IM ChAdOx1 at 2 weeks post boost (Figure 3.4F). The 1- and 2- week interval groups did however have a lower expression of eomes as compared to IM ChAdOx1 alone. Together, these data do not clearly indicate if any group is more terminally differentiated than the others based on the marker expression. In addition, the polyfunctionality of the Reps1-specific CD8 T cell response was assessed and there was only one statistically significant difference between the 2-week interval group and IM ChAdOx1 alone ($p = 0.0081$) in terms of the frequency of polyfunctional CD8 T cells (Figure 3.4G). This higher magnitude polyfunctional response is reflected in the higher proportion of the total response that is polyfunctional in

figure 3.4H. However, the differences in proportion are not particularly striking. This further indicates that no group is more terminally differentiated than any of the others or IM ChAdOx1 alone, therefore when boosting with IM ChAdOx1 the interval between prime and boost seems to have little effect on magnitude or quality of the Reps1-specific CD8 T cell response.

The effect of interval between prime and boost was also assessed when using ChAdOx1 IV, and a complete kinetic is provided in figure 3.5B. In the kinetic, it appears as though the IV heterologous prime boost elicits a higher magnitude response, regardless of interval, over the first 4 weeks, and then coalesces with the IV ChAdOx1 alone group at weeks 8 and 16. As seen previously, there were no significant differences in the magnitude of Reps1-specific CD8 T cell responses following the staggered IV SNP prime vaccinations as they all had the same magnitude at the time of boost (Figure 3.5C). All heterologous prime boost groups had a higher magnitude response 7 days post boost as compared to IV ChAdOx1 alone given at time of boost (Figure 3.5D). However, at 2 weeks post boost, the responses in the 2- and 1- interval groups is not significantly different to the IV ChAdOx1 alone (Figure 3.5E).

In contrast to the IM heterologous prime boost groups, the IV heterologous prime boost groups all had decreased expression of Eomes and PD-1 as compared to IV ChAdOx1 alone 2 weeks post vaccination (Figure 3.5F). This indicates that though the magnitude of the response trends towards being higher, the cells following IV heterologous prime boost are less terminally differentiated at this time point and may be more functional. To corroborate these finding, polyfunctionality was assessed and all three intervals were found to elicit a higher frequency of polyfunctional cells following IV ChAdOx1 boost as compared to IV ChAdOx1 vaccination alone (Figure 3.5G). IFNγ single producers were also significantly different in the 4- and 1- week interval groups as

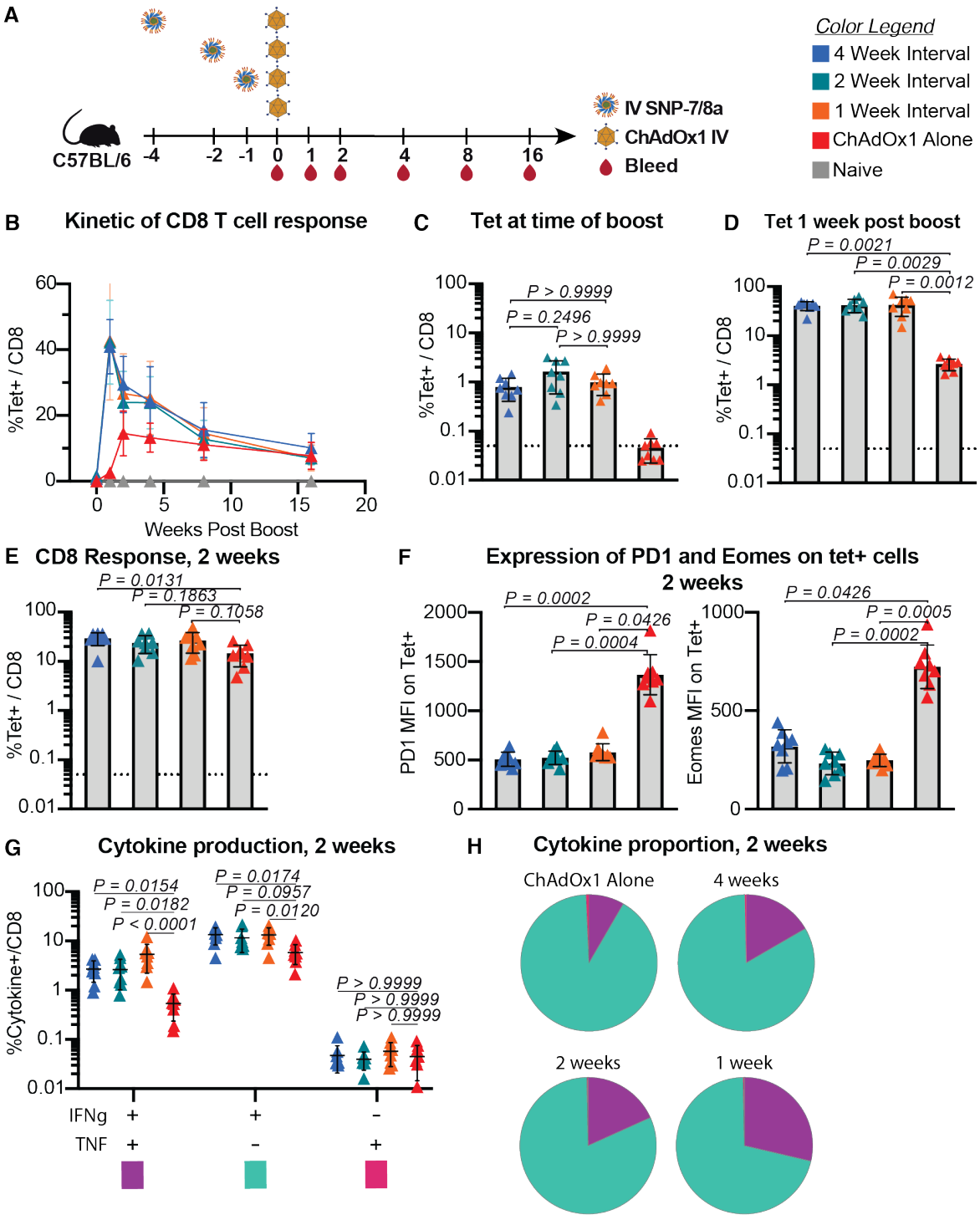

Figure 3.5 Interval between prime and IV ChAdOx1 boost does not affect magnitude or quality of CD8 T cell response. (A) Immunogenicity study vaccination and sampling schedule, legend for entire figure. **(B)** Kinetic of CD8 T cell response over 16 weeks starting at time of boost, measured by tetramer staining. **(C)** Reps1-tetramer response after priming, at time of boost. **(D)** Reps1-tetramer response 1 week post boost. **(E)** Reps1-tetramer response 2 weeks post boost **(F)**MFI of PD-1 and Eomes on Reps1-tetramer positive cells in blood 2 weeks post boost. **(G)** Frequency of IFNγ and TNFα co-producers following peptide restimulation of PBMCs 2 weeks post boost detected by flow cytometry. **(H)** Pie charts showing proportion of response corresponding to cytokine production groups. **Stats: (C-G)** Data represented as mean ± SD, Kruskal-Wallis test with Dunn's correction for multiple comparisons.

compared to IV ChAdOx1 alone ($p = 0.0174$ and 0.0120, respectively) but not significantly different in the 2-week interval group. These differences in functionality are represented by an approximate doubling of the proportion of cells that are polyfunctional in the 4- and 2- week interval groups and a tripling of the proportion in the 1-week interval group (Figure 3.5H).

Collectively, the data presented in figures 3.6 and 3.7 suggest that the interval between SNP prime and ChAdOx1 boost has little to no effect on the magnitude and quality of the antigen-specific response elicited, regardless of the route of boosting. The SNP prime enables a rapid expansion of antigen-specific CD8 T cells following both IM and IV ChAdOx1 boost as evidenced by the difference in magnitude between heterologous prime boost groups and ChAdOx1 alone 7 days post vaccination. However, this difference in magnitude (based on tetramer) is transient for both routes of boosting and disappears by 2-weeks post vaccination. Interestingly, SNP priming of responses does not alter the phenotype or polyfunctionality of the CD8 T cell response following IM ChAdOx1 boost, but does affect the phenotype and cytokine production of IV ChAdOx1 boosted cells as compared to IV ChAdOx1 alone. Finally, the magnitude of the CD8 T cell response achieved by IV ChAdOx1 16 weeks post vaccination is still higher than peak IM ChAdOx1 vaccination in all groups except the 1-week interval, which is a similar trend to what was seen in Figure 3.2.

3.3.5 IV heterologous prime boost elicits the highest magnitude CD8 T cell response and displays improved protection from MC38 tumor challenge

Though the effect of route and interval on heterologous prime boost elicited CD8 T cell responses had been characterized in depth on an immunological level, the T cells had not been tested for their ability to protect from tumor challenge. To test the efficacy of the

heterologous prime boost elicited cells, a prophylactic study was undertaken, whereby mice were primed with SNP and then boosted with ChAdOx1 at a 2 week interval. The mice were then challenged with the MC38 mouse colorectal cancer cell line 2 weeks after the ChAdOx1 vaccination. The mice were sampled for blood to assess T cell responses 7 days post prime and at the time of tumor challenge. In addition to the tumor challenge, the mice would be given a single dose of checkpoint inhibitor – in this case αPD-L1 (Figure 3.6A). IV SNP prime and boost was used as a reference group, given that the expected level of protection is known from previous studies in the lab. All three groups that received a SNP prime had equivalent responses at D7 (Figure 3.6B).

At D28 (time of challenge), the IV ChAdOx1 boosted group had the highest magnitude Reps1-specific CD8 T cell response, and was significantly different to both the IV ChAdOx1 alone ($p = 0.0144$) and the IM ChAdOx1 boosted group ($p < 0.0001$) (Figure 3.6C). There was no difference in magnitude between the SNP primed – IM ChAdOx1 boosted group and the IM ChAdOx1 alone group in terms of magnitude ($p >0.9999$). Interestingly, in this instance the IV ChAdOx1 alone group was not significantly higher than the IM ChAdOx1 alone group ($p = 0.2532$), though this may be due to the use of different statistical tests. In figure 3.2, there were only two groups, so they were compared by using a Mann-Whitney test, whereas in this study it was compared by Kruskal-Wallis with Dunn's correction for multiple comparisons.

In addition to tetramer data, the polyfunctionality of the different groups was assessed and was concordant with the observations made in figures 3.4 and 3.5. The SNP prime – IM ChAdOx1 boosted cells were not significantly different to IM ChAdOx1 alone group, whereas the SNP primed – IV ChAdOx1 boosted group had a higher frequency of both polyfunctional and IFNγ single producers as compared to the IV ChAdOx1 alone group (Figure 3.6D). As there were no differences in TNFα single producers, that data has

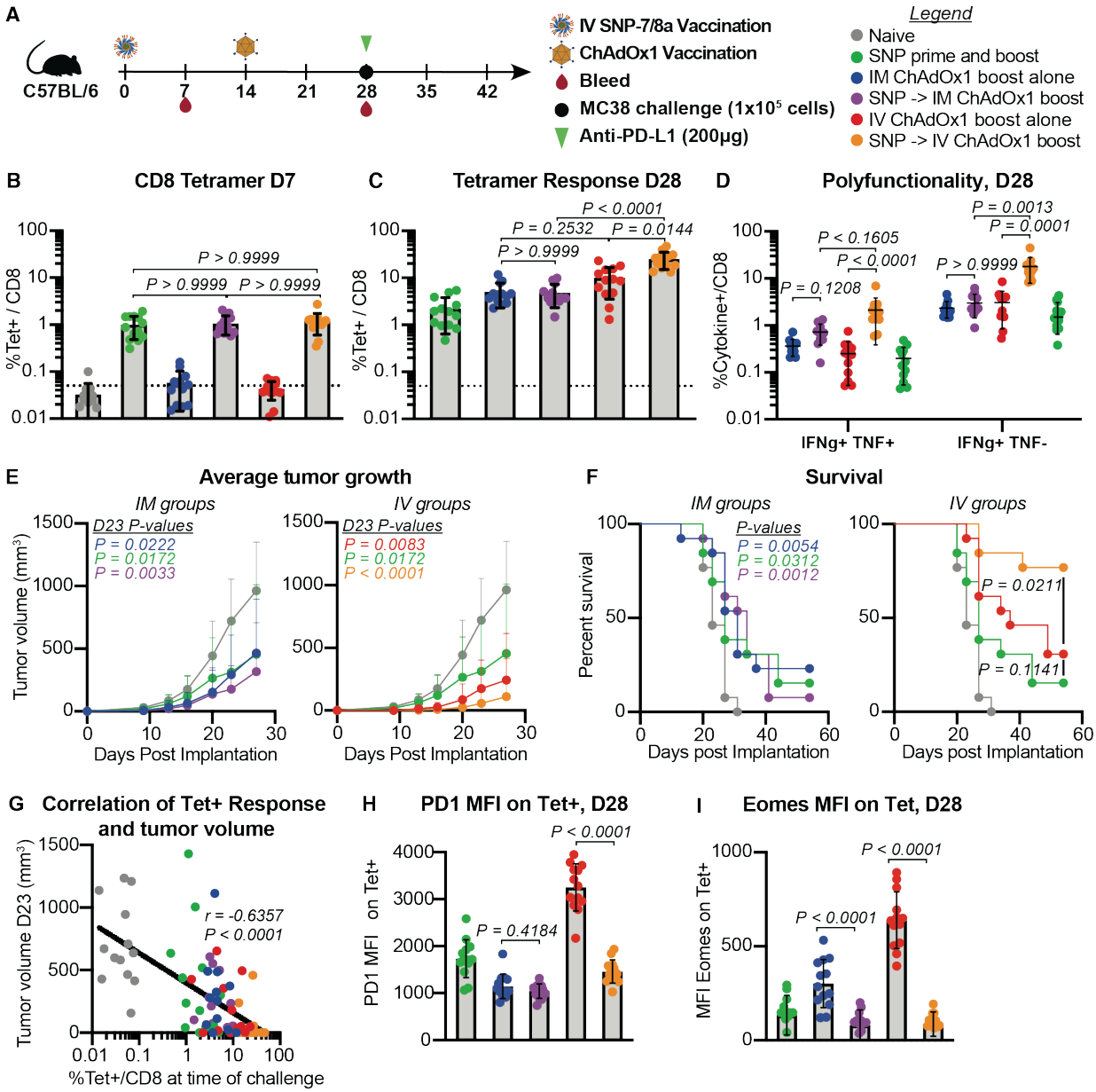

Figure 3.6 IV heterologous prime boost elicits highest magnitude CD8 T cell response and improves protection against MC38 tumor challenge. (**A**) Prophylactic study vaccination and sampling schedule, legend for entire figure. (**B**) Magnitude of Reps1-specific CD8 T cell response in blood 7 days after SNP prime. (**C**) Magnitude of Reps1-specific CD8 T cell response in blood 14 days after boost vaccination. (**D**) Frequency of IFNγ and TNFα co-producers following peptide restimulation of PBMCs 2 weeks post boost detected by flow cytometry. (**E**) Average tumor growth curves following MC38 challenge, groups receiving IM ChAdOx1 (left panel) and IV ChAdOx1 (right panel). (**F**) Survival of groups receiving IM ChAdOx1 (left panel) and IV ChAdOx1 (right panel). (**G**) Correlation of Reps-1 tetramer specific response at time of challenge and tumor volume 23 days after implantation. (**H,I**) MFI of (**H**) PD-1 and (**I**) Eomes on Reps1-tetramer positive cells in blood at time of challenge. **Stats: (B-D)** Data represented as mean ± SD, Kruskal-Wallis test with Dunn's correction for multiple comparisons. (**E**) Two way ANOVA with Bonferroni correction for multiple comparisons, p-values compared to naïve mice. (**F**) Mantel-Cox Log-rank test, compared to naïve mice (left panel). **(G)** Spearman's Rank correlation, line of best fit. **(H, I**) Data represented as mean ± SD, Mann-Whitney test.

been omitted in this figure.

Following tumor challenge, mice were checked regularly for the development of tumors and measured until humane endpoint criteria were met and the mice removed from the study. All vaccinated groups exhibited some level of statistically significant protection as compared to the naïve group based on the differences in tumor volume at day 23 post tumor implantation (Figure 3.6E). This reduced tumor growth translated into longer survival time that was statistically significant for the IM groups as compared to naïve (Figure 3.6F). Interestingly, there was no difference in protection between the SNP prime – IM ChAdOx1 boosted group and the IM ChAdOx1 alone, indicating that for the IM route of vaccination there may be no benefit to heterologous prime boost. The survival in the IV ChAdOx1 groups was better and statistically there was a difference between the SNP primed – IV ChAdOx1 boosted group and IV ChAdOx1 alone ($p = 0.0211$). There was, however, no improvement between IV ChAdOx1 alone as compared to IV SNP given twice ($p = 0.1141$).

Given the dramatic improvement in terms of survival afforded by the SNP primed – IV ChAdOx1 boosted group, and that this group had the highest magnitude CD8 T cell response, it seemed reasonable to attempt to determine whether magnitude of the Reps1-specific CD8 T cell response correlated with outcome. A moderate correlation ($r = -0.6357$, $p < 0.0001$) was calculated across all groups based on their Reps1-specific CD8 T cell response at the time of challenge and tumor volume 23 days post implantation (Figure 3.6G). In addition to magnitude, the expression of PD-1 and Eomes was assessed on the Reps1-specific CD8 T cells to determine if there were any significant differences that might also correlate with outcome. The trends were similar to those observed in figures 3.4 and 3.5, whereby there was no difference in PD-1 expression in the IM ChAdOx1 groups, but IV ChAdOx1 alone had a much higher expression of PD-1 than SNP primed –

IV ChAdOx1 boosted cells (Figure 3.6H). In terms of Eomes expression, both the IM and IV ChAdOx1 alone groups had higher expression as compared to the same vaccination given after SNP prime(Figure 3.6I).

Given that no phenotypic marker or polyfunctionality of cells in the blood had better predictive value of outcome than the magnitude of the Reps1-specific CD8 T cell response, a set of mice were sacrificed at the time of tumor challenge to investigate if there were any differences in T cell phenotype in the spleen that might explain the improved protection in the IV heterologous prime boost group. The trends in terms of magnitude of CD8 T cell response in the spleen for both tetramer and cytokine production were similar to blood, though in some cases not statistically significant likely due to the reduced number of samples per group (Figures 3.7B, 3.7C). The expression of Eomes and PD-1 also followed the same trend in the spleen derived Reps1-specific CD8 T cell responses as in the blood (Figures 3.7D, 3.7E).

One population that can be assessed in the spleen but not the blood is the frequency of stem-like cells. These cells are defined by the co-expression of TCF-1 and PD-1, and have been described as the reservoir of cells that responds to checkpoint inhibitors like αPD-1 [46]. An example of staining for TCF-1 and PD-1 is provided in figure 3.7F. Interestingly, the two groups with the best protection had the lowest proportion of stem-like cells (Figure 3.7G). However, if back-calculated to estimate the total number of stem-like cells present in the spleen, it becomes clear that the SNP primed – IV ChAdOx1 boosted group has the highest absolute number of stem-like cells present in the spleen. This is not statistically significant, likely again due to the limited number of samples. The higher absolute number is due to the higher magnitude of Reps1-specific CD8 T cell responses following SNP prime – IV ChAdOx1 boost, thereby making it possible for a smaller percentage to be a higher absolute count (Figure 3.7H). Regardless,

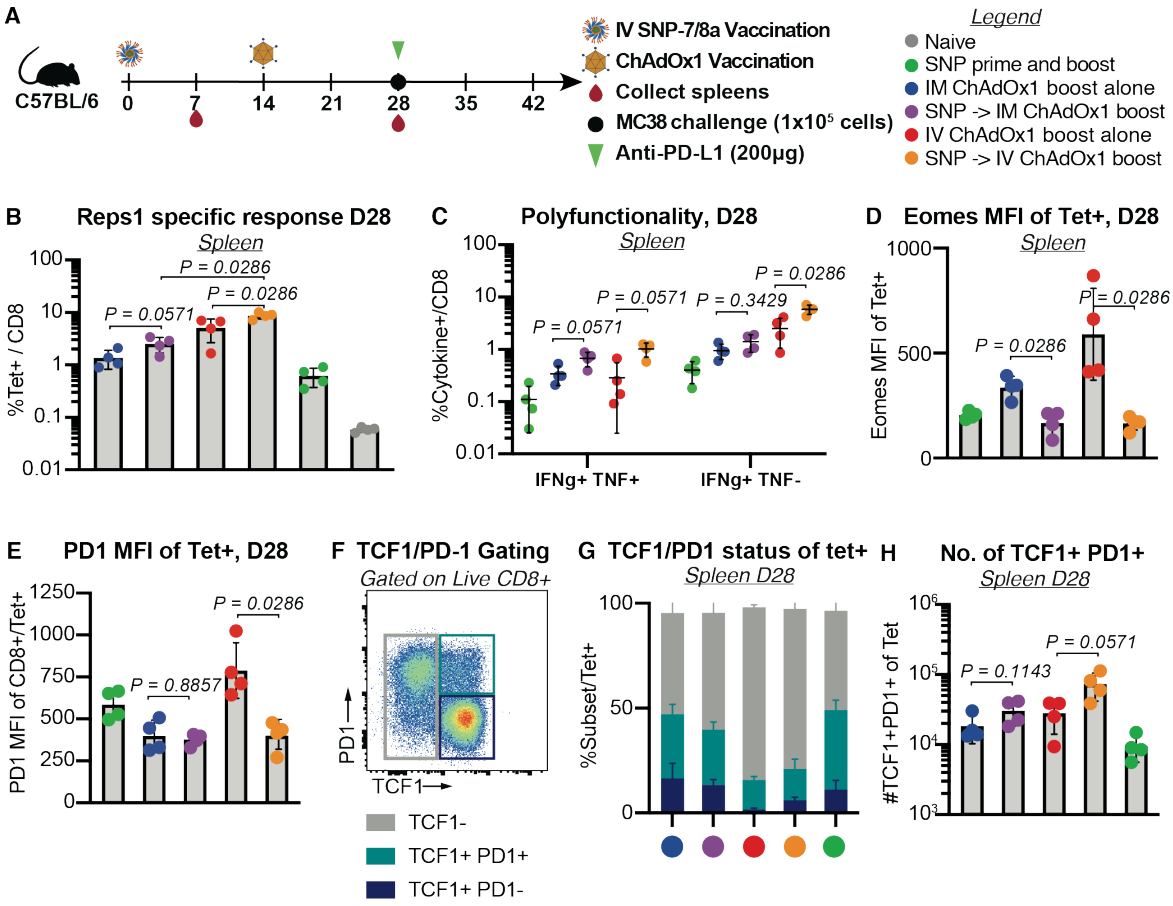

Figure 3.7 IV heterologous prime boost elicits highest magnitude of CD8 T cell responses in spleen and trends towards greatest number of stem-like cells. (**A**) Prophylactic study vaccination and sampling schedule, legend for entire figure. (**B**) Magnitude of Reps1-specific CD8 T cell response in spleen 14 days after boost vaccination. (**C**) Frequency of IFNγ and TNFα co-producers following peptide restimulation of splenocytes 2 weeks post boost detected by flow cytometry. (**D, E**) MFI of (**D**) Eomes and (**E**) PD-1 on Reps1-tetramer positive cells in spleen at time of challenge. (**F**) Gating example on flow plot of TCF1 and PD-1, TCF1+PD-1+ cells are termed stem-like. (**G**) Frequency of Reps1-tetramer+ cells that fall into each category based on TCF1/PD-1 staining in panel. (**H**) Absolute count of stem-like cells in spleen at time of challenge. **Stats: (B)** Data represented as mean ± SD, Kruskal-Wallis test with Dunn's correction for multiple comparisons. (**C-E, H**) Data represented as mean ± SD, Mann-Whitney test.

none of the immunological data provides a better understanding of the factors (in addition to magnitude) that may be affecting protection from tumor challenge.

A CD8 depletion study was done to confirm that the vaccine induced Reps1-specific CD8 T cell response is indeed required for protection from tumor challenge. Mice were primed with SNP and boosted 2 weeks later with IV ChAdOx1. Three days and one day prior to MC38 tumor challenge, mice in one group were treated with an anti-CD8β chain antibody to deplete CD8 T cells. Targeting the CD8β chain is important as other

cells, like cDC1s are known to express CD8α [51] and should not be depleted. Mice were bled at the time of challenge to determine the efficiency of the depletion and the magnitude of the Reps1-specific CD8 T cell response in the non-depleted group (Figure 3.8A). The number of CD8 T cells detected in blood at time of challenge was almost 0 in the depleted group, but there was no difference in the number of CD8 T cells in the naïve and non-depleted group (Figure 3.8B). The magnitude of the CD8 T cell response in the non-depleted group was high as normal (~30% Reps1-specific) (Figure 3.8C). The depletion of CD8 T cells completely abrogated protection as determined by both tumor growth and survival (Figures 3.8D, 3.8E).

Together these data demonstrate that the IV heterologous prime boost group elicits the highest magnitude Reps1-specific CD8 T cell response and provides the best protection as compared to all other tested groups. The best indicator for protection in this model appears to be magnitude of the Reps1-specific CD8 T cell response, regardless of cytokine production or qualitative marker expression. Given the limits of flow cytometry, it may be necessary to investigate the effects of heterologous prime boost on antigen-specific CD8 T cells by scRNA sequencing.

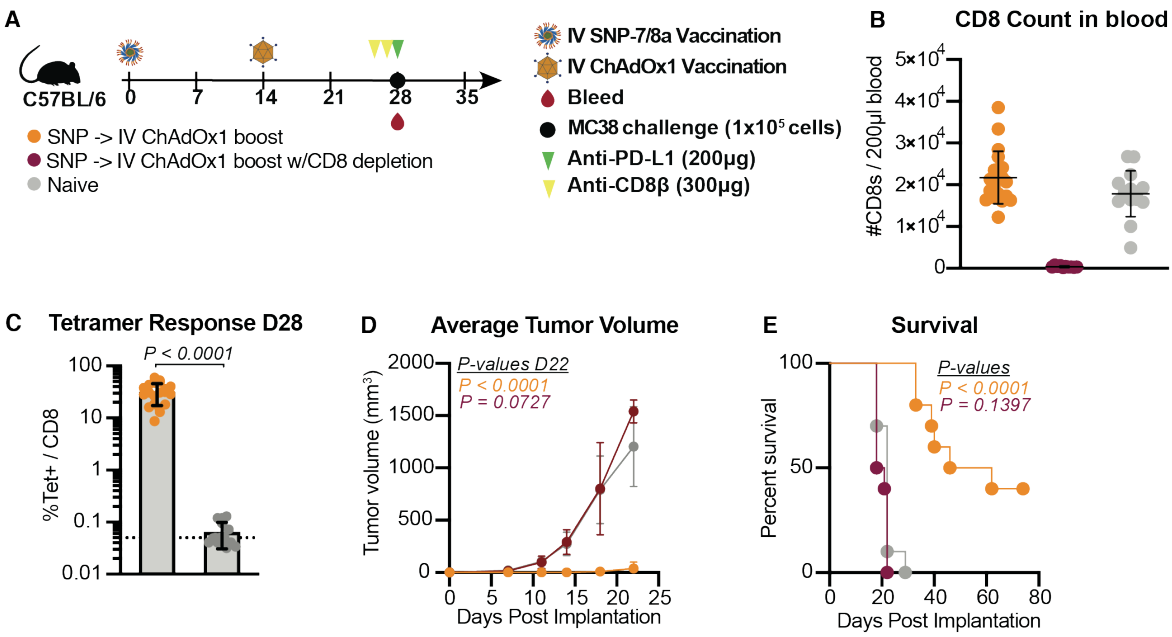

Figure 3.8 Protection from MC38 elicited by IV heterologous prime boost is dependent on the CD8 T cell response. (A) Prophylactic study vaccination and sampling schedule, legend for entire figure. **(B)** CD8 T cell count in blood at time of challenge. **(C)** Magnitude of Reps1-specific CD8 T cell response in blood. **(D)** Average tumor growth curves. **(E)** Survival. **Stats: (C)** Data represented as mean ± SD, Mann-whitney test. **(D)** Two way ANOVA with Bonferroni correction for multiple comparisons, p-values compared to naïve mice. **(E)** Mantel-Cox Log-rank test, compared to naïve mice.

3.4 Conclusions and discussion

3.4.1 The route of ChAdOx1 vaccination is the determining factor for CD8 T cell magnitude, which best correlates with tumor protection in the prophylactic setting

Previous work from the Seder lab has elucidated the importance of vaccination route for eliciting protective immune responses against infectious diseases like TB [191] and cancer [188]. The magnitude and quality (including polyfunctionality) of CD8 T cell responses has been shown to correlate with positive outcomes in cancer and infectious disease across mice [180], non-human primates [197] and humans [198]. This provided a rationale for testing the effect of route (IM or IV) on ChAdOx1 elicited CD8 T cell responses, both in terms of magnitude and quality.

Initially, the goal was to characterize differences between ChAdOx1 primed responses based on the route of immunization. The IV route appears to promote a more terminally differentiated phenotype and less polyfunctional CD8 T cell response as compared to IM ChAdOx1 vaccination (Figure 3.1/3.2). This is surprising as it is the opposite trend to that seen by vaccination with SNP. One possibility is that IV ChAdOx1 vaccination enables systemic distribution of the virus which may then infect long-lived cells. In these cells, ChAdOx1 could continue to produce antigen that would be processed and presented, resulting in chronic antigen stimulation of CD8 T cell responses and the maintenance of high magnitude over time. Previous work has demonstrated that local vaccination SC with SNP also enables antigen persistence for prolonged periods of time and might partially explain why the trends are reversed for these two vaccines [188]. IV ChAdOx1 and SNP SC vaccination may both result in antigen persistence. This suggests vaccine specific features that may be important for vaccine development.

One further interesting finding is that the route of SNP priming did not affect the magnitude and quality of the CD8 T cell response following ChAdOx1 boost (Figure 3.3).

The interval between SNP prime and ChAdOx1 boost similarly had no detectable impact on the magnitude and quality of the antigen-specific CD8 T cell response (Figure 3.4/3.5). Together these data suggest that the route of ChAdOx1 boost was the determining factor of magnitude and quality of the CD8 T cell response.

Given IV ChAdOx1 vaccination elicited high magnitude of CD8 response, it was important to test both routes in the prophylactic setting. This would demonstrate if the CD8 T cell responses were functional, despite IV ChAdOx1 eliciting more terminally differentiated CD8 T cell responses. The IV heterologous prime boost group elicited the highest magnitude of CD8 T cell response and also gave the best protection of all groups tested (Figure 3.6). There was no clear correlation between the polyfunctionality or phenotypic quality of the antigen-specific cells in the blood or spleen at the time of challenge and protection from tumor growth (Figure 3.6/3.7). To demonstrate that protection was indeed dependent on vaccine elicited CD8 T cell responses, a depletion study was undertaken (Figure 3.8). Depleting CD8 T cells in the IV heterologous prime boost group completely abrogated protection, demonstrating that the CD8 T cell responses elicited were functional and capable of mediating protection from tumor challenge. It was important to demonstrate this prior to attempting therapeutic studies, to ensure that the CD8 T cell response could protect from tumor challenge.

3.4.2 Limitations of studies and future studies

The initial studies investigating heterologous prime boost with SNP and ChAdOx1 were focused on testing immune responses against a single neoantigen (Reps1) that has been previously published to provide protection from MC38 tumor challenge [188]. Since all immunogenicity studies have been performed with this antigen, it is not clear if some of the findings are specific to Reps1 and not generalizable to other antigens. To improve

the understanding of how route and interval affect magnitude of CD8 T cell responses, it would be important to repeat the immunogenicity experiments with a different antigen.

Flow cytometry is a biased approach to characterizing immune responses as panels are developed based on prior knowledge. It is descriptive and not typically exploratory. It is possible that there are more qualitative differences dependent on the route of vaccination of ChAdOx1 that have not been identified. Another method to characterize cell states is by the use of single cell RNA sequencing (scRNA seq). This is an unbiased approach that allows the sampling of the transcriptional landscape of cells of interest. The cells can then be characterized in depth to identify unique signatures/states that are dependent on the route of vaccination or vaccine platform used.

Prophylactic studies are useful to determine if the immune response elicited by a vaccination strategy is capable of mediating protection from a tumor model. This is less stringent and clinically relevant than a therapeutic study, which consists of implanting mice with tumors and then beginning intervention. It is possible that what works in the prophylactic setting would not be efficacious in a therapeutic setting. Given that the clinical paradigm is one where a patient presents first with a tumor and then would receive a vaccine intervention, it is important to test the heterologous prime boost strategy using mouse tumor models. This will be the subject of chapter 4.

Chapter 4

Determining the efficacy of heterologous prime boosted CD8 T cell responses in the therapeutic setting

4.1 Introduction

The experiments described in chapter 3 demonstrated the capacity of heterologous prime boost to elicit CD8 T-cell responses capable of providing protection from tumor challenge. However, one serious limitation of the prophylactic setting is its lack of resemblance to the clinical paradigm, whereby a patient presents with a tumor prior to vaccination. For this reason, the next logical step was to test the heterologous prime boost vaccination strategy in mice that already had established tumors, to determine if therapeutic vaccination could also induce tumor regression and clearance.

As therapeutic studies are likely to provide more relevant data to the clinical paradigm, experiments were undertaken with three different tumor models. The MC38 model, as previously described in chapter 3, was targeted by vaccination against either Reps1 or Adpgk. Both neoantigens were validated by mass spectrometry by Yadav et al (Nature, 2015), and so MC38 tumors should respond to therapeutic vaccination and induction of neoantigen-specific CD8 T cell responses against both. In addition, heterologous prime boost vaccination was assessed for efficacy in the TC-1 mouse lung cancer model and in the B16F10 melanoma model. The TC-1 cell line was transformed to express HPV-16 E6 and E7 viral proteins [199], which contain high affinity epitopes that can cause tumor rejection [186]. For B16F10, the self-antigen Trp1 can be targeted to elicit a CD8 T cell responses to promote tumor rejection [186].

For therapeutic studies, mice are implanted with tumor cells subcutaneously in the flank and allowed to develop small, palpable tumors prior to any intervention. Most tumors develop rapidly when implanted subcutaneously and therefore impose a time constraint on treatment regimens. For this reason, all therapeutic studies rely on a one-week interval between prime and boost. As demonstrated in figures 3.6 and 3.7, the

shortened interval should have a limited impact on the magnitude and quality of the CD8 T cell response, regardless of the route of ChAdOx1 vaccination.

Given the emphasis on developing a personalized vaccination strategy, the studies here focus on priming with SNP and boosting with ChAdOx1. The opposite strategy would theoretically be possible in the case of viral- or self-antigens as these vaccines could be mass-produced and given to patients as an off-the-shelf therapy [131]. Targeting viral or self-antigens would remove the manufacturing time constraint inherent to personalized vaccination strategies. Furthermore, the route of priming with SNP in the therapeutic setting is always IV, whereas both IM and IV vaccination will be tested for ChAdOx1. This is because previous data has already demonstrated the need for a systemic vaccination approach to get optimal protection with SNP [188].

In addition, all studies were conducted with the use of αPD-L1 given weekly starting at the time of the boost vaccination. Previous data from the Seder lab has shown that neither MC38 nor B16F10 tumors respond to vaccination in the absence of checkpoint inhibitor. However, the TC-1 model does not require checkpoint inhibitor to respond to vaccination. Nevertheless, for consistency, and due to the likelihood of being given as a combination therapy in humans, all TC-1 studies also received checkpoint inhibitor treatment with their vaccinations.

Blood was sampled from mice one week post boost vaccination in all cases in order to compare the magnitude of the CD8 T cell response between groups. Waiting longer to sample blood would run the risk of losing mice from groups that did not exhibit protection, thereby making it difficult to draw conclusions. The magnitude and quality of CD8 T cell responses in the blood could then be characterized and correlated with the outcome. In addition, some mice in the MC38 tumor model were sacrificed to look at the

CD8 T cell response in the spleen and tumor to determine if there were any other major qualitative differences that correlated with tumor regression.

4.2 Chapter Aims

1. To evaluate heterologous prime boost vaccination strategy in the therapeutic setting
2. To identify a correlation between the blood CD8 T cell response and anti-tumor efficacy
3. To determine if this is a general feature of therapeutic cancer vaccination by using alternative antigens and/or tumor models

4.3 Results

4.3.1 Heterologous prime boost with IM ChAdOx1 improves protection compared to IM ChAdOx1 alone in MC38

Initial testing of heterologous prime boost focused on using ChAdOx1 as an IM vaccination. As this is the standard route of vaccination for ChAdOx1, it could be used to establish a benchmark of protection for heterologous prime boost and begin to determine if there might be a benefit to heterologous prime boost vaccination as compared to either vaccine alone. The experiment was carried out as described in section 4.1 (figure 4.1A). The groups described in the legend are comprised of:

1. ChAdOx1 encoding Reps1 given IM at time of prime, this represents the earliest possible intervention one could attempt with ChAdOx1. Heterologous prime boost must be better than this group to warrant further investigation.
2. Heterologous prime boost using SNP IV followed by ChAdOx1 IM. Both vaccinations provide Reps1 antigen. This is the test group.
3. SNP given twice IV is the positive control for this study as previous data has demonstrated an expected protection rate of 40-60% [188].
4. 'Empty' (no Reps1 antigen) SNP IV prime followed by ChAdOx1 encoding Reps1 IM. This group is a control for the heterologous prime boost to ensure that any protection is dependent on a SNP primed CD8 T cell response and not a generic effect of systemic TLR-7/8a given at the time of priming.
5. Reps1 SNP IV prime followed by IM ChAdOx1 without an antigen insert. This group is a control to determine if efficacy in the heterologous prime boost group is dependent on expanding the CD8 T cell response or not.
6. Naïve tumor bearing mice that receive only the checkpoint inhibitor. This is the negative control of this study.

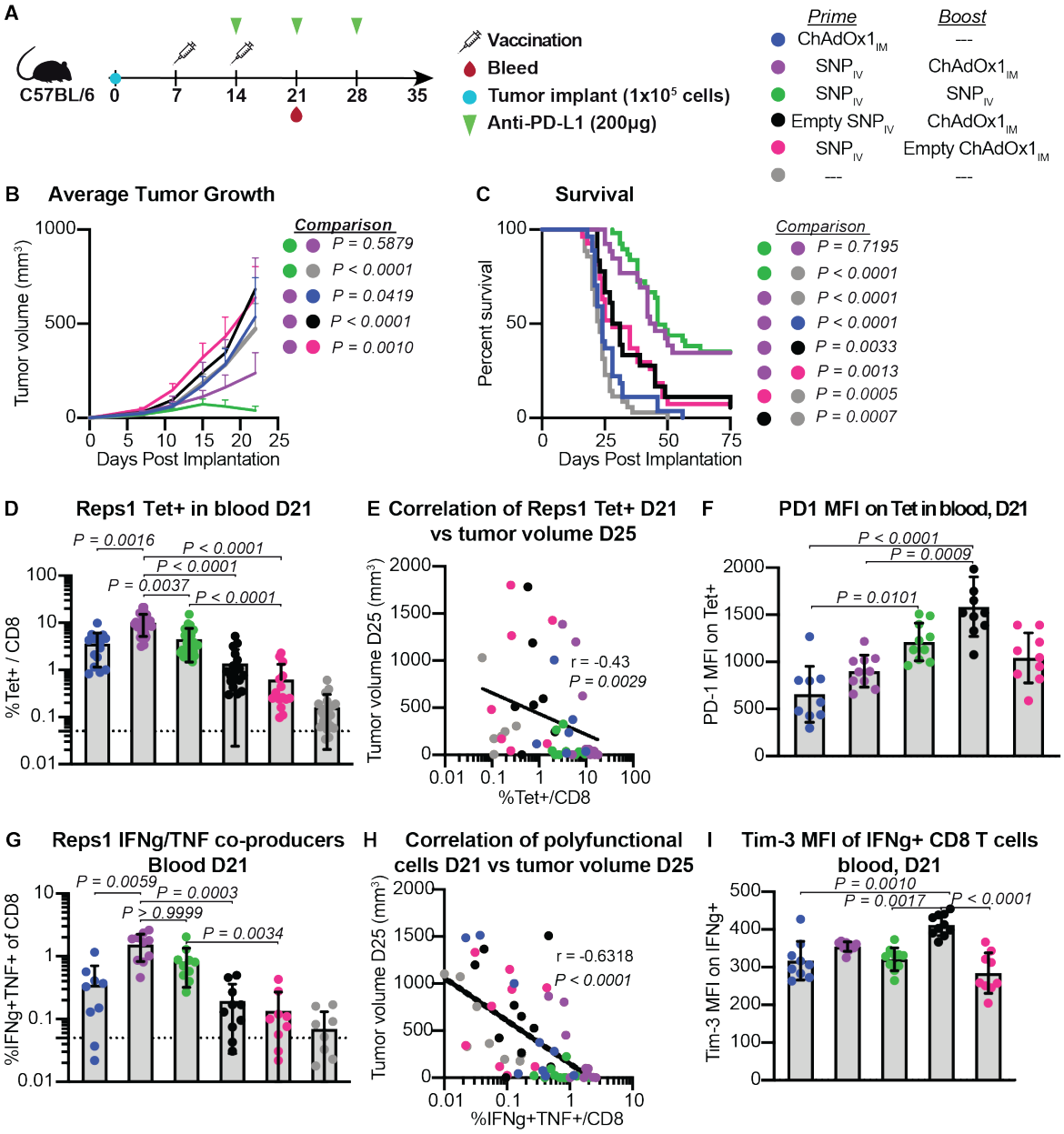

Figure 4.1 IM heterologous prime boost improves protection compared to IM ChAdOx1 alone. (**A**) Therapeutic study treatment and sampling schedule, legend for all figure panels. (**B**) Tumor growth curves plotted as mean + SEM. (**C**) Survival curves for all groups, compiled from 3 studies. (**D**) Immunogenicity at day 21 measured by tetramer staining PBMCs using a Reps1-specific tetramer (**E**) Correlation of Reps1 specific response at day 21 and tumor volume at day 25, plotted with line of best fit. (**F**) MFI of PD-1 on Reps1-tetramer positive cells in blood. (**G**) Frequency of IFNγ and TNFα co-producers following peptide restimulation detected by flow cytometry. (**H**) Correlation of polyfunctional frequency at day 21 and tumor volume at day 25, plotted with line of best fit. (**I**) MFI of Tim-3 on IFNγ producing cells in blood. **Stats:** (**B**) Two way ANOVA with Bonferroni correction for multiple comparisons. (**C**) Mantel-Cox Log-rank test (**D, F, G, I**) Data represented as mean ± standard deviation, Kruskal-Wallis test with Dunn's correction for multiple comparisons. (**E, H**) Spearman's Rank correlation. Data representative of three independent experiments.

Previous experiments in the lab have shown that IV SNP prime alone (no boost) does not provide a therapeutic benefit in this model, and therefore this group has not been included in these studies.

As expected, the SNP IV given twice (positive control) elicited some level of tumor regression (Figure 4.1B) and cleared ~40% of tumors (Figure 4.1C). There was no significant difference between the tumor sizes of SNP IV given twice and the heterologous prime boost group at day 22 ($p = 0.5879$) post tumor inoculation. The overall survival rate was also identical between the heterologous prime boost group and the SNP IV given twice, indicating that heterologous prime boost performs at least as well as the positive control ($p = 0.7195$).

Heterologous prime boost significantly reduced tumor size at day 22 as compared to:

- IM ChAdOx1 alone given at time of prime vaccination, $p = 0.0419$
- Empty SNP followed by ChAdOx1 IM, $p < 0.0001$
- Reps1 SNP IV followed by empty ChAdOx1 IM, $p = 0.0010$

The heterologous prime boost group also significantly improved survival compared to all controls, in line with the improvements in tumor growth. All control groups displayed tumor growth curves similar to the naïve, thereby indicating they did not significantly reduce tumor growth. In addition, the IM ChAdOx1 prime alone group did not improve survival as compared to naïve. However, both the empty SNP followed by Reps1 ChAdOx1 IM group and the Reps1 SNP followed by empty ChAdOx1 groups improved survival as compared to naïve ($p = 0.0007$ and 0.0005, respectively).

Blood was sampled, processed and stained with a Reps1 tetramer as described in chapter 3 to determine if the vaccine elicited CD8 T cell responses elicited by the different vaccination regimens correlated with tumor regression. The highest magnitude response

was elicited by the heterologous prime boost group, and was significantly higher than all other vaccine groups (Figure 4.1D). There was no significant difference in the magnitude of the Reps1-specific CD8 T cell response elicited by IM ChAdOx1 alone at time of prime and the SNP IV given twice (positive control). The SNP IV given twice elicited a higher magnitude response than SNP IV followed by empty ChAdOx1 ($p < 0.0001$), which is expected. The tetramer response was then correlated with the tumor volume at day 25 (Figure 4.1E) across all groups. A significant negative correlation was identified between tumor volume and Reps1 tetramer response ($r = -0.43$, $p = 0.0029$). This indicates that an increased Reps1 T cell response is associated with reduced tumor volume, as was the case in the prophylactic setting.

In addition to correlating magnitude, the expression of PD-1 was assessed on the surface of the Reps1-specific CD8 T cells (Figure 4.1F). Though there were no significant differences between most groups, the IM ChAdOx1 prime alone had a lower expression of PD-1 as compared to Reps1 SNP IV given twice ($p = 0.0101$). This is surprising given the lack of tumor control seen in the IM ChAdOx1 group as compared to the IV SNP given twice, thereby indicating that the expression of PD-1 on antigen-specific CD8 T cells in the blood may not be a good predictive marker for efficacy.

The capacity of Reps1-specific CD8 T cells to produce IFNγ and TNFα was investigated by performing a peptide restimulation assay (described in chapter 3). As the production of IFNγ alone closely follows the tetramer specific response, that data is not shown. However, the different vaccine regimens may affect the frequency of polyfunctional (IFNγ and TNFα co-producing) CD8 T cells. There is no statistically significant difference in the frequency of polyfunctional cells between the heterologous prime boost group and the SNP IV given twice group (Figure 4.1G), even though there was a difference in the tetramer response (Figure 4.1D). The heterologous prime boost

group also had a higher frequency of polyfunctional cells as compared to all other control groups. Correlating the frequency of polyfunctional cells in the blood on day 21 against tumor volume on day 25 (Figure 4.1H) revealed a stronger correlation than the tetramer response ($r = -0.6318$, $p < 0.0001$). The expression of Tim-3 was assessed on the IFNγ producing CD8 T cells, and there were few statistically significant differences between groups indicating similar levels of exhaustion between groups (Figure 4.1I).

Collectively, these data indicate that the magnitude of the T cell response in the blood may moderately correlate with tumor regression in the therapeutic setting. Given the difference in Reps1-tetramer magnitude between the heterologous prime boost group and the SNP IV given twice group and the lack of difference in polyfunctionality between these two groups; it is possible that functionality may be a better predictor than tetramer response for tumor regression. Interestingly, neither the expression of PD-1 or Tim-3 on antigen-specific CD8 T cells from the blood correlated with tumor control, despite using αPD-L1 to promote regression.

4.3.2 IV heterologous prime boost improves tumor regression compared to IV ChAdOx1 alone

Previous data in chapter 3 demonstrated the benefits of heterologous prime boost when using ChAdOx1 IV as a strategy that elicits the highest magnitude antigen-specific CD8 T cell response. Given the correlation seen between magnitude and tumor volume (Figure 4.1), it seemed likely that IV heterologous prime boost could improve tumor regression and clearance compared to the positive control (IV SNP given twice) as it would be expected to elicit much higher magnitude CD8 T cell responses than the IM heterologous prime boost.

Heterologous prime boost using IV ChAdOx1 was tested as shown in figure 4.2A. The groups are the same as in the IM heterologous prime boost study, but with ChAdOx1 given IV in all cases. The IV heterologous prime boost group exhibited the same level of tumor regression as SNP IV given twice (Figure 4.2B, $p > 0.9999$) and provided equivalent survival (Figure 4.C, ~40-45%, $p = 0.8760$). The heterologous prime boost group improved tumor regression compared to all control groups:

- IV ChAdOx1 alone prime, $p < 0.0001$
- Empty SNP followed by Reps1 ChAdOx1 IV, $p = 0.0051$
- Reps1 SNP followed by empty ChAdOx1 IV, $p = 0.0094$

However, in terms of survival the heterologous prime boost group was significantly better than the empty SNP followed by Reps1 ChAdOx1, ($p = 0.0030$) and the ChAdOx1 prime alone ($p < 0.0001$) but was not significantly different to the Reps1 SNP followed by empty ChAdOx1 ($p= 0.0865$). This indicates that for tumor regression and clearance, the SNP must provide antigen to elicit a CD8 T cell response, but perhaps the ChAdOx1 does not need to encode the antigen. The heterologous prime boost is still better when the ChAdOx1 encodes Reps1, but not significantly in terms of survival.

In contrast to the IM control groups, where the tumors grew out at the same rate as the naïve mice, the IV control groups all exhibited a reduction in the rate of tumor growth as compared to naïve (Figure 4.2B). The Reps1 ChAdOx1 IV prime alone slowed growth ($p < 0.0001$), but this did not translate into improved survival ($p = 0.3197$). The empty SNP followed by Reps1 ChAdOx1 and the Reps1 SNP followed by empty ChAdOx1 groups both displayed improved survival by comparison to naïve in addition to the reduced tumor growth rate ($p = 0.0056$, <0.0001, respectively). This may indicate that IV ChAdOx1 vaccination as a boost may provide some therapeutic benefit that is independent of its ability to boost the CD8 T cell response.

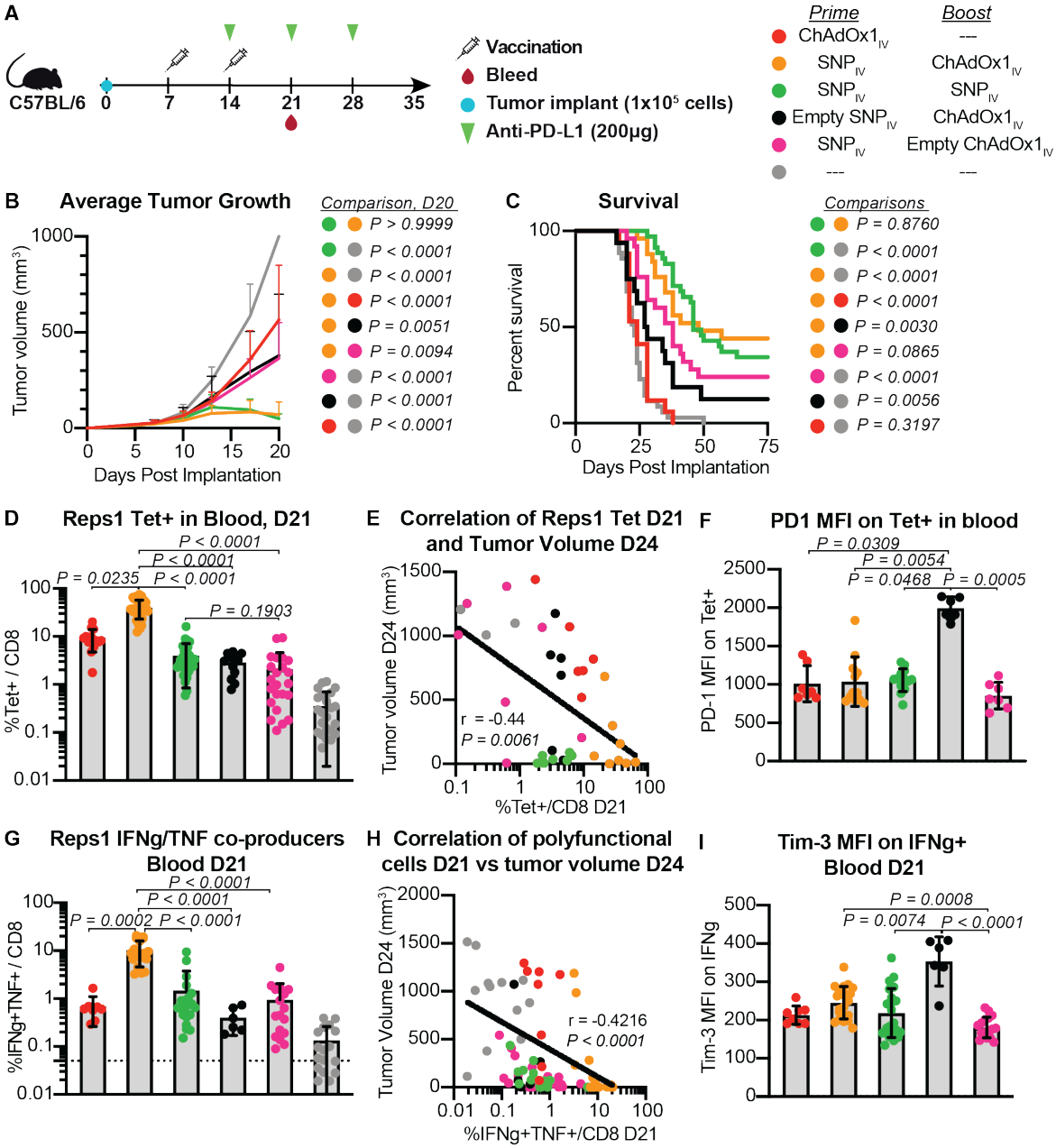

Figure 4.2 IV heterologous prime boost improves protection compared to IV ChAdOx1 alone. (**A**) Therapeutic study treatment and sampling schedule, legend for all figure panels. (**B**) Tumor growth curves plotted as mean + SEM. (**C**) Survival curves for all groups, compiled from 3 studies. (**D**) Immunogenicity at day 21 measured by tetramer staining PBMCs using a Reps1-specific tetramer (**E**) Correlation of Reps1 specific response at day 21 and tumor volume at day 25, plotted with line of best fit. (**F**) MFI of PD-1 on Reps1-tetramer positive cells in blood. (**G**) Frequency of IFNγ and TNFα co-producers following peptide restimulation detected by flow cytometry. (**H**) Correlation of polyfunctional frequency at day 21 and tumor volume at day 25, plotted with line of best fit. (**I**) MFI of Tim-3 on IFNγ producing cells in blood. **Stats:** (**B**) Two way ANOVA with Bonferroni correction for multiple comparisons. (**C**) Mantel-Cox Log-rank test (**D, F, G, I**) Data represented as mean ± standard deviation, Kruskal-Wallis test with Dunn's correction for multiple comparisons. (**E, H**) Spearman's Rank correlation. Data representative of three independent experiments.

The Reps1-specific CD8 T cell response was assessed by tetramer staining as before. The trends are as expected with IV heterologous prime boost eliciting the highest magnitude CD8 T cell response as compared to all other groups (Figure 4.2D). Interestingly, the IV SNP given twice group does not have a significantly higher magnitude response as compared to the IV SNP prime followed by the empty ChAdOx1 IV. As with the IM heterologous prime boost groups, there is a negative correlation between Reps1-specific response on day 21 and tumor volume on day 24 (Figure 4.2E, $r = -0.44$, $p = 0.0061$). Similar to the IM groups, the expression of PD-1 on Reps1-specific cells across vaccination groups is comparable, except for the empty SNP followed by Reps1 ChAdOx1 group, which has higher expression compared to all other groups (Figure 4.2F).

The IV heterologous prime boost group elicited a much higher magnitude of polyfunctional cells as compared to all control groups (Figure 4.2H). As opposed to the IM heterologous prime boost group, the IV heterologous prime boost group also had a higher frequency of polyfunctional cells as compared to the IV SNP given twice ($p < 0.0001$). When correlated with tumor volume on day 24, the frequency of polyfunctional cells did not have an improved correlation (Figure 4.2I, $r = -0.4216$, $p < 0.0001$) as compared to the tetramer correlation, which is different to what was seen with the IM heterologous prime boost groups.

The expression of Tim-3 was assessed in order to determine if the cells were more exhausted following IV ChAdOx1 boost. As with the expression of PD-1 on the Reps1-tetramer specific cells, there were very few differences in expression of Tim-3 (Figure 4.1J), and these were mostly with the empty SNP followed by Reps1 ChAdOx1 group.

Together, these data indicate that magnitude of the antigen-specific response is the only consistent correlate with tumor regression, but is by no means definitive.

Polyfunctionality can be used as a surrogate to predict response to a similar degree. The quality of antigen-specific CD8 T cells in the blood does not appear to vary much regardless of the vaccination strategy used.

4.3.3 There are limited phenotypic differences in Reps1-specific CD8 T cell responses elicited by different vaccination strategies in the spleen and tumor

The heterologous prime boost groups (both IV and IM) exhibited equivalent tumor growth suppression (Figure 4.3B) and survival (Figure 4.3C) as compared to the positive control (SNP IV given twice). However, the heterologous prime boost groups both elicited higher magnitude Reps1 specific CD8 T cell responses than SNP IV given twice (Figure 4.3D, IV – $p < 0.0001$, IM – $p = 0.0217$). In addition, the IV heterologous prime boost group elicited a higher magnitude response than the IM heterologous prime boost group ($p = 0.0027$). Given the differences in the magnitude of the antigen-specific response and the established correlation between magnitude and tumor regression, it is surprising that all three groups perform equivalently in terms of tumor regression and survival. In addition, in figures 4.1 and 4.2, the quality was assessed and there were no differences between the heterologous prime boost groups (IM or IV) and SNP IV given twice. Therefore, it seemed plausible that though there were few differences in the blood CD8 T cell response, there might be detectable differences in the spleen or tumor which may explain the similar levels of protection seen across the three treatment groups.

To probe the magnitude and quality of the T cell response in tissues in the therapeutic setting, mice were inoculated with tumor and treated with vaccinations and checkpoint inhibitor as shown in figure 4.4A. This was done only with the groups that had exhibited protection, and the hypothesis was that the IV heterologous prime boost group

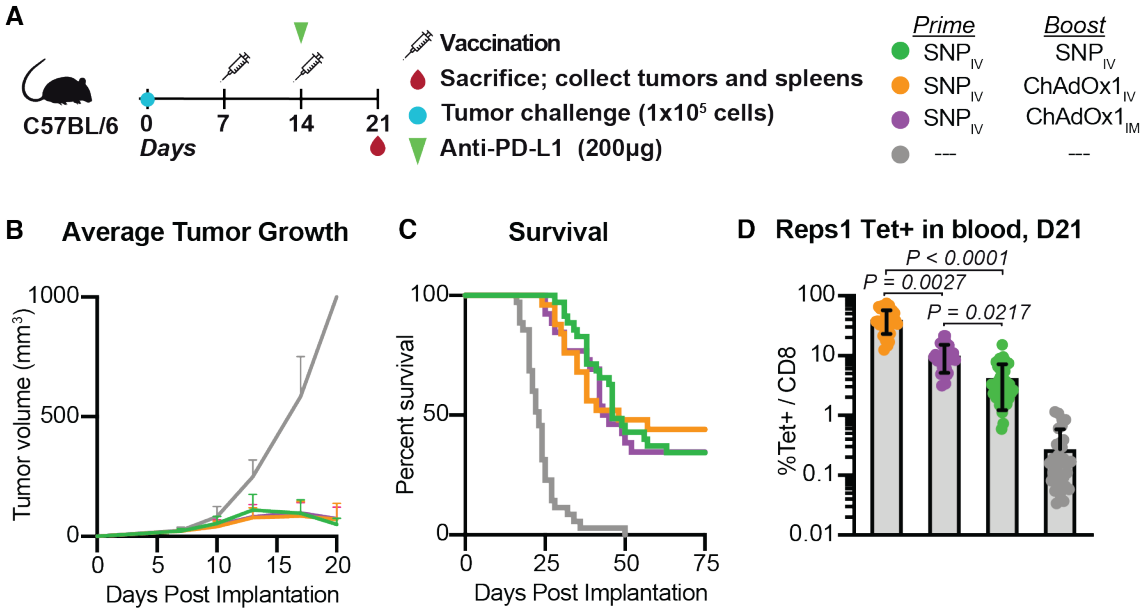

Figure 4.3 There is no difference in tumor regression between heterologous prime boost groups and IV SNP given twice despite dramatically different magnitudes of Reps1-specific CD8 T cell responses in the blood

(**A**) Therapeutic study treatment and sampling schedule, legend for all figure panels. (**B**) Tumor growth curves plotted as mean + SEM. (**C**) Survival curves for all groups, compiled from 3 studies. (**D**) Immunogenicity at day 21 measured by tetramer staining PBMCs using a Reps1-specific tetramer **Stats:** (**B**) Two way ANOVA with Bonferroni correction for multiple comparisons. $P < 0.0001$ for all groups compared to untreated, no difference between vaccinated groups (**C**) Mantel-Cox Log-rank test, $P < 0.0001$ for all groups compared to untreated, no difference between vaccinated groups (**D**) Data represented as mean ± standard deviation, Kruskal-Wallis test with Dunn's correction for multiple comparisons. Data representative of three independent experiments.

would elicit a higher frequency of more exhausted or less functional cells as compared to the other two groups in the tissue. In the spleen, the IV heterologous prime boost elicited a higher magnitude of Reps1-specific CD8 T cells both as a frequency of total CD8 T cells and in terms of absolute count (Figure 4.4B-C). There was no difference in frequency of absolute count of Reps1-specific CD8 T cells between the IM heterologous prime boost group and the IV SNP given twice.

The spleen is one of the reservoirs of the stem-like population of antigen-specific CD8 T cells following infection/vaccination [46]. The stem-like population is defined by co-expression of TCF1 and PD-1, and is the population that responds to checkpoint

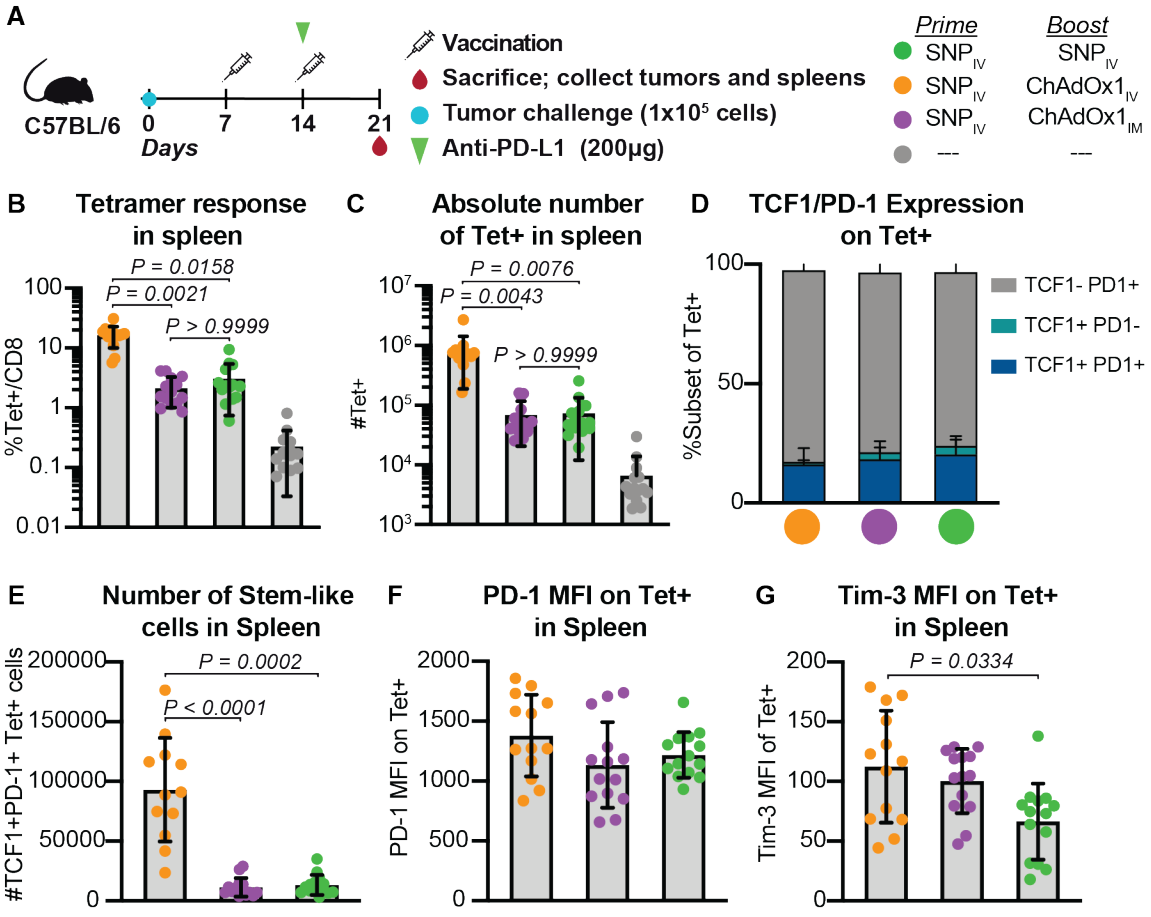

Figure 4.4 IV heterologous prime boost elicits a higher magnitude Reps1-specific CD8 T cell response in the spleen as compared to other vaccine groups.
(**A**) Therapeutic study treatment and sampling schedule, legend for all figure panels. (**B**) Frequency of Reps1-specific CD8 T cells in the spleen (**C**) Absolute number of Reps1-specific CD8 T cells in the spleen for each mouse, calculated by plating a fixed fraction of the spleen for each sample and multiplying by the reciprocal (**D**) Stacked bar graph of proportion of Reps1-tetramer specific cells in each group that fall into each of the subsets described in the legend. TCF1+PD-1+ subset is also known as the stem-like cells. (**E**) Absolute number of stem-like cells in the spleen in each of the vaccinated groups. (**F**) MFI of PD-1 on Reps1-tetramer positive cells in spleen. (**G**) MFI of Tim-3 on Reps1-tetramer positive cells in spleen **Stats:** (**B, C, E, F, G**) Data represented as mean ± standard deviation, Kruskal-Wallis test with Dunn's correction for multiple comparisons. (**D**) 2-way ANOVA with Bonferroni correction for multiple comparisons, no statistically significant differences. Data representative of three independent experiments.

inhibitor [47]. An increased frequency of TCF-1+ CD8 T cells in the tumor is associated with improved prognosis in cancer immunotherapy [200]. There was no difference in the frequency of stem-like cells between the three different vaccination groups (Figure 4.4D). However, if calculating the absolute numbers of stem-like cells (Figure 4.4E), it is clear

that the IV heterologous prime boost group has more stem-like cells than the IM heterologous prime boost group ($p = 0.0002$) and IV SNP given twice ($p < 0.0001$).

The expression of PD-1 and Tim-3 was also assessed on the Reps1-specific CD8 T cells. There was no difference in the PD-1 expression (Figure 4.4F), but there was a slightly higher expression of Tim-3 associated with the IV heterologous prime boost group as compared to IV SNP given twice (Figure 4.4G, $p = 0.0334$). Given the variability of the expression of Tim-3, it seems unlikely that this is as meaningful as the increased number of stem-like cells in the spleen. Given the understanding of factors that affect anti-tumor efficacy, these data would suggest that the IV heterologous prime boost group should outperform both of the other two vaccination strategies, and yet it does not.

In the tumor, IV heterologous prime boost is associated with an increase in the number of Reps1-specific CD8 T cells per mg of tumor (Figure 4.5B) as compared to IV SNP given twice ($p = 0.0415$) but not more cells than IM heterologous prime boost ($p = 0.0785$). There is no statistically significant difference in the number of Reps1-specific CD8 T cells between the IM heterologous prime boost group and IV SNP given twice (Figure 4.5B, $p > 0.9999$) despite the higher magnitude in the blood (Figure 4.3D). All vaccinated groups have a higher number of Reps1-specific CD8 T cells in the tumor compared to the naïve group, which represents the infiltration based on endogenous priming from tumor released antigen.

There is no difference in the expression of PD-1 on the Reps1-specific CD8 T cells across the three vaccine groups (Figure 4.5C). There is a slight difference in Tim-3 expression in the tumor (Figure 4.5D), however as opposed to the spleen, the IV heterologous prime boost group now exhibits the lowest expression (on average), though it's only significant when compared to the IM heterologous prime boost group ($p = 0.0110$).

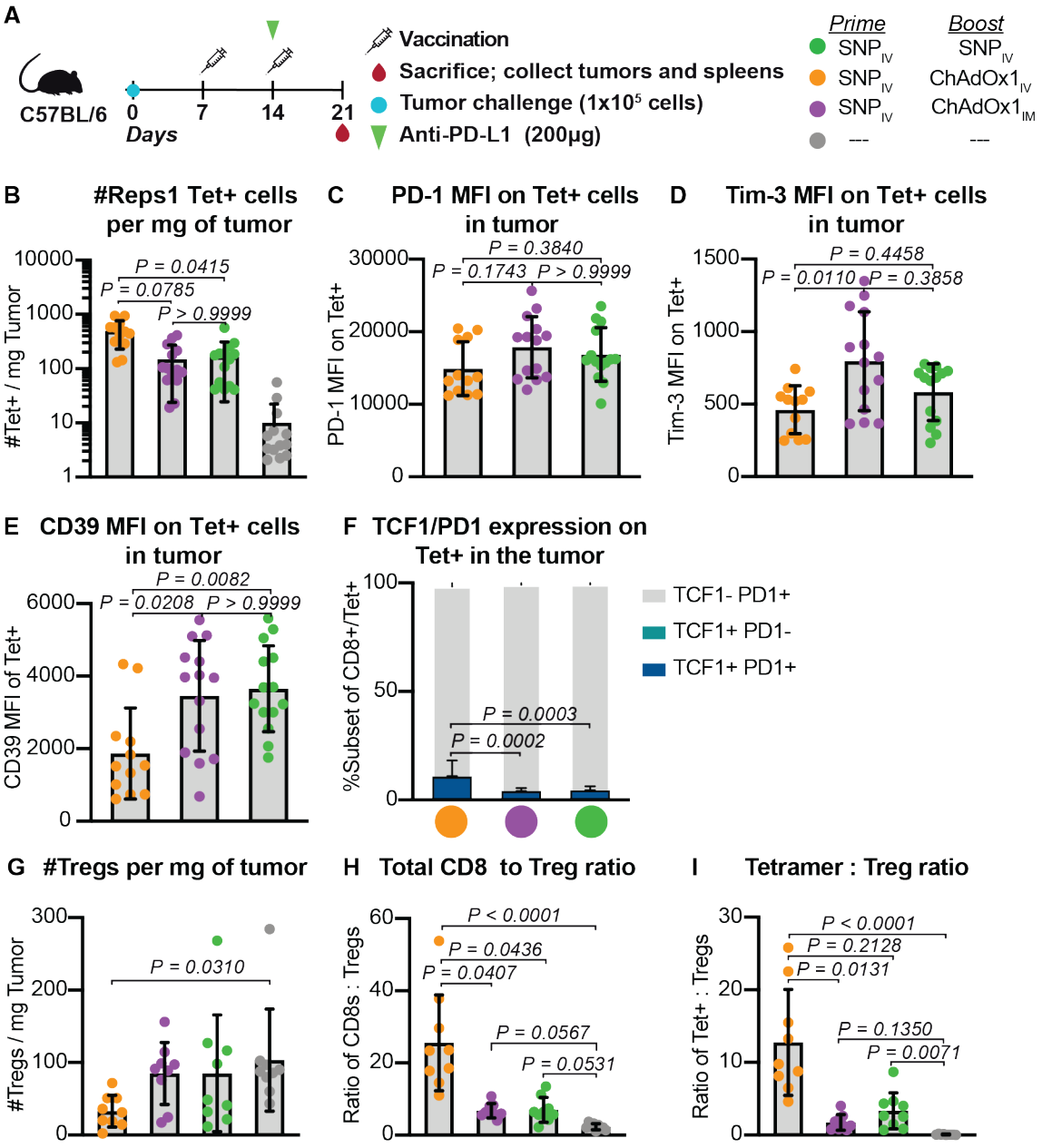

Figure 4.5 IV heterologous prime boost is associated with increased CD8 T cell infiltration and reduction in number of Tregs in the tumor

(**A**) Therapeutic study treatment and sampling schedule, legend for all figure panels. (**B**) Number of Reps1-specific CD8 T cells per mg of tumor calculated by plating a fixed fraction of tumor suspension for flow cytometry staining and reverse calculating from the count on the cytometer. (**C**) MFI of PD-1 on Reps1-tetramer positive cells in the tumor. (**D**) MFI of Tim-3 on Reps1-tetramer positive cells in tumor. (**E**) MFI of CD39 on Reps1-tetramer positive cells in tumor. (**F**) Stacked bar graph of proportion of Reps1-tetramer specific cells in each group that fall into each of the subsets described in the legend. The TCF1+PD-1+ subset are also known as stem-like cells. (**G**) Number of Tregs per mg of tumor calculated as in A (**H**) Ratio of total CD8 T cells to Tregs in the tumor (**I**) Ratio of Reps1-tetramer specific CD8 T cells to Tregs **Stats:** (**B, C, D, E, G, H, I**) Data represented as mean ± standard deviation, Kruskal-Wallis test with Dunn's correction for multiple comparisons. (**F**) 2-way ANOVA with Bonferroni correction for multiple comparisons, (**B-F**) data representative of three independent experiments panel, (**G-I**) data representative of two independent experiments

The expression of CD39 is associated with antigen experience, and when highly upregulated further associated with a more exhausted state [201]. The IV heterologous prime boost group exhibits lower expression of CD39 (Figure 4.5E) as compared to the IM heterologous prime boost group ($p = 0.0208$) and IV SNP given twice ($p = 0.0082$). In addition, the frequency of stem-like cells is also higher in the IV heterologous prime boost group (Figure 4.5F) as compared to the IM heterologous prime boost group ($p = 0.0066$) and the IV SNP given twice group ($p = 0.0060$). Given that there is a higher number of cells per mg of tumor in the IV heterologous prime boost group, the higher frequency means that there is also a higher absolute number of stem-like cells in the tumor. Collectively, the phenotypic data would suggest that the Reps1-specific CD8 T cell response elicited by the IV heterologous prime boost group would outperform either of the other two vaccine strategies.

In addition to characterizing the CD8 T cell response, it is useful to assess the Tregs in the tumor. The IV heterologous prime boost group was the only group to exhibit a decrease in the number of Tregs per mg of tumor as compared to the naïve mice (Figure 4.5G, $p = 0.0310$). A high ratio of CD8 T cells to Tregs has positive prognostic value in ovarian cancer [202] and is likely associated with a more pro-inflammatory anti-tumor immune response [203]. All of the vaccine groups significantly increased the ratio of CD8 T cells to Tregs in the tumor as compared to naïve mice (Figure 4.5H). However, the IV heterologous prime boost group resulted in the greatest increase of the CD8 T cell to Treg ratio, and was significantly higher than the IM heterologous prime boost group ($p = 0.0407$) and the IV SNP given twice group ($p = 0.0436$). This trend is also seen when looking at the ratio of Reps1 tetramer-specific CD8 T cells to Tregs in the tumor (Figure 4.5I).

Altogether, the tissue data suggests that the IV heterologous prime boost group should outperform both of the vaccination strategies. The observation that anti-tumor control is equivalent between these groups suggests a T cell independent factor may be limiting the efficacy.

4.3.4 Immunogenicity and tumor regression trends observed with Reps1 are replicated with the neoantigen Adpgk in the context of IV heterologous prime boost

In order to show that the trends observed with heterologous prime boost are not antigen-specific, the same therapeutic experiments were repeated using another MC38 neoantigen known as Adpgk [168]. In previous studies in the Seder lab, Adpgk has proven to be less protective than Reps1, typically clearing 20-30% of tumors when given as IV SNP twice.

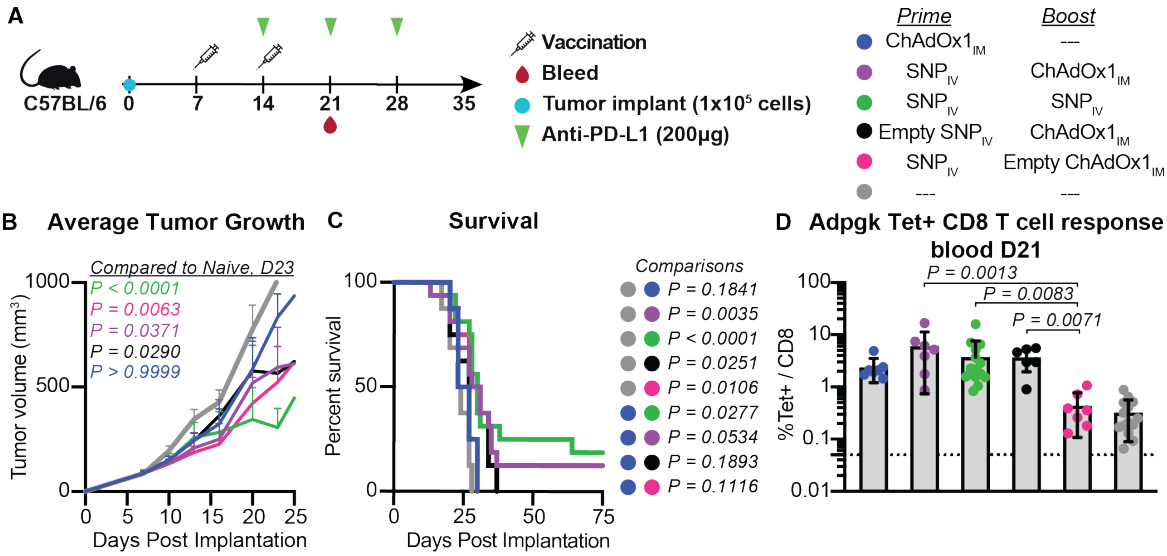

Figure 4.6 IM heterologous prime boost targeting Adpgk elicits modest MC38 tumor regression (**A**) Therapeutic study treatment and sampling schedule, legend for all figure panels. (**B**) Tumor growth curves plotted as mean + SEM. (**C**) Survival curves for all groups (**D**) Immunogenicity at day 21 measured by tetramer staining PBMCs using an Adpgk-specific tetramer. **Stats:** (**B**) Two way ANOVA with Bonferroni correction for multiple comparisons. (**C**) Mantel-Cox Log-rank test (**D**) Data represented as mean ± standard deviation, Kruskal-Wallis test with Dunn's correction for multiple comparisons.

As before, the IM heterologous prime boost vaccination strategy was tested in the therapeutic setting (Figure 4.6A). The groups are identical to those in section 4.3.1. In contrast to the result of the Reps1 study, the IM heterologous prime boost provided modest tumor growth rate reduction (Figure 4.6B). Though there was a significant decrease in the tumor volume at D23 between the IM heterologous prime boost mice and naïve mice (untreated – except for checkpoint inhibitor, $p = 0.0371$), none of the vaccine group tumor growth curves appear to regress. The only group that did not have a significant difference in tumor volume to the naïve was the IM ChAdOx1 prime alone group ($p > 0.9999$), which was consistent with the Reps1 study.

In terms of survival, all groups exhibited significant improvements in survival compared to the naïve group (Figure 4.6C), except for the IM ChAdOx1 prime alone group ($p = 0.1841$). In contrast to the Reps1 study, the IM heterologous prime boost group using Adpgk did not improve survival as compared to IM ChAdOx1 alone prime ($p = 0.0534$). In addition to the lackluster protection data when targeting Adpgk with IM heterologous prime boost, there were no significant differences between most of the vaccinated groups in terms of Adpgk-specific CD8 T cell response magnitude in the blood at day 21. All groups had a higher magnitude response than the SNP followed by empty ChAdOx1 IM group, except for the IM ChAdOx1 alone prime (Figure 4.6D).

Given the lack of significant differences between treatment groups when targeting Adpgk, it would be difficult to tease apart any treatment specific differences in survival and identify key factors mediating protection. For this reason, the IM heterologous prime boost strategy was not further studied when targeting Adpgk.

In contrast to the limited protection with IM heterologous prime boost, the IV heterologous prime boost groups displayed clear evidence of tumor regression and tumor clearance when targeting Adpgk. As seen with Reps1, IV Adpgk ChAdOx1 prime alone

did not reduce tumor growth ($p > 0.9999$) or improve survival ($p = 0.3512$) as compared to naïve mice (Figures 4.7B-C). However, all other vaccinated groups exhibited some level of reduced tumor growth and improved survival compared to naïve. In addition, all vaccinated groups had reduced tumor growth and improved survival as compared to the IV ChAdOx1 prime alone group. The IV heterologous prime boost group also improved survival as compared to the empty SNP followed by IV Adpgk ChAdOx1 ($p = 0.0149$), but was equivalent to Adpgk SNP followed by IV empty ChAdOx1. This was the same trend seen in the Reps1 IV heterologous prime boost study, and implies the requirements of a SNP prime that must provide antigen to prime a CD8 T cell response in order to see protection. However, encoding the antigen in the virus may not be essential for protection.

The IV heterologous prime boost group elicited the highest magnitude Adpgk tetramer-specific CD8 T cell response, and was significantly higher than all other groups except for the IV ChAdOx1 alone group (Figure 4.7D). In contrast to the IM groups, the IV SNP given twice did not elicit a higher magnitude CD8 T cell response than IV Adpgk SNP followed by empty ChAdOx1 IV – which is the same trend as was seen with Reps1. This suggests that the IV empty ChAdOx1 may support the expansion of CD8 T cell responses in an antigen-agnostic way, that is not seen with IM empty ChAdOx1. There is a significant negative correlation between the magnitude of the Adpgk specific CD8 T cell response at day 21 and tumor volume at day 24 (Figure 4.7E, $r = -0.3813$, $p = 0.0139$).

In addition to the similarity of the Adpgk magnitude trends to the data collected from the Reps1 experiments, the phenotypic analysis of PD-1 and Tim-3 also reflect the phenotypic analysis performed in the Reps1 experiments. There is almost no difference in the expression of PD-1 between the different vaccination groups (Figure 4.7F) nor any difference in Tim-3 expression between most groups (Figure 4.7G). In both cases, it is the

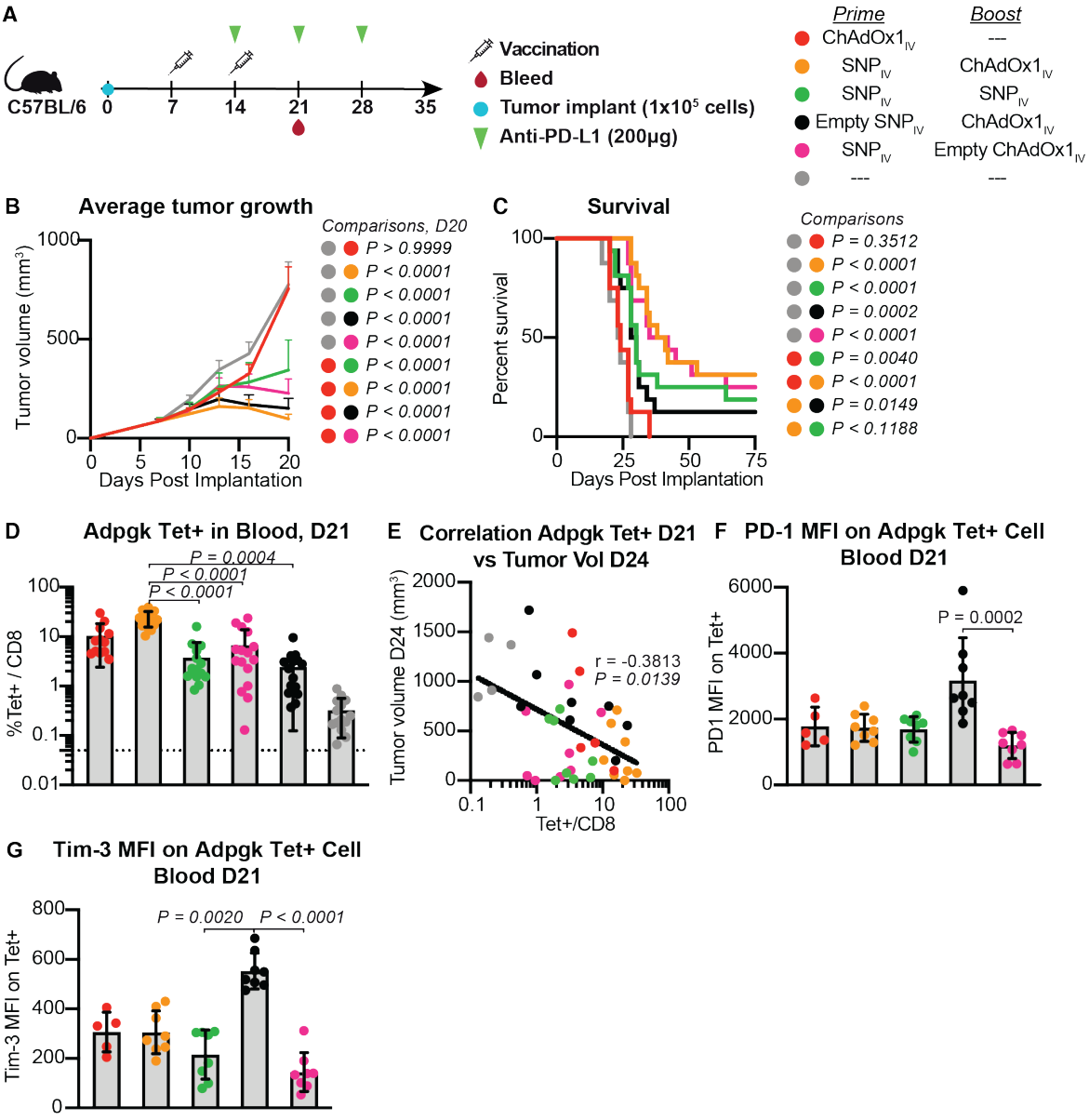

Figure 4.7 IV heterologous prime boost targeting Adpgk improves protection compared to IV ChAdOx1 alone.
(**A**) Therapeutic study treatment and sampling schedule, legend for all figure panels. (**B**) Tumor growth curves plotted as mean + SEM. (**C**) Survival curves for all groups, compiled from 2 studies. (**D**) Immunogenicity at day 21 measured by tetramer staining PBMCs using a Adpgk-specific tetramer (**E**) Correlation of Adpgk specific response at day 21 and tumor volume at day 25, plotted with line of best fit. (**F**) MFI of PD-1 on Adpgk-tetramer positive cells in blood. (**G**) MFI of Tim-3 on Adpgk-tetramer positive cells in blood. **Stats:** (**B**) Two way ANOVA with Bonferroni correction for multiple comparisons. (**C**) Mantel-Cox Log-rank test (**D, F, G**) Data represented as mean ± standard deviation, Kruskal-Wallis test with Dunn's correction for multiple comparisons. (**E**) Spearman's Rank correlation. Data representative of two independent experiments.

empty SNP group followed by Adpgk ChAdOx1 that has slightly elevated expression of both PD-1 and Tim-3.

Taken together, the data collected by targeting Adpgk to treat MC38 tumors therapeutically is generally consistent with the observations made in the Reps1 experiments, particularly with the IV ChAdOx1 groups. The protection afforded by the Adpgk SNP followed by empty ChAdOx1 group further supports the idea that there may be an effect of using IV ChAdOx1 that is independent of its encoding the target antigen in ChAdOx1. Given that the heterologous prime boost group did not significantly outperform the positive control or the Adpgk SNP followed by empty ChAdOx1 IV (as seen with Reps1), it seemed unnecessary to investigate immunological differences in the tissue as this would be unlikely to reveal any further differences not seen with Reps1.

4.3.5 Heterologous prime boost does not provide any added therapeutic benefit in the TC-1 lung cancer model as compared to ChAdOx1 or SNP alone.

To ensure that therapeutic efficacy was not an artefact of testing heterologous prime boost in MC38, the same therapeutic studies were undertaken by using the TC-1 lung cancer model. Previous data has shown that eliciting CD8 T cell responses against the immunodominant epitopes in E6 and E7 HPV proteins can promote tumor regression in this model [186]. For this reason, both immunodominant epitopes were encoded into a single ChAdOx1 vector and SNP vaccines**.**

Mice were implanted with TC-1 tumor cells in the flank and then vaccinated 7 and 14 days later to test IM heterologous prime boost (Figure 4.8A). Checkpoint inhibitor (αPD-L1) was administered once weekly via intraperitoneal route starting at the time of boost for a total of 3 treatments. All groups exhibited a reduction in tumor volume at day 22 compared to unvaccinated mice (Figure 4.8B, $p < 0.0001$ for all). In addition, all

groups that received an E6/E7 SNP prime also had significantly reduced tumor volumes at day 22 as compared to those mice that received empty SNP prime ($p < 0.0001$ for all). There were no discernible differences in tumor growth between the groups that received E6/E7 SNP prime over time, indicating that IV SNP, IM E6/E7 ChAdOx1 and IM empty ChAdOx1 boosts are all equivalent in terms of tumor control.

In addition, the empty SNP prime followed by E6/E7 ChAdOx1 boost group exhibits a reduction in tumor growth after day 22, which coincides with the approximate time when E6/E7-specific CD8 T cell responses would start to appear. This reduction between days 22 – 30 is approximately a week delayed as compared to the mice that received an E6/E7 SNP prime, further supporting that this reduction is likely due to newly primed E6/E7 CD8 T cell responses. However, the protection is short-lived, likely due to the tumors being much larger by the time an E6/E7 CD8 T cell response is primed in the empty SNP followed by E6/E7 ChAdOx1.

The trends in tumor growth match entirely the trends seen in the survival curves (Figure 4.8C). All groups had significantly improved survival as compared to the untreated mice ($p < 0.0001$ for all). In addition, all groups also had significantly improved survival when compared to the empty SNP followed by E6/E7 ChAdOx1. However, there were no statistically significant differences in survival between the IM ChAdOx1 prime alone, the heterologous prime boost group, the IV SNP given twice group or the IV SNP followed by empty ChAdOx1 IM. This is similar to what was observed with the Adpgk IM heterologous prime boost treatment. However, in stark contrast to the Adpgk IM heterologous prime boost, there is significant tumor control in all of these groups.

To assess the E6 and E7 CD8 T cell response in these mice, blood was sampled at day 21 and then split into two pools for a peptide restimulation assay with either E6 or E7. The production of IFNγ was used to identify antigen-specific CD8 T cell responses. There

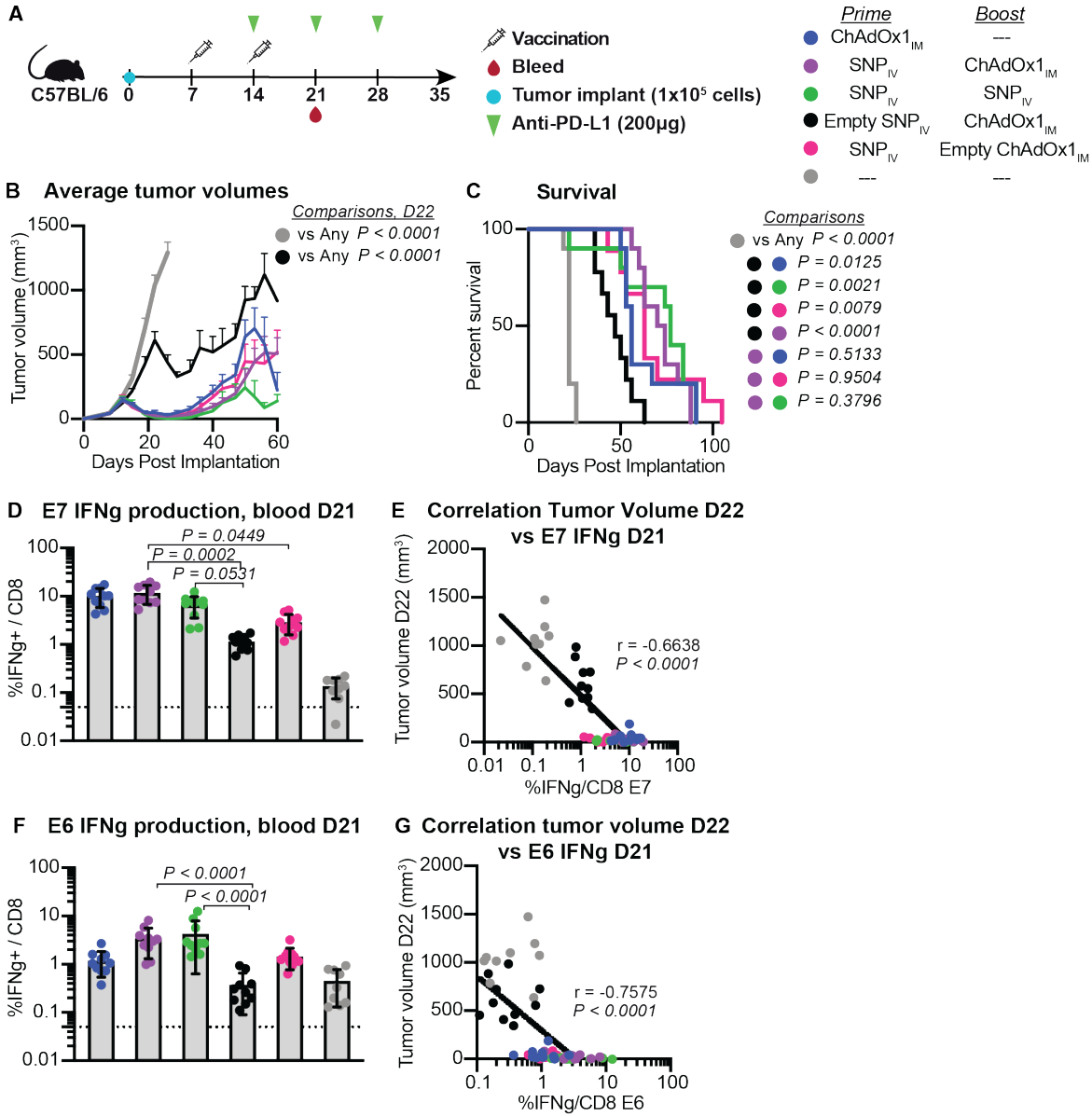

Figure 4.8 IM heterologous prime boost elicits E6/E7 specific CD8 T cell responses and provides comparable protection to IM ChAdOx1 alone.
(**A**) Therapeutic study treatment and sampling schedule, legend for all figure panels. (**B**) Tumor growth curves plotted as mean + SEM. (**C**) Survival curves for all groups (**D**) Immunogenicity at day 21 measured as IFNγ production following peptide restimulation using E7 peptide encoded in SNP and ChAdOx1 (**E**) Correlation of E7 specific response at day 21 and tumor volume at day 22, plotted with line of best fit. (**F**) Immunogenicity at day 21 measured as IFNγ production following peptide restimulation using E6 peptide encoded in SNP and ChAdOx1 (**G**) Correlation of E6 specific response at day 21 and tumor volume at day 22, plotted with line of best fit. **Stats:** (**B**) Two way ANOVA with Bonferroni correction for multiple comparisons. (**C**) Mantel-Cox Log-rank test (**D, F**) Data represented as mean ± standard deviation, Kruskal-Wallis test with Dunn's correction for multiple comparisons. (**E, G**) Spearman's Rank correlation. Data representative of two independent experiments.

was no difference in magnitude of the E7 response between the heterologous prime boost group, the IM ChAdOx1 prime alone group and the IV SNP given twice (Figure 4.8D). The heterologous prime boost group did have an increased magnitude of E7 specific CD8 T cells as compared to both the empty SNP followed by E6/E7 ChAdOx1 group ($p = 0.0002$) and the E6/E7 SNP followed by empty ChAdOx1 group ($p = 0.0449$). This indicates that antigen is required in both vaccinations to achieve the highest magnitude CD8 T cell response. Correlating the E7 CD8 T cell response at day 21 with tumor volume at day 22 reveals a strong negative correlation between magnitude of the E7 response and tumor volume (Figure 4.8E, $r = -0.6638$, $p < 0.0001$). This negative correlation between magnitude of the response and tumor volume is consistent with the trends in MC38 with both Reps1 and Adpgk.

The E6 response was similarly characterized in these mice. In general, the E6 response is lower in magnitude than the E7, for example:

- IM ChAdOx1 alone, E7 average = 10%, E6 average = 1%
- Heterologous prime boost, E7 average = 10%, E6 average = 4%
- IV SNP given twice, E7 average = 8%, E6 = 4%

Regardless of being lower in magnitude, the trends remain similar to E7. There is no significant difference between the IM ChAdOx1 alone, the heterologous prime boost group or the IV SNP given twice group (Figure 4.8F). The heterologous prime boost group continues to elicit a higher magnitude response than the empty SNP followed by E6/E7 ChAdOx1 ($p <0.0001$). The negative correlation between the E6 response and tumor volume (Figure 4.8G) is also significant ($r = -0.7575$, $p < 0.0001$).

Heterologous prime boost using E6/E7 ChAdOx1 IV was also tested, using the same experimental plan as before (Figure 4.9A). One notable difference however, was the exclusion of the empty SNP followed by IV E6/E7 ChAdOx1. This group was excluded

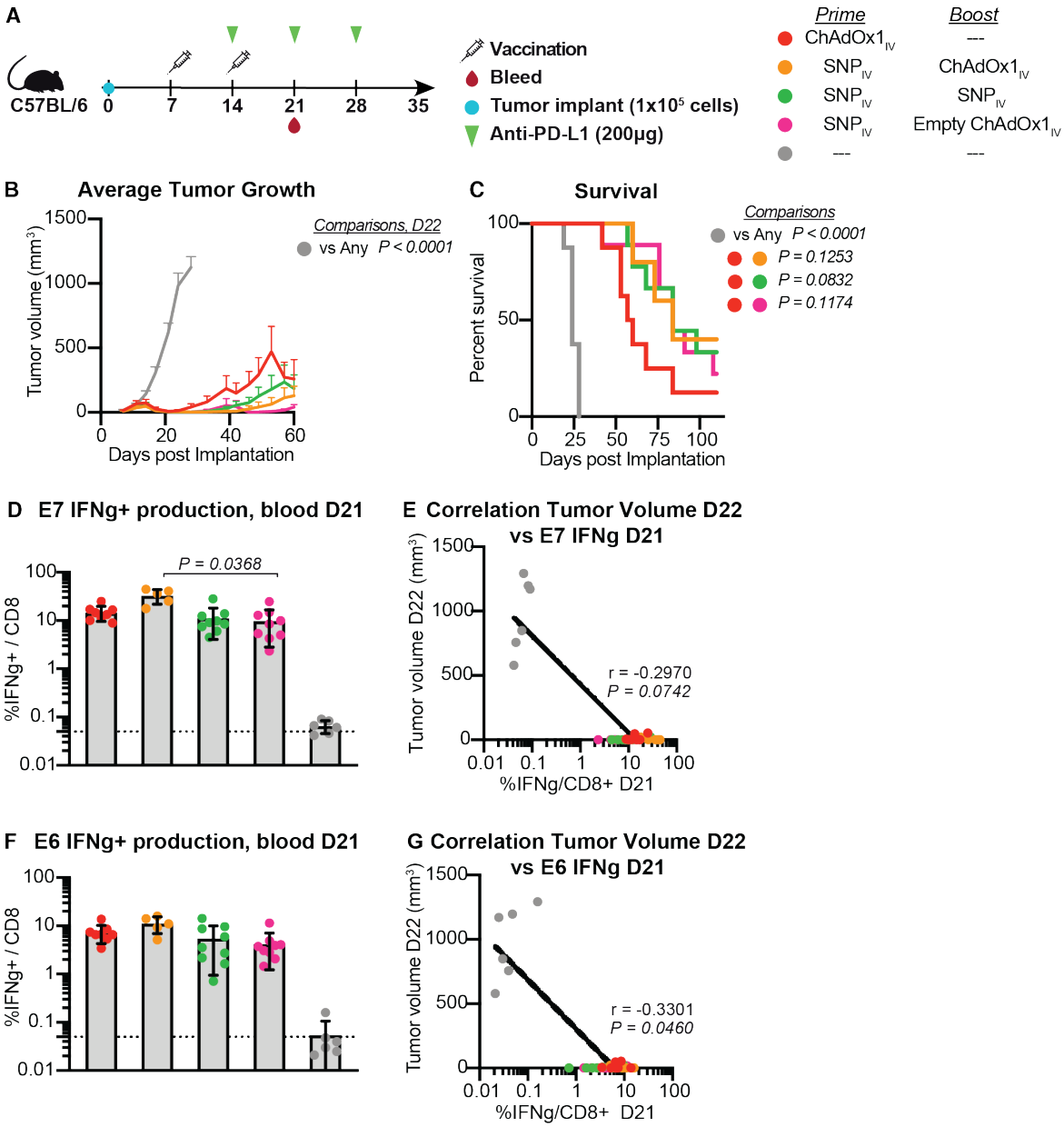

Figure 4.9 IV heterologous prime boost elicits E6/E7 specific CD8 T cell responses and provides comparable protection to IV ChAdOx1 alone.
(**A**) Therapeutic study treatment and sampling schedule, legend for all figure panels. (**B**) Tumor growth curves plotted as mean + SEM. (**C**) Survival curves for all groups (**D**) Immunogenicity at day 21 measured as IFNγ production following peptide restimulation using E7 peptide encoded in SNP and ChAdOx1 (**E**) Correlation of E7 specific response at day 21 and tumor volume at day 22, plotted with line of best fit. (**F**) Immunogenicity at day 21 measured as IFNγ production following peptide restimulation using E6 peptide encoded in SNP and ChAdOx1 (**G**) Correlation of E6 specific response at day 21 and tumor volume at day 22, plotted with line of best fit. **Stats:** (**B**) Two way ANOVA with Bonferroni correction for multiple comparisons. (**C**) Mantel-Cox Log-rank test (**D, F**) Data represented as mean ± standard deviation, Kruskal-Wallis test with Dunn's correction for multiple comparisons. (**E, G**) Spearman's Rank correlation. Data representative of one experiment.

because at the time of boost vaccination, the IV heterologous prime boost group was vaccinated first and it was noticed that 4 out of the 9 animals that received the IV E6/E7 ChAdOx1 died suddenly shortly after vaccination. The decision was made not to boost the empty SNP primed mice with the IV E6/E7 ChAdOx1, given this sudden mortality. This mortality was not seen with any other preparation of ChAdOx1, and may represent a batch specific problem for this viral stock. However, the mice receiving the empty ChAdOx1 IV had already been vaccinated and there were no sudden fatalities in that group. Something about the IV E6/E7 ChAdOx1 boost was not well tolerated in these mice, and it is specifically at the time of boost as the IV E6/E7 ChAdOx1 prime group also did not experience any sudden mortalities. The data presented herein therefore relies on an IV heterologous prime boost group with only 5 animals and is representative of a single experiment. Despite these caveats, this data still provides some insights into heterologous prime boost.

All vaccinated groups displayed reduced tumor growth as compared to the untreated mice (Figure 4.9B, $p < 0.0001$ for all). There were no significant differences in tumor growth between the different vaccinated groups. These trends are supported by the survival curves (Figure 4.9C), where all groups improve survival compared to the untreated ($p < 0.0001$), but there are no significant differences in survival between any of the vaccinated groups.

The E7 response is of a similar magnitude between all vaccine groups (Figure 4.9D) except for between the IV heterologous prime boost group and the IV E6/E7 SNP followed by IV empty ChAdOx1 ($p = 0.0368$). The lack of statistically significant differences may be due to the low number of mice sampled in the IV heterologous prime boost group, as the trend supports a higher magnitude in this group (average heterologous prime boost E7 response = 33.1%, average IV ChAdOx1 prime alone E7 response =

14.7%). The E7 response at day 21 is negatively correlated with tumor volume at day 22 (Figure 4.9E), however it is not significant ($r = -0.2970$, $p = 0.0742$). The lack of a significant correlation could be due to the missing empty SNP followed by IV ChAdOx1 group data, as this would likely have been characterized by larger tumor volumes and lower magnitude CD8 T cell responses - as seen in the IM ChAdOx1 study.

Similarly, there were no differences in the magnitude of the E6 response between the vaccine groups when using IV ChAdOx1 (Figure 4.9F). The E6 response at day 21 is significantly negatively correlated with tumor volume at day 22 (Figure 4.9G, $r = -0.3301$, $p = 0.0460$). Despite the unexpected loss of mice following IV E6/E7 ChAdOx1 boost, the tumor growth and survival was increased in all vaccination groups and correlated with magnitude of the E6 and E7 response. Further experiments would be required to understand the factors underlying the fatalities observed in the IV heterologous prime boost group.

4.3.6 IV heterologous prime boost slightly outperforms ChAdOx1 alone when vaccinating against Trp1 to promote B16F10 tumor regression.

The B16F10 melanoma model is more aggressive than either the MC38 or TC-1 model. Like TC-1, the tumors do not respond to the use of checkpoint inhibitor alone but require a CD8 T cell response to be primed by vaccination or the infusion of antigen-specific CD8 T cells to mediate protection [204]. One of the vaccination targets is the self-antigen Trp-1 [186]. As a more stringent model, it seemed ideal to attempt to separate the different vaccine groups in terms of efficacy, as the heterologous prime boost groups have thus far only performed as well as the positive control (IV SNP given twice).

Given the aggressiveness of the model, the treatment timeline is accelerated with vaccination beginning 2 days after inoculation of the cells in the flank (Figure 4.10A).

Checkpoint inhibitor starts at day 9, with the boost vaccination and is given once weekly for a total of three doses. As this model is more aggressive, the goal of this study was to determine if the IV heterologous prime boost vaccination strategy (predicted to give highest magnitude Trp-1 response) provides sufficient protection to warrant further investigation.

Compared to the untreated animals, all vaccine groups delayed tumor growth significantly based on tumor volumes at day 19 (Figure 4.10B, $p < 0.0001$ for all). In addition, all SNP primed groups delayed tumor growth significantly compared to the IV ChAdOx1 prime alone group (SNP IV given twice – $p = 0.0028$, IV heterologous prime boost – $p = 0.0005$, SNP prime followed by IV empty ChAdOx1 boost – $p = 0.0373$). These trends are supported by the survival curve, where all vaccinated groups improved protection compared to the untreated group (Figure 4.10C, $p < 0.0001$). Both the IV SNP given twice and the IV heterologous prime boost group improved survival compared to the IV ChAdOx1 alone group ($p < 0.0001$, $p = 0.0022$, respectively). As seen with Reps1, Adpgk, and E6/E7, the IV heterologous prime boost group did not improve survival relative to the IV SNP followed by IV empty ChAdOx1 group. Only one mouse in the SNP IV given twice group cleared its tumor, all other mice in vaccinated groups only exhibited a delay in tumor growth.

The magnitude of the Trp-1 response was measured by tetramer staining (Figure 4.10D). The IV heterologous prime boost group elicited the highest magnitude CD8 T cell response against Trp-1 as compared to all other groups (IV ChAdOx1 prime – $p = 0.0186$, IV SNP given twice – $p = 0.0175$, SNP followed by empty ChAdOx1 – $p < 0.0001$). There was a significant negative correlation between magnitude of the Trp-1 specific CD8 T cell response at day 16 and tumor volume at day 19 (Figure 4.10E, $r = -0.4959$, $p = 0.0004$).

This negative correlation is consistent with the negative correlations seen between antigen-specific CD8 T cell response and tumor volume in other models.

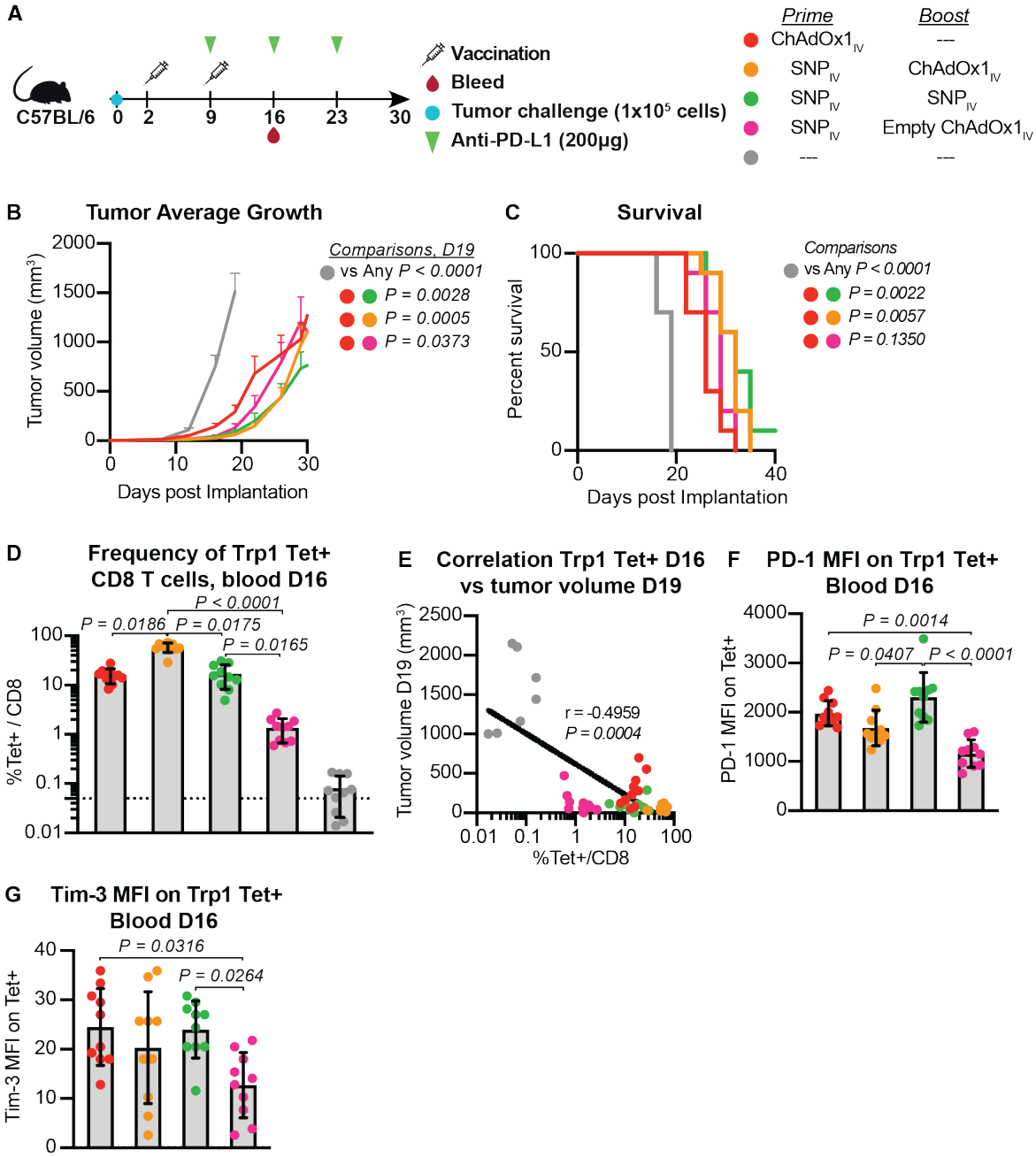

Figure 4.10 IV heterologous prime boost targeting Trp1 improves survival with B16F10 compared to IV ChAdOx1 alone.
(**A**) Therapeutic study treatment and sampling schedule, legend for all figure panels. (**B**) Tumor growth curves plotted as mean + SEM. (**C**) Survival curves for all groups (**D**) Immunogenicity at day 16 measured by tetramer staining PBMCs using a Trp1-specific tetramer (**E**) Correlation of Trp1 specific response at day 21 and tumor volume at day 19, plotted with line of best fit. (**F**) MFI of PD-1 on Trp1-tetramer positive cells in blood. (**G**) MFI of Tim-3 on Trp1-tetramer positive cells in blood. **Stats:** (**B**) Two way ANOVA with Bonferroni correction for multiple comparisons. (**C**) Mantel-Cox Log-rank test (**D, F, G**) Data represented as mean ± standard deviation, Kruskal-Wallis test with Dunn's correction for multiple comparisons. (**E**) Spearman's Rank correlation. Data representative of one experiment.

The expression of PD-1 and Tim-3 on the Trp-1 specific CD8 T cells was also assessed to determine if there were any different trends as compared to what had been previously described for Reps1 and Adpgk specific CD8 T cell responses. The expression of PD-1 was significantly increased in the IV SNP given twice group (Figure 4.10F) as compared to either the IV heterologous prime boost group ($p = 0.0407$) and the IV SNP followed by empty ChAdOx1 group ($p < 0.0001$). This is in contrast to the Reps1 and Adpgk specific responses where there was no difference between these groups (Figures 4.2F, 4.7F). These modest differences in PD-1 expression do not appear to have any bearing on protection against B16F10. The expression of Tim-3 is similar between most of the vaccinated groups (Figure 4.10G), the only differences are between the IV SNP followed by empty ChAdOx1 group and either IV SNP given twice ($p = 0.0264$) or IV ChAdOx1 prime alone ($p = 0.0316$).

Together these data are consistent with the trends observed with Reps1 and Adpgk in the MC38 tumor model. The magnitude of the antigen-specific response is negatively correlated with tumor volume and the phenotype of the antigen-specific cells is similar in the blood one week post boost vaccination between the different vaccine groups. Despite the high magnitude of Trp-1 specific CD8 T cells elicited by the IV heterologous prime boost group, tumor growth and survival were not significantly better than IV SNP given twice. For this reason, further studies testing IM heterologous prime boost or tissue level immunological assessment was not undertaken as it was unlikely to yield new insights.

4.4 Conclusions and discussion

4.4.1 IM heterologous prime boost

Heterologous prime boost using IM ChAdOx1 improved tumor control against MC38 (with both Reps1 and Adpgk) and against TC-1 as compared to untreated mice. However, IM heterologous prime boost only improved survival compared to IM ChAdOx1 alone when targeting Reps1. When vaccinating against Reps1, IM heterologous prime boost elicited higher magnitude CD8 T cell responses than IM ChAdOx1 alone. This was not the case with Adpgk, E6 or E7 and may underpin the lack of improved protection in the heterologous prime boost group as compared to the IM ChAdOx1 alone. In all cases, there was a negative correlation between tumor size and antigen-specific CD8 T cell response. The limitation on therapeutic efficacy was therefore likely due to the the lack of significant boosting of SNP primed responses following IM ChAdOx1 boost. The extent to which this inefficient boosting effect would translate to higher mammals is unknown, but may be a reason to favor IV ChAdOx1 vaccination.

4.4.2 IV heterologous prime boost

Heterologous prime boost using IV ChAdOx1 improved both tumor regression and survival compared to untreated mice across MC38, TC-1 and B16F10 for all antigens tested. In addition, the IV heterologous prime boost group outperformed the IV ChAdOx1 prime alone group in both MC38 and B16F10. The lack of improvement in TC-1 may be due to the sudden unexplained mortality in the IV E6/E7 ChAdOx1 boosted group, which reduced the number of subjects and prevented further studies from being performed, though it is notable that the trend towards better protection is present in both the tumor growth curves and survival.

The highest magnitude response was elicited by the IV heterologous prime boost group, though in the case of Adpgk, E6 and E7, this was not statistically different than the IV ChAdOx1 alone group. Regardless, tumor volume was negatively correlated with magnitude of the antigen-specific response. There were limited differences in the expression of co-inhibitory receptors PD-1 and Tim-3 on the surface of antigen-specific-CD8 T cells for Reps1, Adpgk and Trp1. This suggests that the quality of antigen-specific CD8 T cells in the blood elicited by the different vaccine conditions has limited effects on the quality of the response.

One interesting observation in the IV ChAdOx1 studies is that the antigen-specific SNP followed by the empty ChAdOx1 IV provided equivalent protection to the heterologous prime boost group across all tumor models, despite exhibiting a much lower frequency of antigen-specific CD8 T cells. In contrast, the IV heterologous prime boost group was better than the empty SNP followed by IV antigen-ChAdOx1 for both Reps1 and Adpgk. Together, these two trends suggest that priming the CD8 T cell response with SNP is essential, but encoding the antigen in ChAdOx1 for boosting may not be. There may be a beneficial effect of simply providing empty ChAdOx1 IV, as this effect is not seen with empty ChAdOx1 IM.

4.4.3 CD8 T cell response in spleen and tumor

Both the IV and IM heterologous prime boost groups displayed equivalent protection to the SNP IV given twice, despite having dramatically different magnitudes of antigen-specific CD8 T cell responses in the blood. Assessing the Reps1-specific response in the spleen revealed that the IV heterologous prime boost group continued to have an increase magnitude of Reps1-specific CD8 T cells, and this translated into a greater

absolute number of stem-like cells. There were limited phenotypic differences between these cells based on PD-1 and Tim-3 expression, suggesting similar quality of responses.

In the tumor, the IV heterologous prime boost group also elicited the greatest number of Reps1-specific CD8 T cells, and the phenotype was similar based on PD-1 and Tim-3. The expression of CD39 on IV heterologous prime boosted cells was markedly decreased compared to both other vaccine groups, though what exact functional significance this may have is unclear. As in the spleen, there was a higher frequency of stem-like cells in the tumor in the IV heterologous prime boost group.

Interestingly, there were fewer Tregs observed in the tumor following IV heterologous prime boost as compared to untreated mouse tumors. The ratio of CD8 T cells to Tregs was also highest in the IV heterologous prime boost group, though it was significantly elevated in both other vaccine groups as compared to untreated mice. This may indicate a vaccine-dependent promotion of CD8 T cell infiltration, which is not entirely made up of vaccine elicited cells, as the ratio of Reps1-tetramer positive cells to Tregs is considerably lower than that of total CD8s to Tregs. Together these data suggest that the IV heterologous prime boost group should outperform both of the other vaccine strategies. That this is not the case is currently not understood.

4.4.4 Limitations of studies

The immunological data presented in this chapter is all based on flow cytometry, which is a biased manner of collecting data as markers are only added based on previous understanding. It is possible that performing a single-cell RNA sequencing experiment on the IV heterologous prime boost elicited CD8 T cells at the tumor site and comparing to IV SNP given twice would reveal markers of dysfunctional T cells that might explain why

these two groups provide equivalent protection despite the larger magnitude response elicited by the IV heterologous prime boost strategy.

The rate of tumor growth in mouse tumor models is considerably faster than would be expected in the clinic, and results in accelerated treatment schedules in these studies. The effect of interval between prime and boost on tumor growth in these studies may be important, but due to the nature of the models cannot be further explored. Additionally, these studies focused exclusively on T cells but vaccination may be activating other immune cells that might explain these observations.

4.4.5 Future directions

The heterologous prime boost groups by both routes provided good tumor control. In particular, the IV ChAdOx1 heterologous prime boost also improved prognostic markers associated with positive response in immunotherapy and dramatically boosted antigen-specific CD8 T cell responses. Given these results, a non-human primate study will be undertaken to determine if IV heterologous prime boost elicits higher magnitude responses than IM heterologous prime boost or ChAdOx1 given alone by either route. Previous work with SNP in NHP has demonstrated that it primes low magnitude CD8 T cell responses when given subcutaneously (SC) [186]. For this reason, clinical development of SNP as a vaccine may require a heterologous prime boost approach to reach clinically relevant magnitudes of antigen-specific responses. If this boosting effect translates to non-human primates, then perhaps a clinical trial will be undertaken.

Separately, the efficacy of the heterologous prime boost approach using IV empty ChAdOx1 suggests an effect of vaccination that is independent of encoding the antigen in the vector. This could be due to activation of innate immunity and will be further described and explained in chapter 5.

Chapter 5

IV ChAdOx1 vaccination induced IFNα is required for efficacy in the therapeutic setting

5.1 Introduction

In Chapter 4, the ability of IV heterologous prime boost to mediate tumor regression was established across multiple models with different classes of tumor antigens. However, one interesting observation was that partial tumor regression was also observed in the heterologous prime boost group when administering an empty ChAdOx1 intravenously. This did not boost CD8 T cell responses but did improve survival compared to the untreated mice. This suggested a mechanism of action independent of the CD8 T cell boosting that was hypothesized to be required for optimal protection.

One possibility is that IV vaccination results in systemic activation of antigen presenting cells that may promote anti-tumor immunity. To probe this, it is important to understand which signaling pathways IV ChAdOx1 activates, and how the kinetics of activation compare to IV SNP for example – which is known to cause systemic activation of APCs [188]. Based on the recently described importance of IFNα for ChAdOx1 vaccine elicited CD8 T cell responses [205], and the known importance of IFNα for SNP vaccine elicited CD8 T cell responses, the role of IFNα in the therapeutic setting was selected as the primary avenue of investigation.

5.2 Chapter Aims

1. To characterize the kinetic of APC activation following IV vaccination
2. To determine the effects of vaccine elicited IFNα on therapeutic efficacy
3. To determine the effects of IV vaccine induced IFNα on APCs in the tumor, spleen and tumor-draining lymph node

5.3 Results

5.3.1 IV ChAdOx1 boost is required for tumor regression in the therapeutic setting, but does not need to encode the targeted antigen to enable this effect.

In order to determine that heterologous prime boost using the IV empty ChAdOx1 was indeed improving survival in the therapeutic setting, it was necessary to compare this to a SNP prime alone group. A therapeutic study (Figure 5.1A) was undertaken to test this. As expected, the IV SNP prime alone group exhibited a modest reduction in tumor growth as compared to untreated (Figure 5.1B). However, the heterologous prime boost groups with IV ChAdOx1 (encoding Reps1 or empty) both exhibited far better tumor control than the IV SNP prime alone group ($p < 0.0001$ for both, Figure 5.1B). These trends were reflected in the survival curves, where the SNP prime alone fared no better than untreated mice (Figure 5.1C). However, both the encoding and empty IV ChAdOx1 boosted groups improved survival as compared to SNP prime alone ($p < 0.0001$, $p = 0.0116$, respectively).

The mice were bled at day 21, one week post boost vaccination to compare Reps1-specific T cell responses between vaccinated groups. As expected, the heterologous prime boost group with the IV Reps1-encoding ChAdOx1 elicited the highest magnitude CD8 T cell response (Figure 5.1D), and was significantly greater than both the empty ChAdOx1 heterologous prime boost group ($p = 0.0011$) and SNP prime alone group ($p = 0.0018$). There was no difference in the magnitude of the CD8 T cell response between the IV SNP prime alone group and the empty ChAdOx1 heterologous prime boost group ($p > 0.9999$). In addition, comparing the expression of PD-1 on the Reps1-specific CD8 T cells revealed no significant differences between vaccine groups (Figure 5.1E).

These results suggest that the difference in tumor growth reduction and survival between the IV empty ChAdOx1 heterologous prime boost group and the IV SNP prime

alone group may not be based on the CD8 T cell response. Instead, this effect may be mediated by the activation of innate immunity by systemic administration of ChAdOx1.

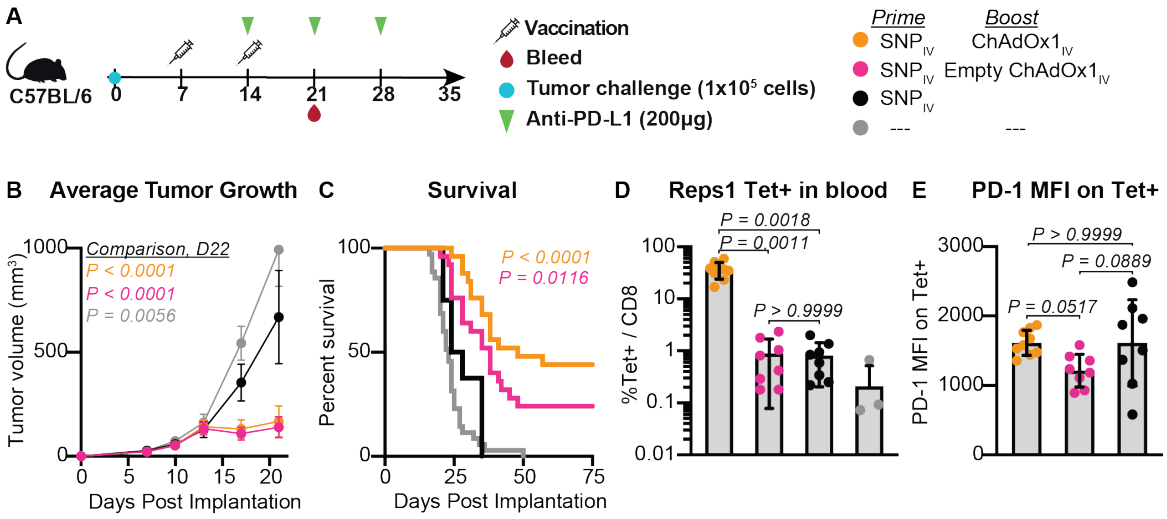

Figure 5.1 Empty ChAdOx1 boost improves tumor regression compared to SNP prime alone. (**A**) Therapeutic study treatment and sampling schedule, legend for all figure panels. (**B**) Tumor growth curves plotted as mean ± SEM. (**C**) Survival curves for all groups, compiled from 3 studies. (**D**) Immunogenicity at day 21 measured by tetramer staining PBMCs using a Reps1-specific tetramer. (**E**) MFI of PD-1 on Reps1-tetramer positive cells in blood. **Stats:** (**B**) Two way ANOVA with Bonferroni correction for multiple comparisons, p-value compared to SNP prime alone. (**C**) Mantel-Cox Log-rank test, p-value compared to SNP prime alone (**D,E**) Data represented as mean ± standard deviation, Kruskal-Wallis test with Dunn's correction for multiple comparisons.

5.3.2 Priming CD8 T cell responses with ChAdOx1 is dependent on Sting and IFNα

Other groups have recently published on the requirement for pDC production of IFNα to prime CD8 T cell responses following ChAdOx1 vaccination [205]. IV administration of SNP is also known to elicit a strong type I IFN response, which is required for eliciting a CD8 T cell response [188]. Given that both vaccinations converge on IFNα, the production of IFNα following IV vaccination with SNP or ChAdOx1 was assessed in mice over a three-day period. Mice were vaccinated intravenously either 72 hours, 24 hours or 6 hours prior to bleeding for serum collection (Figure 5.2A). The standard therapeutic dose for each vaccine was used.

Both vaccines elicited transient production of IFNα, which peaked at 6 hours and was undetectable by 3 days (Figure 5.2B). The IV ChAdOx1 elicited a higher amount of

IFNα at peak ($p < 0.0001$), and interestingly still had detectable levels of IFNα 24 hours after vaccination, whereas the SNP elicited IFNα was undetectable by 24 hours ($p < 0.0001$). The production of CXCL-10 (IP-10) can also be assessed by ELISA. Increased levels of CXCL-10 are the result of functional IFNα signaling [206]. As expected, the levels of CXCL-10 followed the trends of the IFNα (Figure 5.2C). IV ChAdOx1 elicited a higher amount of CXCL-10 at peak ($p = 0.0156$) and 24 hours ($p = 0.0388$) as compared to IV SNP, with undetectable levels at 72 hours.

In addition to IFNα, SNP is also known to elicit IL-12, which skews T cells towards a Th1 type response and may be beneficial in the context of anti-tumor immunity [188]. For comparison, the production of IL-12 following IV ChAdOx1 vaccination was tested. IV ChAdOx1 elicited very little IL-12, as based on the IL-12p40 ELISA and followed the same kinetic as the IFNα and CXCL-10 (Figure 5.2D).

To follow up on the cytokine data, wild-type (WT) mice and IFNα receptor (IFNar) knock-out (KOs) mice were vaccinated with IV ChAdOx1 to determine if IFNα produced by vaccination was required for CD8 T cell response priming (Figure 5.2E). IL-12 KOs were also vaccinated, despite the low IL-12 production to determine if this had any effect on CD8 T cell response magnitude. Mice were bled 14 days after vaccination to assess T cell responses in the blood. The IL-12 KO did not display any loss in magnitude of CD8 T cell response as compared to the WT mice. However, the IFNαr KO mice failed to prime a response following vaccination as they had responses similar to naïve mice ($p = 0.8439$). This finding was consistent with works published earlier in 2021 [188].

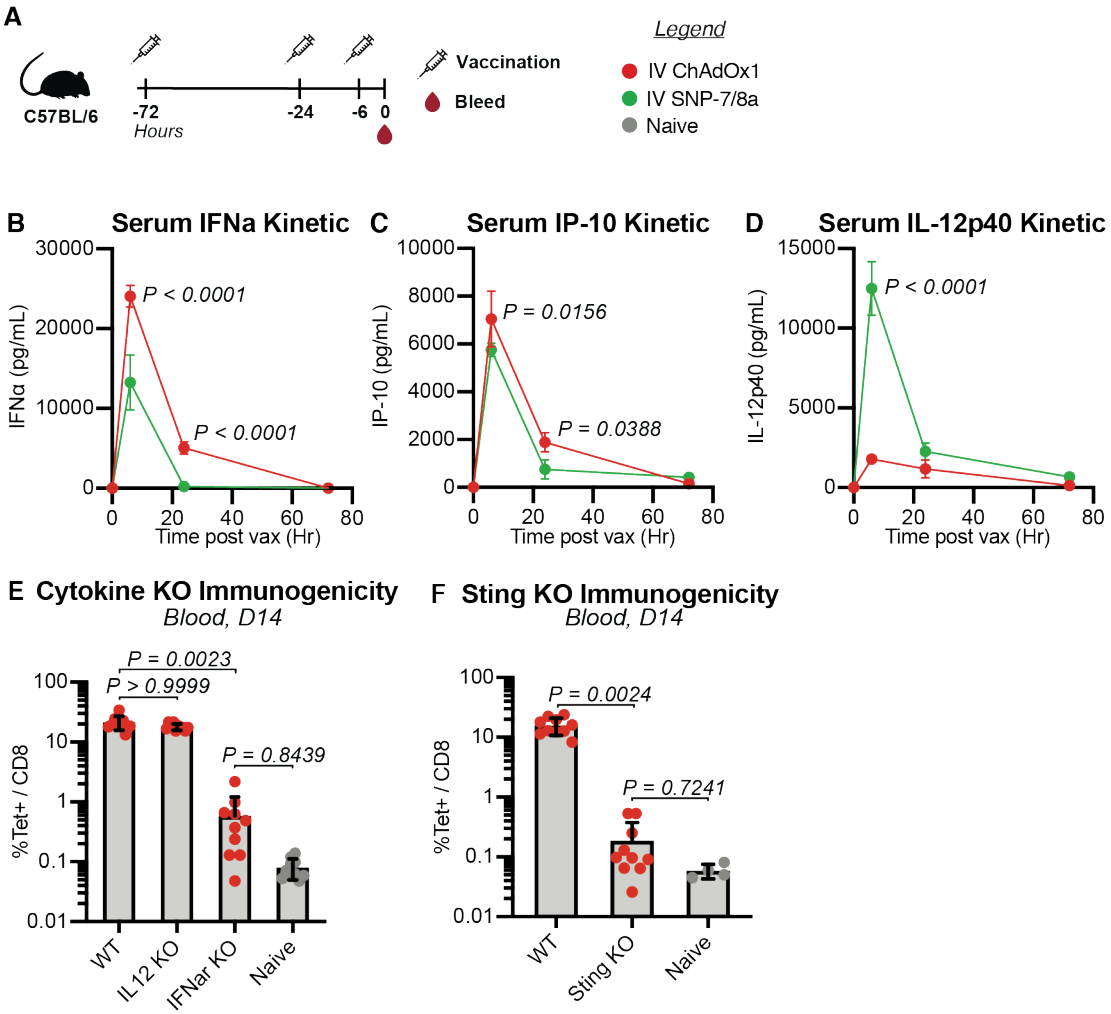

Figure 5.2 Priming CD8 T cell responses with ChAdOx1 is dependent on Sting and IFNα, but not IL-12.(**A**) Groups of mice were vaccinated in a staggered fashion with IV ChAdOx1 or IV SNP either 72, 24 or 6 hours prior to bleeding. (**B-D**) Cytokine production 6, 24, and 72 hours after IV vaccination (**B**) IFNα (**C**) IP-10 (**D**) IL-12p40. (**E**) Immunogenicity 14 days post IV ChAdOx1 vaccination of wild-type, IL-12 KO and IFNar KO mice - measured by tetramer staining PBMCs. (**F**) Immunogenicity 14 days post IV ChAdOx1 vaccination of wild-type and Sting KO mice - measured by tetramer staining PBMCs. **Stats:** (**B-F**) Data represented as mean ± standard deviation, Kruskal-Wallis test with Dunn's correction for multiple comparisons.

Quinn and colleagues published on the requirement of functional Sting signaling to prime CD8 T cell responses following vaccination with species E adenoviruses [207]. ChAdOx1 is also a species E adenovirus, but the requirement of Sting signaling is unknown. To test the requirement of Sting for ChAdOx1 CD8 T cell priming, Sting KO were vaccinated and bled 14 days later to assess T cell responses in the blood. Similar to the IFNα KOs, the Sting KOs failed to prime a CD8 T cell response that was greater than

naïve mice (Figure 5.2F, p = 0.7241). Collectively, the data suggests that ChAdOx1 activates Sting dependent IFNα production, which is required for priming CD8 T cell responses.

5.3.3 IV ChAdOx1 vaccination causes transient activation of DCs in the spleen, similar to IV SNP

The transient production of IFNα suggests that IV vaccination with ChAdOx1 or SNP likely causes transient activation of APCs systemically. Mice were vaccinated as before (Figure 5.3A), and were sacrificed to collect spleens from the mice. Spleens were processed into single cell suspensions and stained with a flow cytometry panel to assess activation of DCs. The expression of co-stimulatory molecules CD80 and CD86 are used as markers of activation on DC subsets [75]. In addition, the expression of CCR7 was used as a marker for maturation, which is upregulated on activated DCs that are homing towards secondary lymph nodes [57]. In the spleen, 4 distinct DC subsets were assessed:

- Conventional DC1s (cDC1) – cross-presenting antigen to activate CD8 T cells
- cDC2s – activation of CD4 responses, may promotes Th1, Th2 or Th17 responses [51]
- Monocyte derived DCs (moDCs) – induced by inflammation to support (and take on functions) of DCs pertaining to activating CD8 T cell responses [49].
- Plasmacytoid DCs (pDCs) – rapid production of IFNα and initiation of anti-viral immune responses [52].

Across all DC subsets, IV ChAdOx1 elicited a higher expression of both CD80 and CD86 at 24 hours post vaccination (Figures 5.3B/C, $p < 0.0001$ for all). There was no significant difference between these vaccinations 6 hours post vaccination, thereby suggesting that though cytokines peak ~6 hours post vaccination (Figure 5.2B), activation

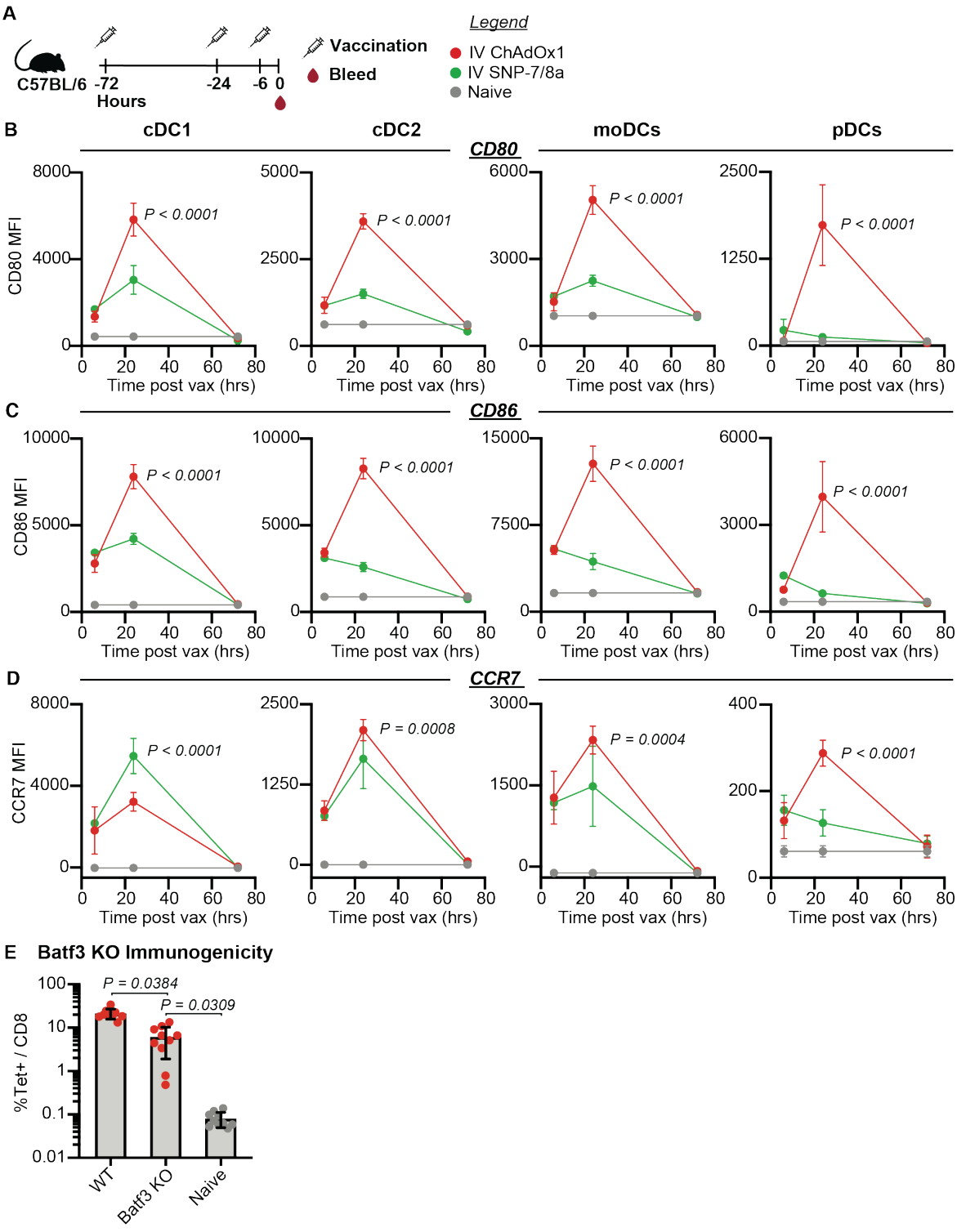

Figure 5.3 IV ChAdOx1 causes transient activation of DCs and requires cDC1s to elicit high magnitude CD8 T cell responses.
(**A**) Groups of mice were vaccinated in a staggered fashion with IV ChAdOx1 or IV SNP either 72, 24 or 6 hours prior to sacrificing mice to collect spleens. (**B-D**) Expression of different activation and maturation markers on DC subsets following IV vaccination (**B**) CD80 (**C**) CD86 (**D**) CCR7. (**E**) Immunogenicity 14 days post IV ChAdOx1 vaccination of wild-type and Batf3 KO mice - measured by tetramer staining PBMCs. (**B-E**) Data represented as mean ± standard deviation, Kruskal-Wallis test with Dunn's correction for multiple comparisons.

of DC subsets peaks later. As with the cytokines, activation of DC subsets was decreased to baseline levels (indicated by unvaccinated DC marker expression) by 72 hours. The trends of CCR7 expression are similar to CD80 and CD86 except for the cDC1s where IV SNP vaccination elicits a greater expression as compared to IV ChAdOx1 (Figure 5.3D, $P < 0.0001$).

Interestingly, the expression CD80/CD86 on pDCs was only seen to peak in the IV ChAdOx1 groups (Figures 5.3B/C). At 6 hours post vaccination, the IV SNP group pDCs have the highest expression of CD80, CD86, and CCR7. This suggests that IV SNP likely activates pDCs more rapidly that ChAdOx1 (< 6 hours).

The role of pDCs in priming CD8 T cell responses following ChAdOx1 vaccination has been studied, however the role of cDC1s has not. Batf3 KO mice are readily available to determine whether cDC1s play a role in the priming of ChAdOx1 elicited CD8 T cell responses. Vaccination and CD8 T cell response assessment were carried out as in previous KO experiments. Batf3 KOs (average tetramer response = 6%) were found to have a ~3.5-fold lower magnitude CD8 T cell response as compared to WT mice (Figure 5.3E) average tetramer response = 21%, $p = 0.0384$). This suggests that cDC1s are not required for priming CD8 T cell responses, but are required to achieve high magnitude responses, and therefore may play a critical role in eliciting high magnitude anti-tumor CD8 T cell responses.

5.3.4 Tumor regression and survival in the therapeutic setting is dependent on IFNα signaling

Given the necessity of functional IFNα signaling for priming CD8 T cell responses following SNP and ChAdOx1 vaccination, and the known effects of type I IFNs on antigen presenting cells to promote CD8 T cell immunity, it seemed likely that IFNα

elicited by vaccination may be promoting tumor regression in the therapeutic setting. To assess this, a therapeutic experiment was undertaken to test the effect of blocking IFNα signaling at the time of boost vaccination (Figure 5.4A). One day before and after vaccination, mice were given a saturating dose of IFNα receptor blocking antibody. The only tested vaccination groups were heterologous prime boost using the Reps1-encoding ChAdOx1 and the IV SNP given twice group. By comparing between the blocked and unblocked groups, a role for IFNα could be established.

The blockade of the IFNα receptor was associated with a loss of tumor growth control in both the IV Reps1-ChAdOx1 boosted group and the IV SNP boosted group relative to the same vaccination strategy without blockade (Figure 5.4B, $p < 0.0001$, $p = 0.0038$, respectively). This trend is reflected by the survival curves. The IFNα receptor blocked heterologous prime boost group displayed survival equivalent to the untreated group ($p > 0.9999$), and thus represents a total loss of protection as compared to the unblocked heterologous prime boost group (Figure 5.4C, $p < 0.0001$). In the IV SNP given twice group, blockade significantly affected survival and was not as good as the unblocked IV SNP given twice ($p = 0.0012$). However, even with IFNα receptor blockade the IV SNP given twice group had significantly improved survival as compared to the untreated group ($p = 0.0119$), suggesting that IV SNP given twice is not as reliant on functional IFNα signaling as the IV ChAdOx1 heterologous prime boost group.

It was important to assess the production of cytokines following vaccination in the blocked and unblocked groups to determine if the IFNα receptor blocking antibody had successfully inhibited IFNα signaling. Mice were bled 6 hours after the vaccination, which had been previously identified as the peak time post vaccination for IFNα in the serum (Figure 5.2B). The amount of IFNα present in the serum was significantly reduced in the IFNα receptor blocked groups for both vaccination strategies as compared to unblocked

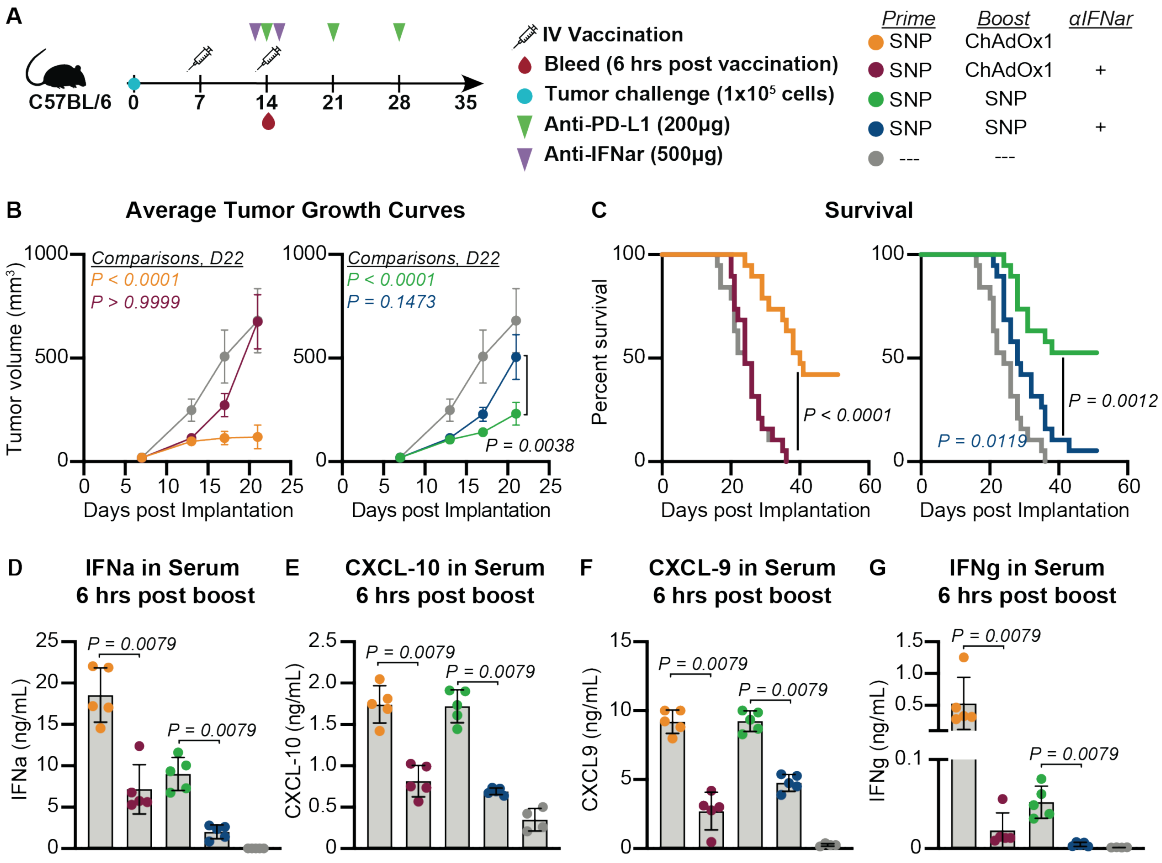

Figure 5.4 Tumor regression and survival in the therapeutic setting is dependent on IFNα signaling. (**A**) Therapeutic study treatment and sampling schedule, legend for all figure panels. (**B**) Tumor growth curves plotted as mean ± SEM. (**C**) Survival curves for all groups, compiled from 2 studies. (**D-G**) Cytokine production 6 hours post boost vaccination in serum (**D**) IFNα (**E**) CXCL-10 (**F**) CXCL-9 (**G**) IFNγ. **Stats:** (**B**) Two way ANOVA with Bonferroni correction for multiple comparisons, p-values compared to untreated. (**C**) Mantel-Cox Log-rank test. (**D-G**) Data represented as mean ± standard deviation, Mann-Whitney test.

(Figure 5.4D, p = 0.0079 for both). However, there was still some IFNα production in the blocked groups as compared to the untreated animals. This likely represents IFNα induced directly by the vaccines that is not capable of inducing production of further IFNα through positive feedback given the presence of the blocking antibody.

The use of a Luminex kit provided further information about multiple cytokines post vaccination. CXCL-9 and CXCL-10 were both significantly reduced in the blocked groups compared to the unblocked groups (Figure 5.4E/F, p = 0.0079 for both). Given that CXCL-10 is upregulated by IFNα, the lack of upregulation in the blocked groups implies a functional block of IFNα signaling by the blocking antibody. These chemokines are

associated with CD8 T cell infiltration into the tumor and are positive prognostic markers for outcome in tumor immunotherapy [62]. In addition, the presence of IFNγ in the serum is significantly increased in the unblocked groups as compared to the blocked groups for both vaccination strategies (Figure 5.4G, $p = 0.0079$ for both).

5.3.5 IFNα blockade does not affect magnitude of the antigen-specific CD8 T cell response post IV ChAdOx1 boost, but eliminates correlation between magnitude and tumor regression.

In addition to assessing the effect of IFNα blockade on systemic cytokine production, it was important to characterize the effects of this intervention on the Reps1-specific CD8 T cell response elicited by these vaccination strategies. To do this, mice were bled 7 days post boost and PBMCs stained with Reps1-tetramer or stimulated with peptide to assess cytokine production (Figure 5.5A). By tetramer staining, there was no difference in magnitude between the IFNα-receptor blocked and unblocked heterologous prime boost groups (Figure 5.5B, $p = 0.2675$). This was surprising given the requirement of IFNα for priming CD8 T cell responses following ChAdOx1 prime (Figure 5.2E). By comparison, the IV SNP given twice group with IFNα receptor blockade elicited significantly lower magnitude Reps1-specific CD8 T cell responses as compared to the unblocked group (Figure 5.5B, $p = 0.0431$).

As expected, the magnitude of the Reps1-specific CD8 T cell response at day 21 negatively correlated with tumor volume at day 24 (Figure 5.5C, $r = -0.6952$, $p < 0.0001$). In contrast, IFNα blockade completely negated any correlation between magnitude and tumor volume (Figure 5.5D, $r = -0.0454$, $p = 0.8184$). Together, these data indicate that in the absence of IFNα signaling, the CD8 T cell response may be unable to mediate anti-tumor functions.

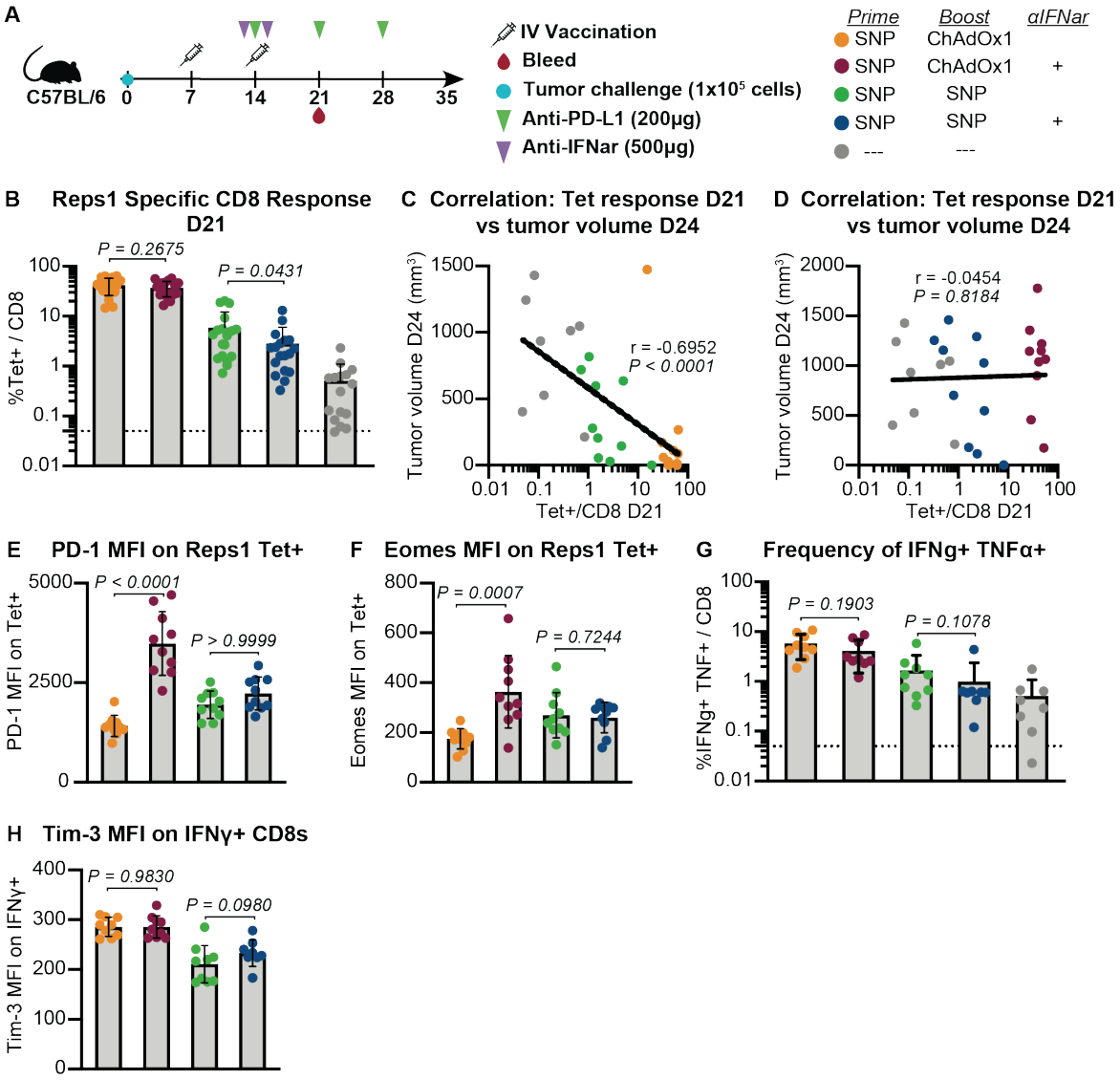

Figure 5.5 IFNα blockade does not affect magnitude of CD8 T cell responses following heterologous prime boost and minimally affects phenotype.
(**A**) Therapeutic study treatment and sampling schedule, legend for all figure panels. (**B**) Immunogenicity at day 21 measured by tetramer staining PBMCs using a Reps1-specific tetramer. (**C-D**) Correlation of Reps1 specific response at day 21 and tumor volume at day 24 plotted with line of best fit. (**C**) Groups without IFNα receptor blockade (**D**) Groups with IFNα receptor blockade. (**E**) MFI of PD-1 on Reps1-tetramer positive cells in blood. (**F**) MFI of Eomes on Reps1-tetramer positive cells in blood. (**G**) Frequency of IFNγ and TNFα co-producers following peptide restimulation detected by flow cytometry. (**H**) MFI of Tim-3 on IFNγ producing cells in blood. **Stats:** (**B, E-H**) Data represented as mean ± standard deviation, Mann-Whitney test. (**C-D**) Spearman's rank correlation.

The phenotype of the T cell responses was assessed by measuring the expression of PD-1 and Eomes on the Reps1-specific CD8 T cells. Interestingly, IFNα blockade was associated with an increase in the expression of PD-1 and Eomes in the heterologous prime boost group compared to without blockade (Figure 5.5E/F, $p < 0.0001$, $p = 0.0007$, respectively), whereas there was no difference in PD-1 and Eomes expression in the IV SNP given twice groups.

Increased expression of PD-1 and Eomes had previously been associated with a decrease in polyfunctionality (Chapter 3), so the co-production of IFNγ and TNFα was assessed by peptide restimulation. There was no difference in the frequency of polyfunctional cells between the IV heterologous prime boost groups with or without IFNα receptor blockade (Figure 5.5G, $p = 0.1903$) and the same was true for the IV SNP given twice groups ($p = 0.1078$). The expression of Tim-3 was assessed on the IFNγ producing cells to determine if these were perhaps more exhausted, as might be suggested by the increased PD-1 expression in the IFNα receptor blocked group. This was not the case for either IV heterologous prime boost groups (Figure 5.5H, $p = 0.9830$) or IV SNP given twice groups ($p = 0.0980$).

5.3.6 IFNα blockade is associated with a loss of activation of cDC1s in the spleen, tumor, and tumor draining lymph node.

The importance of cDC1s for CD8 T cell priming, and the time to reach peak activation of DCs following IV ChAdOx1 vaccination was established in figure 5.3. A therapeutic study was undertaken to assess the effects on the DC subsets, in particular cDC1s, of IV vaccination in the presence of IFNα receptor blockade (Figure 5.6A). Mice were sacrificed 24 hours after vaccination to collect spleens, tumors and tumor draining lymph nodes (td-LNs). The expression of co-stimulatory molecules CD80 and CD86, and

maturation marker CCR7 were assessed as before. The expression of CD40 was also assessed due to its role in DC maturation to promote Th1 T cell responses [64]. In addition, Tim-3 is expressed by cDC1s at steady state and is down-regulated upon activation. Tim-3 blockade is associated with an increase in CXCL-9 production and improved anti-tumor efficacy [208]. Therefore the expression of Tim-3 on cDC1s was also assessed.

In the spleen, the expression of CD80, CD86, and CD40 was significantly increased in the IFNα receptor unblocked groups relative to the same vaccination strategy with IFNα receptor blockade (Figure 5.6B, $p < 0.0079$ for all). Interestingly, the expression of CCR7 was unaffected by IFNα receptor blockade in the IV heterologous prime boost ($p = 0.5476$), but was dependent on IFNα in the SNP IV given twice group ($p = 0.0079$). The expression of Tim-3 followed the same trend as CCR7, though the expression of Tim-3 was still significantly different between IFNα receptor blocked and unblocked in the IV heterologous prime boost groups ($p = 0.0159$). This suggests that the maturation of cDC1s in the spleen following ChAdOx1 vaccination is not entirely dependent on IFNα, whereas it is IFNα dependent for SNP.

In the tumor, IV ChAdOx1 was the only vaccine that consistently upregulated all three activation markers (CD80/CD86/CD40) and this was IFNα dependent in all cases (Figure 5.6C, $p = 0.0079$). Of those three markers, IV SNP only significantly upregulated CD86, and this was also IFNα dependent ($p = 0.0238$). When assessing CCR7 however, only IV SNP increased expression of this maturation marker ($p = 0.0159$) in an IFNα dependent manner. Finally, Tim-3 expression in the tumor remains highly expressed on cDC1s in both vaccinated groups in the presence of IFNα receptor blockade as compared to the unblocked groups ($p = 0.0079$ for both).

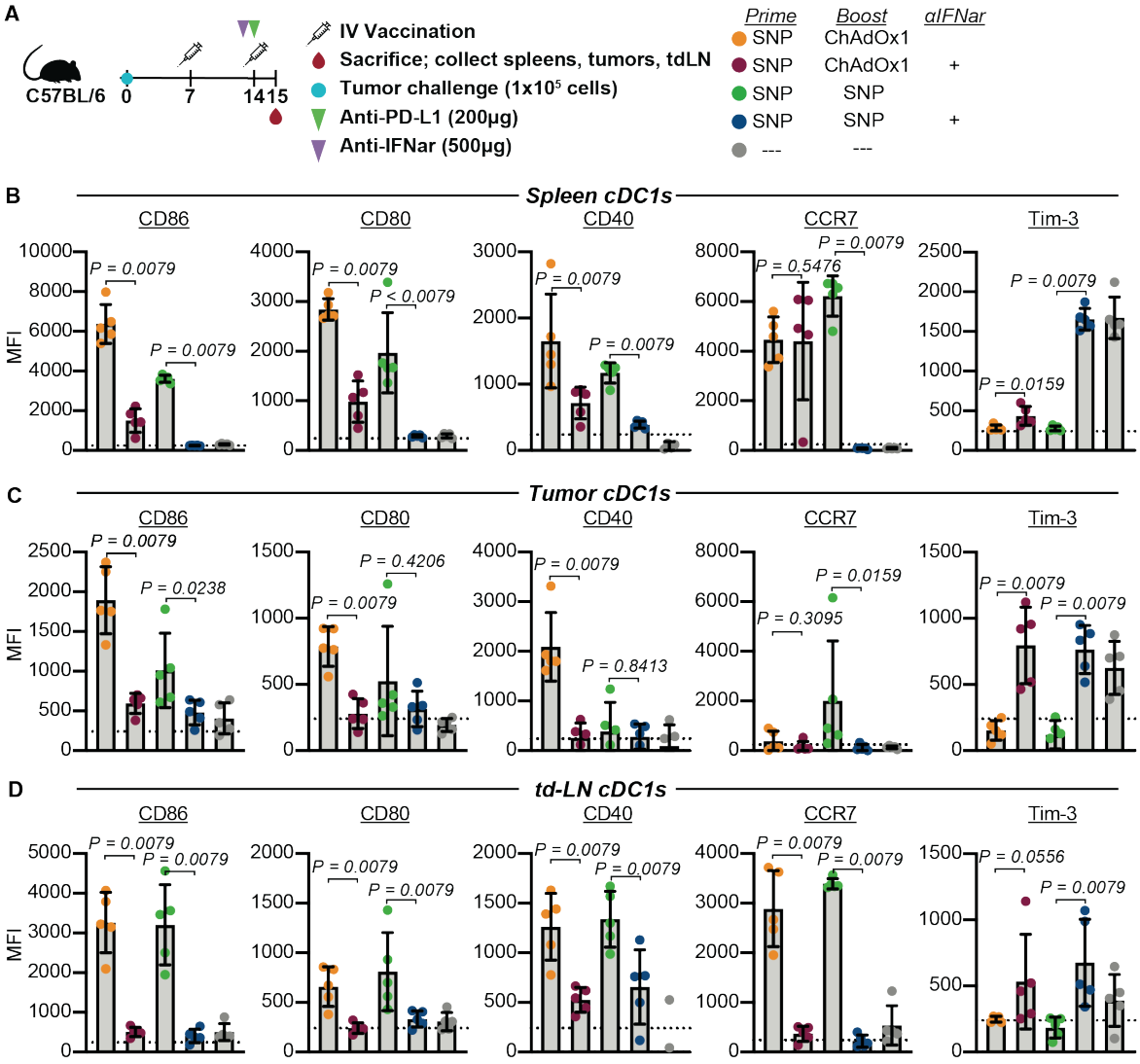

Figure 5.6 IV vaccine elicited IFNα causes activation of cDC1s in the spleen, tumor and td-LN. (**A**) Therapeutic study treatment and sampling schedule, legend for all figure panels. (**B-D**) Expression of CD86, CD80, CD40, CCR7 and Tim-3, as measured by median fluorescence intensity (MFI) on cDC1s in the (**B**) Spleen (**C**) Tumor (**D**) Tumor draining lymph node, td-LN. **Stats:** (**B-D**) Data represented as mean ± standard deviation, Mann-Whitney test.

In the td-LN, both IV vaccinations induce expression of CD86, CD80, CD40, and CCR7 in an IFNα dependent manner (Figure 5.6D, $p = 0.0079$). The expression of Tim-3 in the td-LN is more heterogenous, but the IV SNP given twice group still shows IFNα dependent down-regulation ($p = 0.0079$). Together these data demonstrate that IV vaccination with either ChAdOx1 or SNP causes activation of cDC1s in the spleen, tumor and td-LN. These trends in activation, particularly with CD80, CD86 and CD40 are also observed in cDC2s and moDCs (data not shown). Together these data suggest that IFNα induced by IV vaccination activates DCs systemically and may result in tumor microenvironment modulation that supports anti-tumor CD8 T cell responses.

5.4 Conclusions and discussion

5.4.1 IFNα is required for IV vaccination mediated tumor regression in the therapeutic setting

The finding that IV ChAdOx1 and IV SNP both elicit transient production of IFNα suggested the possibility of a common mechanism of action that might explain why IV SNP given twice is as protective as IV heterologous prime boost with Reps1-encoding ChAdOx1, despite eliciting ~10 fold lower magnitude antigen-specific CD8 T cell response. Blocking IFNα signaling in the therapeutic setting abrogated vaccine elicited protection, providing the evidence that IFNα signaling was required for both vaccination strategies. IFNα production following IV vaccination was associated with production of chemokines that promote CD8 T cell infiltration of tumors and activation of cDC1s (and other DCs) in the spleen, tumor and td-LN. Together, these data suggest that vaccine induced IFNα promotes tumor regression by promoting CD8 T cell infiltration into the tumor and modulating the APCs in the tumor microenvironment.

One intriguing comparison between the IV vaccinations was the pattern of activation of cDC1s in the spleen with IFNα receptor blockade (Figure 5.6B/C/D). The absolute dependence of cDC1 maturation (based on CCR7 upregulation and Tim-3 down-regulation) on IFNα following IV SNP given twice may be due to the difference in the pattern recognitions receptors (PRRs) through which SNP and ChAdOx1 are activating innate immunity. SNP contains a TLR-7/8 agonist and therefore signals through TLR-7 in mice [187] (mice do not have TLR-8), while ChAdOx1 signals through Sting. TLR-7 is not expressed by cDC1s in mice [209], and therefore the activation relies entirely on IFNα. However, Sting is expressed by cDC1s and therefore the maturation (based on CCR7 and Tim-3 expression) in the spleen is likely the result of direct activation by ChAdOx1 in the cDC1s. The lack of upregulation of costimulatory molecules by IV ChAdOx1 with IFNα blockade suggests that Sting activation alone is insufficient to fully activate cDC1s. This fits with previously published work that IFNα promotes cross-presentation of cDC1s [66], which is supported by the increased expression of co-stimulatory markers CD80/CD86 in the IFNα unblocked group.

The effects of IFNα on tumor regression are perhaps unsurprising given that others have published on the loss of efficacy of immunotherapies in IFNα deficient mouse models . However, these experiments are (to my knowledge), the first reports of vaccine induced IFNα being considered as a therapeutic component of intervention, separate and yet synergistic with the antigen-specific CD8 T cell response elicited. Collectively these data suggest that a low magnitude CD8 T cell response may be capable of mediating tumor regression, provided the appropriate tumor microenvironment modulation is provided. IV vaccination therefore provides a two-pronged approach to tumor therapy by providing both the CD8 T cell response and the immunomodulatory signals to alter the tumor microenvironment.

5.4.2 Limitations of the studies

The effects of IFNα are pleiotropic in nature, and so blocking IFNα affects multiple different cell types and the production of numerous cytokines/chemokines. This makes it difficult to pin-point exactly which cell types are critical for mediating anti-tumor immunity following IV vaccination, and thus results in a general statement about the requirement of IFNα for tumor regression. In addition, IFNα is a family of cytokines and not a single entity. The ELISA kit detects multiple IFNα family members but does not discriminate between the different family members. Therefore it is unclear if ChAdOx1 and SNP are eliciting the same IFNα response, or if there are nuanced differences between the IFNα family members induced that may have further implications on tumor regression.

The IFNα receptor blocking studies were only performed by targeting Reps1 in MC38. It is unknown to what extent this phenomenon is generalizable to other tumor models or whether it is specific to the MC38 tumor model.

The studies on APCs in the tumor and td-LN are correlational and do not determine the relative importance of subsets, like cDC1s, in the anti-tumor effect of heterologous prime boost.

5.4.3 Future studies

This chapter began by showing that empty ChAdOx1 IV vaccination provided a therapeutic benefit as compared to SNP prime alone in the therapeutic setting (Figure 5.1). IFNα was identified as a critical mediator of tumor control in the therapeutic setting when using antigen-encoding ChAdOx1. A follow up study would assess if the protection seen with the IV empty ChAdOx1 boost is also IFNα dependent.

Another way to demonstrate the effects of IFNα would be to provide IFNα alone as a therapeutic agent. Historically, IFNα has been given clinically to promote anti-tumor

immunity [7]. SNP prime alone and SNP prime followed by exogenous IFNα given at the time of boost (no vaccine/no antigen) in the therapeutic setting could be compared to see if IFNα alone is sufficient to improve protection provided by SNP primed responses. This would be similar to the empty ChAdOx1 alone boost, except it would not cause activation through Sting and may have more limited effects. This could inform on the importance of Sting signaling activated by ChAdOx1 vaccination for therapeutic effect.

IFNα blockade was associated with an increased expression of PD-1 in the heterologous prime boost group, though by all other assessments the phenotype of the cells looked similar. It would be interesting to see if the blockade of IFNα is associated with a reduction of CD8 T cell infiltration into the tumor or with a change in phenotype of the CD8 T cells present at the tumor site.

The activation of APCs in the spleen, tumor and td-LN following IV vaccination with ChAdOx1 or SNP is similar by flow cytometry. However, these vaccines signal through different PRRs and thus may elicit different cell states following vaccination. To better understand how each of the vaccines affects the APCs to promote tumor regression, a scRNA sequencing experiment could be undertaken to compare APCs in the spleen, tumor and td-LN following IV vaccination in combination with or without the IFNα receptor blocking antibody. This data set could reveal vaccine specific activation states of APCs that promote tumor regression which could then be tested in vivo.

Finally, the same IFNα receptor blocking experiment could be repeated in a different mouse tumor model. Though based on the data in chapter 4, it is likely that neither TC-1 nor B16F10 would be good candidates for this given their sensitivity to CD8 T cell responses and aggressiveness, respectively.

Chapter 6

Conclusions and Future Work

6.1 Conclusions and future work

Neoantigens have emerged as critical targets for cancer immunity across multiple cancer types [152]. However, not all patients naturally prime CD8 T cell responses against neoantigens and this may underpin their lack of responsiveness to CPIs. This has led to the development of neoantigen based vaccination strategies to prime *de novo* (or boost pre-existing) neoantigen T cell responses in humans [210]. Though the neoantigen SLP and poly-ICLC vaccine clinical trial was able to elicit CD8 T cell responses in patients, it was against a very low number of neoantigens relative to the number tested (16%) and no vaccine specific therapeutic outcomes were reported. One reason for this may be that SLP-adjuvant emulsions like SLP and poly-ICLC are suboptimal for inducing broad antigen-specific CD8 T cell responses. Formulating 7 mass-spectrometry validated neoantigens as SNP-7/8a demonstrated that CD8 T cell responses could be primed against all 7 neoantigens, whereas poly-ICLC formulation was only able to elicit CD8 T cell responses against three of these. In addition, the magnitude of SLP + poly-ICLC primed CD8 T cell responses in humans, as detected by IFNγ production following peptide stimulation with pools of neoantigens, was found to be very low (<0.5%) [185]. This low magnitude following SLP + poly-ICLC is similar to findings in rhesus macaques tested with the SNP vaccine, indicating that peptide vaccines may be well suited for priming T cell responses but would likely need to receive a heterologous boost to elicit high magnitude responses in primates. In contrast, ChAdOx1 elicits high magnitude CD8 T cell responses in humans against a variety of tested antigens – though neoantigens have not been tested to date.

The fundamental purpose of this thesis therefore was to assess whether the combination of SNP and ChAdOx1 elicited higher magnitude neoantigen-specific CD8 T cell responses than either platform alone, and if this resulted in improved survival in preclinical mouse models. As the target was neoantigens, the studies focused on SNP

prime followed by ChAdOx1 boost, given that in the clinical setting SNP vaccines would likely be ready earlier than personalized ChAdOx1 vaccines. With this information, a decision could be made about whether or not to pursue this combination in NHPs and if successful later in humans.

The project began by testing the effect of route of ChAdOx1 vaccination on magnitude and quality of the induced neoantigen-specific CD8 T cell response. This is because the route of vaccination has been shown to be important in eliciting protective immune responses against tuberculosis [191] and cancer [188], with IV vaccination providing superior protection in both cases. In the case of ChAdOx1 vaccination, the IV route was associated with higher magnitude, but more terminally differentiated T cell responses as characterized by a lower frequency of polyfunctional CD8 T cells and higher expression of PD-1 and the transcription factor Eomes [192]. The cells induced by IV ChAdOx1 may also be more exhausted as evidenced by the higher frequency of PD-1+ Tim-3+ cells when compared to IM ChAdOx1. These double positive cells have been previously described to be less capable of producing cytokines in response to TCR stimulation, and may represent a more 'exhausted' T cell phenotype [126]. Together, the immunological data suggested that in the case of ChAdOx1 vaccination, the IV route might be suboptimal for inducing T cell responses.

However, in the prophylactic setting IV ChAdOx1 outperformed the IM ChAdOx1 and protected a greater percentage of mice challenged with MC38. This indicates that with a sufficiently large magnitude T cell response, the quality of the T cells may become less important – similar to findings in the prophylactic setting when comparing SNP given SC or IV. Though with SNP, the trend is reversed, localized vaccination (SC or IM) is associated with more terminally differentiated T cell responses and IV vaccination elicits lower magnitude but more 'stem-like' responses [188].

Interestingly, despite the more terminally differentiated phenotype of IV ChAdOx1 primed CD8 T cell responses, these did not contract over 16 weeks as much as IM ChAdOx1 primed responses, resulting in prolonged high magnitude CD8 T cell responses detectable in the blood and spleen. In fact, the CD8 T cell response at 16 weeks following IV ChAdOx1 vaccination remained higher than the peak magnitude achieved by IM ChAdOx1. This may be important in the context of cancer as inducing stable high magnitude responses over prolonged periods of time may enable better control of tumor growth and allow for treatment of more advanced metastatic disease in patients.

Having noticed this effect of route of vaccination on CD8 T cell responses primed by ChAdOx1, and with the understanding that route affects the quality and magnitude of SNP primed CD8 T cell responses, it was important to determine the effect of different routes of both prime and boost vaccinations on heterologous prime boosted T cell responses. Interestingly, the route of SNP prime had no effect on the magnitude or quality of CD8 T cell responses elicited after ChAdOx1 boost. However, the route of ChAdOx1 boost was critical, with IV ChAdOx1 eliciting higher magnitude responses than IM, as would be expected. Given this finding, and that the IV route of vaccination elicits a greater frequency of 'stem-like' cells – which are associated with better response to CPIs, all subsequent experiments focused on the use of IV SNP as a prime vaccination.

Having selected a route for SNP prime vaccination, the next variable to understand was the effect of interval between IV SNP prime and ChAdOx1 boost. Longer intervals between prime and boost have been associated with increased boosting of T cell responses [211]. Three intervals were tested (1-, 2- and 4-weeks) between prime and boost. Interestingly, the magnitude of the CD8 T cell response immediately prior to ChAdOx1 boosting was equivalent between groups regardless of how much time had elapsed since IV SNP vaccination – indicating that IV SNP induces stable, albeit low magnitude, CD8 T

cell responses, which has not been previously reported. This may be why there was no difference in the magnitude of CD8 T cell responses following ChAdOx1 boost between the different intervals for both IM and IV boosted groups. All IV ChAdOx1 groups elicited higher magnitude CD8 T cell responses than IM boosted groups. It was clear that SNP primes a pool of neoantigen-specific T cell responses that can be boosted dramatically by ChAdOx1 at early time points, though after 4 weeks the magnitude of the response is approximately equivalent between SNP primed groups and ChAdOx1 alone. In the clinic, the decline in response over time may be less dramatic as patient tumors would provide a constant source of antigen for stimulating T cell responses and the use of checkpoint inhibitors may promote MHC-I presentation of tumor antigens on DCs to maintain the response elevated. Together these factors may preserve the magnitude differences seen initially between heterologous prime boosted groups and ChAdOx1 alone groups over time and may prove beneficial in patients.

There was also an observation unique to the IV ChAdOx1 boosted groups as compared to the IV ChAdOx1 alone, which is that SNP priming appears to limit the terminal differentiation induced by IV ChAdOx1. The expression of PD-1 and Eomes was significantly lower in the IV heterologous prime boost groups as compared to IV ChAdOx1 alone, and this was associated with a greater frequency of polyfunctional cells. It is unclear what significance this may have in the tumor, but immunologically one might expect the heterologous prime boosted cells to exhibit better effector functions as a result.

The effect of route and interval were well characterized in these studies, however only one dose of ChAdOx1 was tested. It is unclear what effects a lower dose might have on the magnitude and quality of T cell responses, and this is something that will be investigated in follow up studies, likely in NHPs. The reason being that finding the lowest dose possible that maintains potent T cell response boosting is likely to reduce side effects

in patients, without compromising anti-tumor efficacy. The rationale for not determining this in mice is because scaling doses from mice to NHP is non-trivial and so findings in mice may not be representative of what would be observed in NHP or humans.

The ability of heterologous prime boosted T cells to mediate protection from tumor challenge was then assessed in a prophylactic study. A 2-week interval was used between prime and boost for two reasons, 1) interval did not have a detectable effect on magnitude or quality of T cell responses and 2) previous experiments in the lab had used the same interval and could be included as controls or compared with historical data. The prophylactic experiments demonstrated the ability of heterologous prime boosted cells to mediate anti-tumor protection, and protection was correlated with magnitude of response thereby making the IV heterologous prime boost group the best performing group. Interestingly there was no difference between IM ChAdOx1 alone and heterologous prime boost with SNP and IM ChAdOx1, further accentuating the difference that route of vaccination can make. The protection was shown to be CD8 T cell dependent through a depletion study, which validated the model system of Reps1 vaccine mediated protection from MC38.

Collectively, these data supported the utility of heterologous prime boosted CD8 T cells in eliciting anti-tumor immunity and provided reason to explore how this might be applied in a more clinical setting. The prophylactic setting was only tested in MC38 because even low magnitude responses against E6/E7 can confer near sterile protection from TC-1 challenge in the prophylactic setting and so it would be very difficult to tease apart vaccination strategy differences in this model. However, the effect of the prophylactic setting should be repeated with another model in order to ensure the robustness of the finding.

Following the success of heterologous prime boost in the prophylactic setting, it was important to test the heterologous prime boost strategy in the therapeutic setting, which might better model the therapeutic nature of this cancer vaccination strategy. The interval between prime and boost was shortened to 1 week due to the fast-growing nature of the tumors, but was not expected to dramatically influence the heterologous prime boost immunogenicity based on the previous data on the effect of interval. In the therapeutic setting with MC38, heterologous prime boost using ChAdOx1 IM or IV both performed as well as the positive control (SNP IV given twice) despite having vastly different magnitude Reps1-specific CD8 T cell responses. IV or IM ChAdOx1 alone did not provide any therapeutic benefit against MC38 in this setting despite eliciting CD8 T cell responses of a similar magnitude to SNP IV given twice. These data indicate that for MC38, heterologous prime boost is a more potent therapeutic intervention than ChAdOx1 alone.

Moreover, this trend was also seen with a second neoantigen (Adpgk) when tested as an IV heterologous prime boost strategy. Tumor regression was less striking in the case of targeting the Adpgk neoantigen, though it is unclear exactly why this might be. All previous work in the Seder lab has shown that Adpgk is a less protective neoantigen in the prophylactic and therapeutic settings (unpublished). A number of factors may explain this discrepancy between neoantigens, for example a lower expression level of Adpgk as compared to Reps1, lower MHC-I binding affinity of Adpgk peptide, or more effective central tolerance to screen out potentially cross-reactive CD8 T cell clones against Adpgk than against Reps1. The selection of effective neoantigens is a topic of much debate, but it is clear that there are many differences between neoantigens that may determine the effectiveness of targeting them to induce T cell responses capable of mediating tumor regression. What is clear is that IV heterologous prime boost does elicit a CD8 T cell

response when targeting Adpgk and improves protection as compared to controls. Adpgk is expressed by the tumors as unvaccinated tumor-challenged mice develop Adpgk specific-CD8 T cell responses. The reasons why protection is less efficacious when vaccinating with Adpgk than when targeting Reps1 are beyond the scope of this thesis.

Given the disparities in magnitude between the three partially protective groups, a study was undertaken to assess differences in the quality of the antigen-specific CD8 T cell response in the spleen and tumor. It was assumed that the groups with higher magnitude had likely elicited more exhausted or less functional T cell responses as they did not improve survival compared to the SNP control. In the spleen, the quality of T cell responses was found to be similar between groups, the major difference was in the numbers of antigen-specific CD8 T cells, which were ~10x higher in the IV heterologous prime boost groups compared to the other groups. In the tumor, there were also limited differences in T cell quality between groups, but IV heterologous prime boost resulted in an increase in T cell infiltration into the tumor. This could be a result of the increased CXCL-9/CXCL-10 produced following IV ChAdOx1 vaccination. There were also fewer Tregs in the tumor following IV heterologous prime boost as compared to the other groups and this has a positive prognostic value. The analysis at the tissue sites did not reveal any striking differences between the groups that would explain why IV heterologous prime boost does not definitively outperform the other two groups as the magnitude elicited is the highest.

One interesting observation was that the SNP followed by ‘empty’ ChAdOx1 IV exhibited partial tumor growth control in MC38 despite having lower magnitude responses. Interestingly, SNP followed by ‘empty’ ChAdOx1 IM did not display improved survival or display tumor regression. This indicated that perhaps the systemic distribution of ChAdOx1 following IV vaccination may promote anti-tumor immunity as compared to

the locally administered IM ChAdOx1. In addition, the varied magnitude T cell responses in the 3 best responding groups, indicated that perhaps the magnitude of the CD8 T cell response is not the determining factor for whether or not MC38 will respond to an intervention. This prompted investigation of the factors that might explain these observations, one of which was the activation of innate immunity following systemic vaccination with SNP or ChAdOx1.

Some adenoviruses are known to activate innate immunity through the activation of STING and subsequent production of IFNα [207]. IFNα has pleiotropic effects on multiple different cell types. However, one effect of IFNα is to activate cDC1s to promote cross-presentation to activate CD8 T cells, and also to activate cDC1s to produce chemokines CXCL-9/CXCL-10, which are required to recruit T cells [62]. Thus, the possibility emerged that IV vaccination with ChAdOx1 or SNP resulted in production of IFNα which potently activated cDC1s to promote anti-tumor immunity.

To begin testing this hypothesis, the production of IFNα and IL-12 was assessed in mice at multiple times post IV vaccination. A significant amount of IFNα was produced in response to both ChAdOx1 and SNP vaccination. However, IL-12 was only elicited by SNP. The CD8 T cell response primed by ChAdOx1 was entirely dependent on STING and IFNα as demonstrated through the vaccination of KOs. Multiple DC populations displayed transient activation that peaked 24 hours following vaccination. Furthermore, ChAdOx1 vaccination of *Batf3* KO mice revealed a ~4-fold reduction in magnitude of the antigen-specific response, indicating a key role for cDC1s in priming high magnitude CD8 T cell responses. The reason this was not tested with heterologous prime boost is because *Batf3* KO mice also exhibit deficient priming with SNP [188]. This demonstrated that IV vaccination could elicit IFNα and activate cDC1s, and made plausible the theory that these two features of IV vaccination may be linked to the anti-tumor efficacy of IV vaccination.

Further support for this was provided by the IFNα receptor blocking experiments in the therapeutic setting. These demonstrated that functional IFNα signaling was required for protection following IV boost vaccination with either SNP or ChAdOx1. Blocking IFNα signaling completely at the time of boost abrogated tumor control when using ChAdOx1 IV, and mostly abrogated protection with IV SNP. IFNα receptor blockade was associated with lower levels of CXCL-9 and CXCL-10 in the serum. Moreover, the T cell response magnitude in the blood after ChAdOx1 boost was not affected in the IFNα receptor blocked group, though the phenotype of these cells was slightly more terminally differentiated. Given this data, it is possible that the magnitude in the blood is unchanged, but due to the lower expression of CXCL-9 and CXCL-10 there are fewer CD8 T cells in the tumor itself, thereby preventing effective tumor clearance. A follow up study will be undertaken to determine if IFNα receptor blockade reduces T cell infiltration into the tumors.

Finally, the activation of cDC1s in the spleen, tumor and td-LN was assessed in the context of IFNα receptor blockade. IFNα receptor blockade totally abrogated activation of these cells in the tumor and td-LN, indicating that IV ChAdOx1 does indeed activate cDC1s through the production of IFNα. These data support the hypothesis that vaccine induced IFNα production activates cDC1s and may be promote anti-tumor immunity, in part through the production of chemokines and licensing of CD8 T cell responses. To definitively show this, an inducible *Batf3* conditional KO mouse could be used for a therapeutic experiment. Depleting cDC1s specifically just prior to boost and comparing to mice with intact immune systems would reveal the role of cDC1s in both boosting T cell responses and orchestrating anti-tumor immunity.

Though the cDC1 activation hypothesis is appealing, IFNα has pleiotropic effects on multiple different cell types. It is possible that IFNα is also affecting the

immunosuppressive TME by altering tumor cells or other immune cells [7]. This is something that will be pursued by single cell RNA sequencing of tumor preparations following vaccination with or without IFNα receptor blockade in an attempt to characterize the mechanism of protection in this model as precisely as possible.

In addition, it is possible that the ChAdOx1 prime alone groups in the therapeutic setting prime fully functional T cell responses but the absence of an IFNα inducing signal at the time of boost prevents these from homing into the tumor. A follow up study where ChAdOx1 is given as a prime (no protection) and then recombinant mouse IFNα is provided at the time of boost would demonstrate that efficacy in the therapeutic setting for MC38 is dependent on both a T cell response and an immunostimulatory signal that could activate APCs/revert immunosuppression in the tumor as a result. This would not be unlike the studies in the 1990s that tested IFNα2 in clinical trials [9]. A T cell response is known to be required to treat MC38 from CD8 T cell depletion studies performed with SNP [188]. For MC38 treatment, the framework may be that some low level of anti-tumor T cell response is required or anti-tumor efficacy, but must be supplemented with an immunostimulatory signal to enable effective function. In the context of heterologous prime boost, IV ChAdOx1 provides both the T cell response boosting and the inflammatory signal to enable anti-tumor function, and this may be an important paradigm for the clinic.

Collectively, the data in this thesis provides sufficient evidence for pursuing a NHP study to determine if heterologous prime boost elicits higher magnitude T cell responses than either SNP or ChAdOx1 alone. Whilst in MC38, the magnitude of the T cell response does not determine efficacy, it is highly likely that in humans it will play a role. This is based on two major lines of evidence:

1. High numbers of T cells infused for efficacious ACT with expanded TILs or CAR T cells [165].
2. The correlation of high numbers of TILs with a favorable prognosis in ovarian[212] and colorectal [213] cancers.
3. The positive correlation between TILs and TMB, and therefore positive association with outcome [162].

Therefore, the magnitude of the T cell response generated through vaccination is important for clinical development. Given the low magnitude CD8 T cell responses that SNP primed in NHPs [186], it is unlikely that SNP alone will induce sufficient magnitude T cell responses in humans to be clinically viable. The evidence from the heterologous prime boost mouse studies in this tome supports the use of an IV ChAdOx1 boost to increase T cell magnitude from the perspective of SNP. It will have to be demonstrated in NHPs that heterologous prime boost elicits higher magnitude responses than ChAdOx1 alone to determine if this combination is suitable for clinical development as opposed to using ChAdOx1 alone.

In summary, IV heterologous prime boost was shown to be the most potent strategy for eliciting high magnitude antigen-specific CD8 T cells across a range of antigens. IV heterologous prime boost exhibited the best tumor regression, even if not significantly better than the positive control. In addition to boosting T cell responses, IV vaccination with SNP or ChAdOx1 elicits high levels of IFNα which promotes anti-tumor immunity, and builds on decades of previous work in understanding the anti-tumor effects of the IFNα cytokine family. This represents a new paradigm for cancer vaccinology, whereby the vaccine is desired not solely to elicit potent anti-tumor T cell responses but also to modulate the TME to promote tumor regression. The Seder lab has dubbed this paradigm Vax-Innate.

"I have often had a fancy for writing a romance about an English yachtsman who slightly miscalculated his course and discovered England under the impression that it was a new island in the South Seas. There will probably be a general impression that the man who landed….to plant the British flag….felt rather a fool…..But I have a peculiar reason for mentioning the man in a yacht, who discovered England. For I am that man in a yacht….I am the man who with the utmost daring discovered what had been discovered before."

G. K. Chesterton, *Orthodoxy*

References

1. Sung, H., et al., *Global Cancer Statistics 2020: GLOBOCAN Estimates of Incidence and Mortality Worldwide for 36 Cancers in 185 Countries.* CA: A Cancer Journal for Clinicians, 2021. **71**(3): p. 209-249.
2. Hanahan, D. and Robert, *Hallmarks of Cancer: The Next Generation.* Cell, 2011. **144**(5): p. 646-674.
3. Quaresma, M., M.P. Coleman, and B. Rachet, *40-year trends in an index of survival for all cancers combined and survival adjusted for age and sex for each cancer in England and Wales, 1971–2011: a population-based study.* The Lancet, 2015. **385**(9974): p. 1206-1218.
4. Neoptolemos, J.P., et al., *Therapeutic developments in pancreatic cancer: current and future perspectives.* Nature Reviews Gastroenterology & Hepatology, 2018. **15**(6): p. 333-348.
5. Pennathur, A., et al., *Oesophageal carcinoma.* The Lancet, 2013. **381**(9864): p. 400-412.
6. Decker, W.K. and A. Safdar, *Bioimmunoadjuvants for the treatment of neoplastic and infectious disease: Coley's legacy revisited.* Cytokine & Growth Factor Reviews, 2009. **20**(4): p. 271-281.
7. Borden, E.C., *Interferons α and β in cancer: therapeutic opportunities from new insights.* Nature Reviews Drug Discovery, 2019. **18**(3): p. 219-234.
8. Gresser, I., et al., *Increased Survival in Mice Inoculated with Tumor Cells and Treated with Interferon Preparations.* Proceedings of the National Academy of Sciences, 1969. **63**(1): p. 51-57.
9. Rai, K.R., et al., *Recombinant alpha-2b-interferon in therapy of previously untreated hairy cell leukemia: long-term follow-up results of study by Cancer and Leukemia Group B.* Leukemia, 1995. **9**(7): p. 1116-20.
10. Kirkwood, J.M., et al., *Interferon alfa-2b adjuvant therapy of high-risk resected cutaneous melanoma: the Eastern Cooperative Oncology Group Trial EST 1684.* Journal of Clinical Oncology, 1996. **14**(1): p. 7-17.
11. Morgan, D.A., F.W. Ruscetti, and R. Gallo, *Selective in Vitro Growth of T Lymphocytes from Normal Human Bone Marrows.* Science, 1976. **193**(4257): p. 1007-1008.
12. Rosenberg, S.A., et al., *Biological Activity of Recombinant Human Interleukin-2 Produced in Escherichia coli.* Science, 1984. **223**(4643): p. 1412-1415.
13. Rosenberg, S.A., et al., *Use of Tumor-Infiltrating Lymphocytes and Interleukin-2 in the Immunotherapy of Patients with Metastatic Melanoma.* New England Journal of Medicine, 1988. **319**(25): p. 1676-1680.
14. Rosenberg, S.A., et al., *Observations on the Systemic Administration of Autologous Lymphokine-Activated Killer Cells and Recombinant Interleukin-2 to Patients with Metastatic Cancer.* New England Journal of Medicine, 1985. **313**(23): p. 1485-1492.
15. Rosenberg, S.A., et al., *Durable Complete Responses in Heavily Pretreated Patients with Metastatic Melanoma Using T-Cell Transfer Immunotherapy.* Clinical Cancer Research, 2011. **17**(13): p. 4550-4557.
16. Perica, K., et al., *Adoptive T Cell Immunotherapy For Cancer.* Rambam Maimonides Medical Journal, 2015. **6**(1): p. e0004.

17. Graham, C., et al., *Cancer immunotherapy with CAR-T cells – behold the future.* Clinical Medicine, 2018. **18**(4): p. 324-328.
18. Guedan, S., et al., *Engineering and Design of Chimeric Antigen Receptors.* Molecular Therapy - Methods & Clinical Development, 2019. **12**: p. 145-156.
19. Maude, S.L., et al., *Chimeric Antigen Receptor T Cells for Sustained Remissions in Leukemia.* New England Journal of Medicine, 2014. **371**(16): p. 1507-1517.
20. Sermer, D., et al., *Outcomes in patients with DLBCL treated with commercial CAR T cells compared with alternate therapies.* Blood Advances, 2020. **4**(19): p. 4669-4678.
21. Park, J.H., et al., *Long-Term Follow-up of CD19 CAR Therapy in Acute Lymphoblastic Leukemia.* New England Journal of Medicine, 2018. **378**(5): p. 449-459.
22. O'Leary, M.C., et al., *FDA Approval Summary: Tisagenlecleucel for Treatment of Patients with Relapsed or Refractory B-cell Precursor Acute Lymphoblastic Leukemia.* Clinical Cancer Research, 2019. **25**(4): p. 1142-1146.
23. Bouchkouj, N., et al., *FDA Approval Summary: Axicabtagene Ciloleucel for Relapsed or Refractory Large B-cell Lymphoma.* Clinical Cancer Research, 2019. **25**(6): p. 1702-1708.
24. Hargadon, K.M., C.E. Johnson, and C.J. Williams, *Immune checkpoint blockade therapy for cancer: An overview of FDA-approved immune checkpoint inhibitors.* International Immunopharmacology, 2018. **62**: p. 29-39.
25. Ribas, A. and J.D. Wolchok, *Cancer immunotherapy using checkpoint blockade.* Science, 2018. **359**(6382): p. 1350-1355.
26. Wolchok, J.D., et al., *Nivolumab plus Ipilimumab in Advanced Melanoma.* New England Journal of Medicine, 2013. **369**(2): p. 122-133.
27. Hellmann, M.D., et al., *Nivolumab plus Ipilimumab in Lung Cancer with a High Tumor Mutational Burden.* New England Journal of Medicine, 2018. **378**(22): p. 2093-2104.
28. Motzer, R.J., et al., *Nivolumab plus ipilimumab versus sunitinib in first-line treatment for advanced renal cell carcinoma: extended follow-up of efficacy and safety results from a randomised, controlled, phase 3 trial.* The Lancet Oncology, 2019. **20**(10): p. 1370-1385.
29. Larkin, J., et al., *Five-Year Survival with Combined Nivolumab and Ipilimumab in Advanced Melanoma.* New England Journal of Medicine, 2019. **381**(16): p. 1535-1546.
30. Fisher, R.A. and J. Larkin, *Malignant melanoma (metastatic).* BMJ clinical evidence, 2010. **2010**: p. 1718.
31. Vaddepally, R.K., et al., *Review of Indications of FDA-Approved Immune Checkpoint Inhibitors per NCCN Guidelines with the Level of Evidence.* Cancers, 2020. **12**(3): p. 738.
32. Jonathan, et al., *Resistance Mechanisms to Immune-Checkpoint Blockade in Cancer: Tumor-Intrinsic and -Extrinsic Factors.* Immunity, 2016. **44**(6): p. 1255-1269.
33. Baruch, E.N., et al., *Fecal microbiota transplant promotes response in immunotherapy-refractory melanoma patients.* Science, 2021. **371**(6529): p. 602-609.

34. Sotillo, E., et al., *Convergence of Acquired Mutations and Alternative Splicing of CD19 Enables Resistance to CART-19 Immunotherapy.* Cancer Discovery, 2015. **5**(12): p. 1282-1295.
35. Braig, F., et al., *Resistance to anti-CD19/CD3 BiTE in acute lymphoblastic leukemia may be mediated by disrupted CD19 membrane trafficking.* Blood, 2017. **129**(1): p. 100-104.
36. Fry, T.J., et al., *CD22-targeted CAR T cells induce remission in B-ALL that is naive or resistant to CD19-targeted CAR immunotherapy.* Nature Medicine, 2018. **24**(1): p. 20-28.
37. Shah, N.N. and T.J. Fry, *Mechanisms of resistance to CAR T cell therapy.* Nature Reviews Clinical Oncology, 2019. **16**(6): p. 372-385.
38. Ramos-Casals, M., et al., *Immune-related adverse events of checkpoint inhibitors.* Nature Reviews Disease Primers, 2020. **6**(1).
39. Hodi, F.S., et al., *Nivolumab plus ipilimumab or nivolumab alone versus ipilimumab alone in advanced melanoma (CheckMate 067): 4-year outcomes of a multicentre, randomised, phase 3 trial.* The Lancet Oncology, 2018. **19**(11): p. 1480-1492.
40. Abdel-Wahab, N., et al., *Use of Immune Checkpoint Inhibitors in the Treatment of Patients With Cancer and Preexisting Autoimmune Disease: A Systematic Review.* Annals of Internal Medicine, 2018. **168**.
41. Brudno, J.N. and J.N. Kochenderfer, *Recent advances in CAR T-cell toxicity: Mechanisms, manifestations and management.* Blood Reviews, 2019. **34**: p. 45-55.
42. Hirayama, A.V. and C.J. Turtle, *Toxicities of CD19 CAR-T cell immunotherapy.* American Journal of Hematology, 2019. **94**(S1): p. S42-S49.
43. Potluri, R., et al., *Healthcare cost comparison analysis of nivolumab in combination with ipilimumab versus nivolumab monotherapy and ipilimumab monotherapy in advanced melanoma.* Experimental Hematology & Oncology, 2019. **8**(1).
44. Haslam, A. and V. Prasad, *Estimation of the Percentage of US Patients With Cancer Who Are Eligible for and Respond to Checkpoint Inhibitor Immunotherapy Drugs.* JAMA Network Open, 2019. **2**(5): p. e192535.
45. Furzer, J., et al., *Cost-effectiveness of Tisagenlecleucel vs Standard Care in High-risk Relapsed Pediatric Acute Lymphoblastic Leukemia in Canada.* JAMA Oncology, 2020. **6**(3): p. 393.
46. Im, S.J., et al., *Defining CD8+ T cells that provide the proliferative burst after PD-1 therapy.* Nature, 2016. **537**(7620): p. 417-421.
47. Siddiqui, I., et al., *Intratumoral Tcf1+PD-1+CD8+ T Cells with Stem-like Properties Promote Tumor Control in Response to Vaccination and Checkpoint Blockade Immunotherapy.* Immunity, 2019. **50**(1): p. 195-211.e10.
48. Daniel, C. and I. Mellman, *Oncology Meets Immunology: The Cancer-Immunity Cycle.* Immunity, 2013. **39**(1): p. 1-10.
49. Wculek, S.K., et al., *Dendritic cells in cancer immunology and immunotherapy.* Nature Reviews Immunology, 2020. **20**(1): p. 7-24.
50. Engblom, C., C. Pfirschke, and M.J. Pittet, *The role of myeloid cells in cancer therapies.* Nature Reviews Cancer, 2016. **16**(7): p. 447-462.

51. Durai, V. and Kenneth, *Functions of Murine Dendritic Cells.* Immunity, 2016. **45**(4): p. 719-736.
52. Fitzgeraldbocarsly, P., J. Dai, and S. Singh, *Plasmacytoid dendritic cells and type I IFN: 50 years of convergent history.* Cytokine & Growth Factor Reviews, 2008. **19**(1): p. 3-19.
53. Crozat, K., et al., *Cutting Edge: Expression of XCR1 Defines Mouse Lymphoid-Tissue Resident and Migratory Dendritic Cells of the CD8α+ Type.* The Journal of Immunology, 2011. **187**(9): p. 4411-4415.
54. Hildner, K., et al., *Batf3 Deficiency Reveals a Critical Role for CD8a+ Dendritic Cells in Cytotoxic T Cell Immunity.* Science, 2008. **322**(5904): p. 1097-1100.
55. Spranger, S., R. Bao, and T.F. Gajewski, *Melanoma-intrinsic β-catenin signalling prevents anti-tumour immunity.* Nature, 2015. **523**(7559): p. 231-235.
56. Wculek, S.K., et al., *Effective cancer immunotherapy by natural mouse conventional type-1 dendritic cells bearing dead tumor antigen.* Journal for ImmunoTherapy of Cancer, 2019. **7**(1).
57. Roberts, E.W., et al., *Critical Role for CD103+/CD141+ Dendritic Cells Bearing CCR7 for Tumor Antigen Trafficking and Priming of T Cell Immunity in Melanoma.* Cancer Cell, 2016. **30**(2): p. 324-336.
58. Brewitz, A., et al., *CD8 + T Cells Orchestrate pDC-XCR1 + Dendritic Cell Spatial and Functional Cooperativity to Optimize Priming.* Immunity, 2017. **46**(2): p. 205-219.
59. Mashayekhi, M., et al., *CD8α+ Dendritic Cells Are the Critical Source of Interleukin-12 that Controls Acute Infection by Toxoplasma gondii Tachyzoites.* Immunity, 2011. **35**(2): p. 249-259.
60. Otani, T., et al., *Identification of IFN-γ-Producing Cells in IL-12/IL-18-Treated Mice.* Cellular Immunology, 1999. **198**(2): p. 111-119.
61. Zaidi, M.R., *The Interferon-Gamma Paradox in Cancer.* Journal of Interferon & Cytokine Research, 2019. **39**(1): p. 30-38.
62. Spranger, S., et al., *Tumor-Residing Batf3 Dendritic Cells Are Required for Effector T Cell Trafficking and Adoptive T Cell Therapy.* Cancer Cell, 2017. **31**(5): p. 711-723.e4.
63. Binnewies, M., et al., *Unleashing Type-2 Dendritic Cells to Drive Protective Antitumor CD4+ T Cell Immunity.* Cell, 2019. **177**(3): p. 556-571.e16.
64. Ferris, S.T., et al., *cDC1 prime and are licensed by CD4+ T cells to induce anti-tumour immunity.* Nature, 2020. **584**(7822): p. 624-629.
65. Mouriès, J., et al., *Plasmacytoid dendritic cells efficiently cross-prime naive T cells in vivo after TLR activation.* Blood, 2008. **112**(9): p. 3713-3722.
66. Diamond, M.S., et al., *Type I interferon is selectively required by dendritic cells for immune rejection of tumors.* Journal of Experimental Medicine, 2011. **208**(10): p. 1989-2003.
67. Wynn, T.A. and K.M. Vannella, *Macrophages in Tissue Repair, Regeneration, and Fibrosis.* Immunity, 2016. **44**(3): p. 450-462.
68. Forssell, J., et al., *High Macrophage Infiltration along the Tumor Front Correlates with Improved Survival in Colon Cancer.* Clinical Cancer Research, 2007. **13**(5): p. 1472-1479.
69. Ohno, S., et al., *The Degree of Macrophage Infiltration into the Cancer Cell Nest is a Significant Predictor of Survival in Gastric Cancer Patients.* Anticancer research, 2003. **23**: p. 5015-22.

70. Harney, A.S., et al., *Real-Time Imaging Reveals Local, Transient Vascular Permeability, and Tumor Cell Intravasation Stimulated by TIE2hi Macrophage–Derived VEGFA.* Cancer Discovery, 2015. **5**(9): p. 932-943.
71. Kuang, D.-M., et al., *Activated monocytes in peritumoral stroma of hepatocellular carcinoma foster immune privilege and disease progression through PD-L1.* Journal of Experimental Medicine, 2009. **206**(6): p. 1327-1337.
72. Noy, R. and Jeffrey, *Tumor-Associated Macrophages: From Mechanisms to Therapy.* Immunity, 2014. **41**(1): p. 49-61.
73. Kessenbrock, K., V. Plaks, and Z. Werb, *Matrix Metalloproteinases: Regulators of the Tumor Microenvironment.* Cell, 2010. **141**(1): p. 52-67.
74. Smith-Garvin, J.E., G.A. Koretzky, and M.S. Jordan, *T Cell Activation.* Annual Review of Immunology, 2009. **27**(1): p. 591-619.
75. Lenschow, D.J., et al., *Differential up-regulation of the B7-1 and B7-2 costimulatory molecules after Ig receptor engagement by antigen.* The Journal of Immunology, 1994. **153**(5): p. 1990.
76. Esensten, J.H.H., Ynes A., et al., *CD28 Costimulation: From Mechanism to Therapy.* Immunity, 2016. **44**(5): p. 973-988.
77. Harding, F.A., et al., *CD28-mediated signalling co-stimulates murine T cells and prevents induction of anergy in T-cell clones.* Nature, 1992. **356**(6370): p. 607-609.
78. Seder, R.A., et al., *Interleukin 12 acts directly on CD4+ T cells to enhance priming for interferon gamma production and diminishes interleukin 4 inhibition of such priming.* Proceedings of the National Academy of Sciences, 1993. **90**(21): p. 10188-10192.
79. Seder, R.A., et al., *The presence of interleukin 4 during in vitro priming determines the lymphokine-producing potential of CD4+ T cells from T cell receptor transgenic mice.* Journal of Experimental Medicine, 1992. **176**(4): p. 1091-1098.
80. Curtsinger, J.M., D.C. Lins, and M.F. Mescher, *Signal 3 Determines Tolerance versus Full Activation of Naive CD8 T Cells.* Journal of Experimental Medicine, 2003. **197**(9): p. 1141-1151.
81. Díaz-Montero, C.M., et al., *Priming of naive CD8+ T cells in the presence of IL-12 selectively enhances the survival of CD8+CD62Lhi cells and results in superior anti-tumor activity in a tolerogenic murine model.* Cancer Immunology, Immunotherapy, 2008. **57**(4): p. 563-572.
82. Szabo, S.J., et al., *A Novel Transcription Factor, T-bet, Directs Th1 Lineage Commitment.* Cell, 2000. **100**(6): p. 655-669.
83. Szabo, S.J., et al., *Distinct Effects of T-bet in TH1 Lineage Commitment and IFN-gamma Production in CD4 and CD8 T Cells.* Science, 2002. **295**(5553): p. 338-342.
84. Gramaglia, I., et al., *Ox-40 Ligand: A Potent Costimulatory Molecule for Sustaining Primary CD4 T Cell Responses.* The Journal of Immunology, 1998. **161**(12): p. 6510.
85. De Smedt, T., et al., *Ox40 Costimulation Enhances the Development of T Cell Responses Induced by Dendritic Cells In Vivo.* The Journal of Immunology, 2002. **168**(2): p. 661-670.
86. Tanaka, A. and S. Sakaguchi, *Regulatory T cells in cancer immunotherapy.* Cell Research, 2017. **27**(1): p. 109-118.
87. Fontenot, J.D., M.A. Gavin, and A.Y. Rudensky, *Foxp3 programs the development and function of CD4+CD25+ regulatory T cells.* Nature Immunology, 2003. **4**(4): p. 330-336.

88. Debes, G.F., et al., *Chemokine receptor CCR7 required for T lymphocyte exit from peripheral tissues.* Nature Immunology, 2005. **6**(9): p. 889-894.
89. Loetscher, M., et al., *Chemokine receptor specific for IP10 and mig: structure, function, and expression in activated T-lymphocytes.* Journal of Experimental Medicine, 1996. **184**(3): p. 963-969.
90. Mikucki, M.E., et al., *Non-redundant requirement for CXCR3 signalling during tumoricidal T-cell trafficking across tumour vascular checkpoints.* Nature Communications, 2015. **6**(1): p. 7458.
91. Fujita, M., et al., *Effective Immunotherapy against Murine Gliomas Using Type 1 Polarizing Dendritic Cells—Significant Roles of CXCL10.* Cancer Research, 2009. **69**(4): p. 1587-1595.
92. Chow, M.T., et al., *Intratumoral Activity of the CXCR3 Chemokine System Is Required for the Efficacy of Anti-PD-1 Therapy.* Immunity, 2019. **50**(6): p. 1498-1512.e5.
93. Huang, B., et al., *Identification of immune-related biomarkers associated with tumorigenesis and prognosis in cutaneous melanoma patients.* Cancer Cell International, 2020. **20**(1).
94. Mlecnik, B., et al., *Biomolecular Network Reconstruction Identifies T-Cell Homing Factors Associated With Survival in Colorectal Cancer.* Gastroenterology, 2010. **138**(4): p. 1429-1440.
95. Liu, J., et al., *Local production of the chemokines CCL5 and CXCL10 attracts CD8+ T lymphocytes into esophageal squamous cell carcinoma.* Oncotarget, 2015. **6**(28): p. 24978-24989.
96. Tumeh, P.C., et al., *PD-1 blockade induces responses by inhibiting adaptive immune resistance.* Nature, 2014. **515**(7528): p. 568-571.
97. Van Der Woude, L.L., et al., *Migrating into the Tumor: a Roadmap for T Cells.* Trends in Cancer, 2017. **3**(11): p. 797-808.
98. Martínez-Lostao, L., A. Anel, and J. Pardo, *How Do Cytotoxic Lymphocytes Kill Cancer Cells?* Clinical Cancer Research, 2015. **21**(22): p. 5047-5056.
99. Dobrzanski, M.J., J.B. Reome, and R.W. Dutton, *Immunopotentiating Role of IFN-γ in Early and Late Stages of Type 1 CD8 Effector Cell-Mediated Tumor Rejection.* Clinical Immunology, 2001. **98**(1): p. 70-84.
100. Chin, Y.E., et al., *Activation of the STAT signaling pathway can cause expression of caspase 1 and apoptosis.* Molecular and Cellular Biology, 1997. **17**(9): p. 5328-5337.
101. Fulda, S. and K.-M. Debatin, *IFNγ sensitizes for apoptosis by upregulating caspase-8 expression through the Stat1 pathway.* Oncogene, 2002. **21**(15): p. 2295-2308.
102. Liao, F., et al., *Human Mig chemokine: biochemical and functional characterization.* Journal of Experimental Medicine, 1995. **182**(5): p. 1301-1314.
103. Martini, M., et al., *IFN-γ-mediated upmodulation of MHC class I expression activates tumor-specific immune response in a mouse model of prostate cancer.* Vaccine, 2010. **28**(20): p. 3548-3557.
104. Takeda , K., et al., *Critical Role for Tumor Necrosis Factor–related Apoptosis-inducing Ligand in Immune Surveillance Against Tumor Development.* Journal of Experimental Medicine, 2002. **195**(2): p. 161-169.
105. Josephs, S.F., et al., *Unleashing endogenous TNFA-alpha as a cancer immunotherapeutic.* Journal of Translational Medicine, 2018. **16**(1).

106. Voskoboinik, I., J.C. Whisstock, and J.A. Trapani, *Perforin and granzymes: function, dysfunction and human pathology.* Nature Reviews Immunology, 2015. **15**(6): p. 388-400.
107. Van Den Broek, M.E., et al., *Decreased tumor surveillance in perforin-deficient mice.* Journal of Experimental Medicine, 1996. **184**(5): p. 1781-1790.
108. Garg, A.D., et al., *Danger signalling during cancer cell death: origins, plasticity and regulation.* Cell Death & Differentiation, 2014. **21**(1): p. 26-38.
109. Gardai, S.J., et al., *Cell-Surface Calreticulin Initiates Clearance of Viable or Apoptotic Cells through trans-Activation of LRP on the Phagocyte.* Cell, 2005. **123**(2): p. 321-334.
110. Gregory, C.D. and J.D. Pound, *Cell death in the neighbourhood: direct microenvironmental effects of apoptosis in normal and neoplastic tissues.* The Journal of Pathology, 2011. **223**(2): p. 178-195.
111. Bondanza, A., et al., *Inhibition of phosphatidylserine recognition heightens the immunogenicity of irradiated lymphoma cells in vivo.* The Journal of experimental medicine, 2004. **200**(9): p. 1157-1165.
112. Böttcher, J.P., et al., *NK Cells Stimulate Recruitment of cDC1 into the Tumor Microenvironment Promoting Cancer Immune Control.* Cell, 2018. **172**(5): p. 1022-1037.e14.
113. Gabrilovich, D., et al., *Vascular Endothelial Growth Factor Inhibits the Development of Dendritic Cells and Dramatically Affects the Differentiation of Multiple Hematopoietic Lineages In Vivo: Presented in part at the Keystone Symposium "Cellular and Molecular Biology of Dendritic Cells," Santa Fe, NM, March 3-9, 1998, and at the annual meeting of the American Association for Cancer Research, March 28-April 1, 1998.* Blood, 1998. **92**(11): p. 4150-4166.
114. Ruffell, B., et al., *Macrophage IL-10 Blocks CD8+ T Cell-Dependent Responses to Chemotherapy by Suppressing IL-12 Expression in Intratumoral Dendritic Cells.* Cancer Cell, 2014. **26**(5): p. 623-637.
115. Feig, C., et al., *Targeting CXCL12 from FAP-expressing carcinoma-associated fibroblasts synergizes with anti-PD-L1 immunotherapy in pancreatic cancer.* Proceedings of the National Academy of Sciences, 2013. **110**(50): p. 20212-20217.
116. Muthuswamy, R., et al., *Functional reprogramming of human prostate cancer to promote local attraction of effector CD8+T cells.* The Prostate, 2016. **76**(12): p. 1095-1105.
117. Molon, B., et al., *Chemokine nitration prevents intratumoral infiltration of antigen-specific T cells.* Journal of Experimental Medicine, 2011. **208**(10): p. 1949-1962.
118. Griffioen, A.W., et al., *Endothelial Intercellular Adhesion Molecule-1 Expression Is Suppressed in Human Malignancies: The Role of Angiogenic Factors.* Cancer Research, 1996. **56**(5): p. 1111.
119. McLane, L.M., M.S. Abdel-Hakeem, and E.J. Wherry, *CD8 T Cell Exhaustion During Chronic Viral Infection and Cancer.* Annual Review of Immunology, 2019. **37**(1): p. 457-495.
120. Barber, D.L., et al., *Restoring function in exhausted CD8 T cells during chronic viral infection.* Nature, 2006. **439**(7077): p. 682-687.
121. Dong, H., et al., *Tumor-associated B7-H1 promotes T-cell apoptosis: A potential mechanism of immune evasion.* Nature Medicine, 2002. **8**(8): p. 793-800.

122. Utzschneider, D.T., et al., *T Cell Factor 1-Expressing Memory-like CD8+ T Cells Sustain the Immune Response to Chronic Viral Infections.* Immunity, 2016. **45**(2): p. 415-427.
123. Monney, L., et al., *Th1-specific cell surface protein Tim-3 regulates macrophage activation and severity of an autoimmune disease.* Nature, 2002. **415**(6871): p. 536-541.
124. Sánchez-Fueyo, A., et al., *Tim-3 inhibits T helper type 1–mediated auto- and alloimmune responses and promotes immunological tolerance.* Nature Immunology, 2003. **4**(11): p. 1093-1101.
125. Jin, H.T., et al., *Cooperation of Tim-3 and PD-1 in CD8 T-cell exhaustion during chronic viral infection.* Proceedings of the National Academy of Sciences, 2010. **107**(33): p. 14733-14738.
126. Zhou, Q., et al., *Coexpression of Tim-3 and PD-1 identifies a CD8+ T-cell exhaustion phenotype in mice with disseminated acute myelogenous leukemia.* Blood, 2011. **117**(17): p. 4501-4510.
127. Fourcade, J., et al., *Upregulation of Tim-3 and PD-1 expression is associated with tumor antigen–specific CD8+ T cell dysfunction in melanoma patients.* Journal of Experimental Medicine, 2010. **207**(10): p. 2175-2186.
128. Wolf, Y., A.C. Anderson, and V.K. Kuchroo, *TIM3 comes of age as an inhibitory receptor.* Nature Reviews Immunology, 2020. **20**(3): p. 173-185.
129. Restifo, N.P., et al., *Loss of Functional Beta2-Microglobulin in Metastatic Melanomas From Five Patients Receiving Immunotherapy.* JNCI Journal of the National Cancer Institute, 1996. **88**(2): p. 100-108.
130. Zaretsky, J.M., et al., *Mutations Associated with Acquired Resistance to PD-1 Blockade in Melanoma.* New England Journal of Medicine, 2016. **375**(9): p. 819-829.
131. Guo, C., et al., *Therapeutic Cancer Vaccines*. 2013, Elsevier. p. 421-475.
132. Nemunaitis, J. and J. Nemunaitis, *Granulocyte-Macrophage Colony-Stimulating Factor Gene–Transfected Autologous Tumor Cell Vaccine: Focus on Non–Small-Cell Lung Cancer.* Clinical Lung Cancer, 2003. **5**(3): p. 148-157.
133. Hanna, M.G., et al., *Adjuvant active specific immunotherapy of stage II and stage III colon cancer with an autologous tumor cell vaccine: first randomized phase III trials show promise.* Vaccine, 2001. **19**(17-19): p. 2576-2582.
134. Antonia, S.J., et al., *Phase I Trial of a B7-1 (CD80) Gene Modified Autologous Tumor Cell Vaccine in Combination With Systemic Interleukin-2 in Patients With Metastatic Renal Cell Carcinoma.* Journal of Urology, 2002. **167**(5): p. 1995-2000.
135. Cheever, M.A. and C.S. Higano, *PROVENGE (Sipuleucel-T) in Prostate Cancer: The First FDA-Approved Therapeutic Cancer Vaccine.* Clinical Cancer Research, 2011. **17**(11): p. 3520-3526.
136. Coulie, P.G., et al., *Tumour antigens recognized by T lymphocytes: at the core of cancer immunotherapy.* Nature Reviews Cancer, 2014. **14**(2): p. 135-146.
137. Gilbert, S.C., *T-cell-inducing vaccines - what's the future.* Immunology, 2012. **135**(1): p. 19-26.
138. Kawakami, Y., et al., *Identification of the immunodominant peptides of the MART-1 human melanoma antigen recognized by the majority of HLA-A2-restricted tumor infiltrating lymphocytes.* Journal of Experimental Medicine, 1994. **180**(1): p. 347-352.

139. Wölfel, T., et al., *Two tyrosinase nonapeptides recognized on HLA-A2 melanomas by autologous cytolytic T lymphocytes.* European Journal of Immunology, 1994. **24**(3): p. 759-764.
140. Kawakami, Y. and S.A. Rosenberg, *Immunobiology of Human Melanoma Antigens MART-1 and gp100 and their Use for Immuno-Gene Therapy.* International Reviews of Immunology, 1997. **14**(2-3): p. 173-192.
141. Gulley, J.L., et al., *Immune Impact Induced by PROSTVAC (PSA-TRICOM), a Therapeutic Vaccine for Prostate Cancer.* Cancer Immunology Research, 2014. **2**(2): p. 133-141.
142. Kantoff, P.W., J.L. Gulley, and C. Pico-Navarro, *Revised Overall Survival Analysis of a Phase II, Randomized, Double-Blind, Controlled Study of PROSTVAC in Men With Metastatic Castration-Resistant Prostate Cancer.* Journal of Clinical Oncology, 2017. **35**(1): p. 124-125.
143. Gulley, J.L., et al., *Phase III Trial of PROSTVAC in Asymptomatic or Minimally Symptomatic Metastatic Castration-Resistant Prostate Cancer.* Journal of Clinical Oncology, 2019. **37**(13): p. 1051-1061.
144. Scanlan, M.J., et al., *Cancer/testis antigens: an expanding family of targets for cancer immunotherapy.* Immunological Reviews, 2002. **188**(1): p. 22-32.
145. Van Den Eynde, B., et al., *Presence on a human melanoma of multiple antigens recognized by autologous CTL.* International Journal of Cancer, 1989. **44**(4): p. 634-640.
146. Chen, Y.T., et al., *A testicular antigen aberrantly expressed in human cancers detected by autologous antibody screening.* Proceedings of the National Academy of Sciences, 1997. **94**(5): p. 1914-1918.
147. Dreno, B., et al., *MAGE-A3 immunotherapeutic as adjuvant therapy for patients with resected, MAGE-A3-positive, stage III melanoma (DERMA): a double-blind, randomised, placebo-controlled, phase 3 trial.* The Lancet Oncology, 2018. **19**(7): p. 916-929.
148. Vansteenkiste, J.F., et al., *Efficacy of the MAGE-A3 cancer immunotherapeutic as adjuvant therapy in patients with resected MAGE-A3-positive non-small-cell lung cancer (MAGRIT): a randomised, double-blind, placebo-controlled, phase 3 trial.* Lancet Oncol, 2016. **17**(6): p. 822-835.
149. Tomaić, V., *Functional Roles of E6 and E7 Oncoproteins in HPV-Induced Malignancies at Diverse Anatomical Sites.* Cancers, 2016. **8**(10): p. 95.
150. Castle, P.E. and M. Maza, *Prophylactic HPV vaccination: past, present, and future.* Epidemiology and Infection, 2016. **144**(3): p. 449-468.
151. Yang, A., et al., *Perspectives for therapeutic HPV vaccine development.* Journal of Biomedical Science, 2016. **23**(1).
152. Schumacher Ton, N. and D. Schreiber Robert, *Neoantigens in cancer immunotherapy.* Science, 2015. **348**(6230): p. 69-74.
153. Turajlic, S., et al., *Insertion-and-deletion-derived tumour-specific neoantigens and the immunogenic phenotype: a pan-cancer analysis.* The Lancet Oncology, 2017. **18**(8): p. 1009-1021.
154. Yang, W., et al., *Immunogenic neoantigens derived from gene fusions stimulate T cell responses.* Nature Medicine, 2019. **25**(5): p. 767-775.
155. Rizvi, N.A., et al., *Mutational landscape determines sensitivity to PD-1 blockade in non–small cell lung cancer.* Science, 2015. **348**(6230): p. 124-128.

156. Le, D.T., et al., *PD-1 Blockade in Tumors with Mismatch-Repair Deficiency.* New England Journal of Medicine, 2015. **372**(26): p. 2509-2520.
157. Le, D.T., et al., *Mismatch repair deficiency predicts response of solid tumors to PD-1 blockade.* Science, 2017. **357**(6349): p. 409-413.
158. Yarchoan, M., A. Hopkins, and E.M. Jaffee, *Tumor Mutational Burden and Response Rate to PD-1 Inhibition.* New England Journal of Medicine, 2017. **377**(25): p. 2500-2501.
159. Samstein, R.M., et al., *Tumor mutational load predicts survival after immunotherapy across multiple cancer types.* Nature Genetics, 2019. **51**(2): p. 202-206.
160. Valero, C., et al., *The association between tumor mutational burden and prognosis is dependent on treatment context.* Nature Genetics, 2021. **53**(1): p. 11-15.
161. Gandara, D.R., et al., *Blood-based tumor mutational burden as a predictor of clinical benefit in non-small-cell lung cancer patients treated with atezolizumab.* Nature Medicine, 2018. **24**(9): p. 1441-1448.
162. Brown, S.D., et al., *Neo-antigens predicted by tumor genome meta-analysis correlate with increased patient survival.* Genome Research, 2014. **24**(5): p. 743-750.
163. Rooney, Michael S., et al., *Molecular and Genetic Properties of Tumors Associated with Local Immune Cytolytic Activity.* Cell, 2015. **160**(1): p. 48-61.
164. Schreiber, R.D., L.J. Old, and M.J. Smyth, *Cancer Immunoediting: Integrating Immunity's Roles in Cancer Suppression and Promotion.* Science, 2011. **331**(6024): p. 1565-1570.
165. Tran, E., et al., *T-Cell Transfer Therapy Targeting Mutant KRAS in Cancer.* New England Journal of Medicine, 2016. **375**(23): p. 2255-2262.
166. Tran, E., et al., *Cancer Immunotherapy Based on Mutation-Specific CD4+ T Cells in a Patient with Epithelial Cancer.* Science, 2014. **344**(6184): p. 641-645.
167. Castle, J.C., et al., *Exploiting the Mutanome for Tumor Vaccination.* Cancer Research, 2012. **72**(5): p. 1081-1091.
168. Yadav, M., et al., *Predicting immunogenic tumour mutations by combining mass spectrometry and exome sequencing.* Nature, 2014. **515**(7528): p. 572-6.
169. Kreiter, S., et al., *Mutant MHC class II epitopes drive therapeutic immune responses to cancer.* Nature, 2015. **520**(7549): p. 692-696.
170. Sahin, U., et al., *Personalized RNA mutanome vaccines mobilize poly-specific therapeutic immunity against cancer.* Nature, 2017. **547**(7662): p. 222-226.
171. Sasso, E., et al., *New viral vectors for infectious diseases and cancer.* Seminars in Immunology, 2020. **50**: p. 101430.
172. Wilson, J.M., *Adenoviruses as Gene-Delivery Vehicles.* New England Journal of Medicine, 1996. **334**(18): p. 1185-1187.
173. Swadling, L., et al., *A human vaccine strategy based on chimpanzee adenoviral and MVA vectors that primes, boosts, and sustains functional HCV-specific T cell memory.* Science Translational Medicine, 2014. **6**(261): p. 261ra153.
174. Hancock, G., et al., *A multi-genotype therapeutic human papillomavirus vaccine elicits potent T cell responses to conserved regions of early proteins.* Scientific Reports, 2019. **9**(1).
175. Reyes-Sandoval, A., et al., *Prime-Boost Immunization with Adenoviral and Modified Vaccinia Virus Ankara Vectors Enhances the Durability and*

Polyfunctionality of Protective Malaria CD8+ T-Cell Responses. Infection and Immunity, 2010. **78**(1): p. 145-153.
176. Dicks, M.D.J., et al., *A Novel Chimpanzee Adenovirus Vector with Low Human Seroprevalence: Improved Systems for Vector Derivation and Comparative Immunogenicity.* PLoS ONE, 2012. **7**(7): p. e40385.
177. Cappuccini, F., et al., *Immunogenicity and efficacy of the novel cancer vaccine based on simian adenovirus and MVA vectors alone and in combination with PD-1 mAb in a mouse model of prostate cancer.* Cancer Immunology, Immunotherapy, 2016. **65**(6): p. 701-713.
178. Cappuccini, F., et al., *5T4 oncofoetal glycoprotein: an old target for a novel prostate cancer immunotherapy.* Oncotarget, 2017. **8**(29): p. 47474-47489.
179. Cappuccini, F., et al., *Safety and immunogenicity of novel 5T4 viral vectored vaccination regimens in early stage prostate cancer: a phase I clinical trial.* Journal for ImmunoTherapy of Cancer, 2020. **8**(1): p. e000928.
180. McAuliffe, J., et al., *Heterologous prime-boost vaccination targeting MAGE-type antigens promotes tumor T-cell infiltration and improves checkpoint blockade therapy.* Journal for ImmunoTherapy of Cancer, 2021. **9**(9): p. e003218.
181. Hailemichael, Y., et al., *Persistent antigen at vaccination sites induces tumor-specific CD8+ T cell sequestration, dysfunction and deletion.* Nature Medicine, 2013. **19**(4): p. 465-472.
182. Bijker, M.S., et al., *Superior induction of anti-tumor CTL immunity by extended peptide vaccines involves prolonged, DC-focused antigen presentation.* European Journal of Immunology, 2008. **38**(4): p. 1033-1042.
183. Baumgaertner, P., et al., *Vaccination of stage III/IV melanoma patients with long NY-ESO-1 peptide and CpG-B elicits robust CD8+ and CD4+ T-cell responses with multiple specificities including a novel DR7-restricted epitope.* OncoImmunology, 2016. **5**(10): p. e1216290.
184. Alspach, E., et al., *MHC-II neoantigens shape tumour immunity and response to immunotherapy.* Nature, 2019. **574**(7780): p. 696-701.
185. Ott, P.A., et al., *An immunogenic personal neoantigen vaccine for patients with melanoma.* Nature, 2017. **547**(7662): p. 217-221.
186. Lynn, G.M., et al., *Peptide-TLR-7/8a conjugate vaccines chemically programmed for nanoparticle self-assembly enhance CD8 T-cell immunity to tumor antigens.* Nat Biotechnol, 2020. **38**(3): p. 320-332.
187. Lynn, G.M., et al., *In vivo characterization of the physicochemical properties of polymer-linked TLR agonists that enhance vaccine immunogenicity.* Nature Biotechnology, 2015. **33**(11): p. 1201-1210.
188. Baharom, F., et al., *Intravenous nanoparticle vaccination generates stem-like TCF1+ neoantigen-specific CD8+ T cells.* Nat Immunol, 2021. **22**(1): p. 41-52.
189. Cristescu, R., et al., *Pan-tumor genomic biomarkers for PD-1 checkpoint blockade–based immunotherapy.* Science, 2018. **362**(6411): p. eaar3593.
190. Saxena, M., et al., *Therapeutic cancer vaccines.* Nature Reviews Cancer, 2021. **21**(6): p. 360-378.
191. Darrah, P.A., et al., *Prevention of tuberculosis in macaques after intravenous BCG immunization.* Nature, 2020. **577**(7788): p. 95-102.
192. Wherry, E.J. and M. Kurachi, *Molecular and cellular insights into T cell exhaustion.* Nature Reviews Immunology, 2015. **15**(8): p. 486-499.

193. Joshi, N.S., et al., *Inflammation Directs Memory Precursor and Short-Lived Effector CD8+ T Cell Fates via the Graded Expression of T-bet Transcription Factor.* Immunity, 2007. **27**(2): p. 281-295.
194. Obar, J.J., et al., *Pathogen-Induced Inflammatory Environment Controls Effector and Memory CD8+ T Cell Differentiation.* The Journal of Immunology, 2011. **187**(10): p. 4967-4978.
195. Pais Ferreira, D., et al., *Central memory CD8+ T cells derive from stem-like Tcf7hi effector cells in the absence of cytotoxic differentiation.* Immunity, 2020. **53**(5): p. 985-1000.e11.
196. Kardani, K., A. Bolhassani, and S. Shahbazi, *Prime-boost vaccine strategy against viral infections: Mechanisms and benefits.* Vaccine, 2016. **34**(4): p. 413-423.
197. Stanley, D.A., et al., *Chimpanzee adenovirus vaccine generates acute and durable protective immunity against ebolavirus challenge.* Nature Medicine, 2014. **20**(10): p. 1126-1129.
198. Betts, M.R., *HIV nonprogressors preferentially maintain highly functional HIV-specific CD8+ T cells.* Blood, 2006. **107**(12): p. 4781-4789.
199. Ji, H., et al., *Antigen-specific immunotherapy for murine lung metastatic tumors expressing human papillomavirus type 16 E7 oncoprotein.* International Journal of Cancer, 1998. **78**(1): p. 41-45.
200. Sade-Feldman, M., et al., *Defining T Cell States Associated with Response to Checkpoint Immunotherapy in Melanoma.* Cell, 2018. **175**(4): p. 998-1013.e20.
201. Moesta, A.K., X.-Y. Li, and M.J. Smyth, *Targeting CD39 in cancer.* Nature Reviews Immunology, 2020. **20**(12): p. 739-755.
202. Sato, E., et al., *Intraepithelial CD8+ tumor-infiltrating lymphocytes and a high CD8+/regulatory T cell ratio are associated with favorable prognosis in ovarian cancer.* Proceedings of the National Academy of Sciences, 2005. **102**(51): p. 18538-18543.
203. Deng, W., et al., *Recombinant Listeria promotes tumor rejection by CD8+ T cell-dependent remodeling of the tumor microenvironment.* Proceedings of the National Academy of Sciences, 2018. **115**(32): p. 8179-8184.
204. Overwijk, W.W., et al., *Tumor Regression and Autoimmunity after Reversal of a Functionally Tolerant State of Self-reactive CD8+ T Cells.* Journal of Experimental Medicine, 2003. **198**(4): p. 569-580.
205. Provine Nicholas, M., et al., *MAIT cell activation augments adenovirus vector vaccine immunogenicity.* Science, 2021. **371**(6528): p. 521-526.
206. Qian, C., et al., *TLR agonists induce regulatory dendritic cells to recruit Th1 cells via preferential IP-10 secretion and inhibit Th1 proliferation.* Blood, 2007. **109**(8): p. 3308-3315.
207. Quinn, K.M., et al., *Antigen expression determines adenoviral vaccine potency independent of IFN and STING signaling.* Journal of Clinical Investigation, 2015. **125**(3): p. 1129-1146.
208. De Mingo Pulido, Á., et al., *TIM-3 Regulates CD103+ Dendritic Cell Function and Response to Chemotherapy in Breast Cancer.* Cancer Cell, 2018. **33**(1): p. 60-74.e6.
209. Edwards, A.D., et al., *Toll-like receptor expression in murine DC subsets: lack of TLR7 expression by CD8α+ DC correlates with unresponsiveness to imidazoquinolines.* European Journal of Immunology, 2003. **33**(4): p. 827-833.

210. Blass, E. and P.A. Ott, *Advances in the development of personalized neoantigen-based therapeutic cancer vaccines.* Nature Reviews Clinical Oncology, 2021. **18**(4): p. 215-229.
211. Ring, S.S., et al., *Heterologous Prime Boost Vaccination Induces Protective Melanoma-Specific CD8+ T Cell Responses.* Molecular Therapy - Oncolytics, 2020. **19**: p. 179-187.
212. Zhang, L., et al., *Intratumoral T Cells, Recurrence, and Survival in Epithelial Ovarian Cancer.* New England Journal of Medicine, 2003. **348**(3): p. 203-213.
213. Galon, J., et al., *Type, Density, and Location of Immune Cells Within Human Colorectal Tumors Predict Clinical Outcome.* Science, 2006. **313**(5795): p. 1960-1964.

Appendix

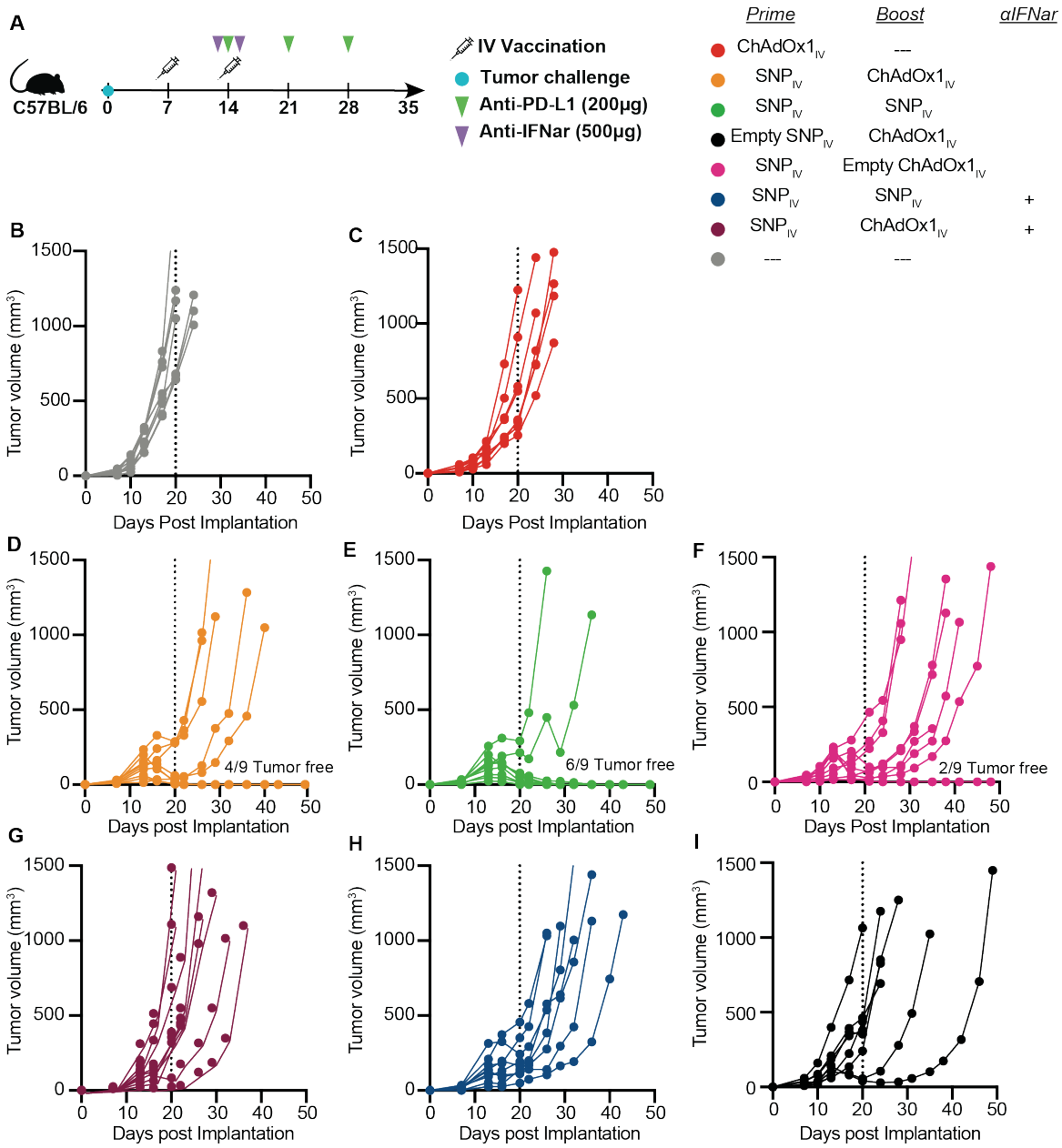

Figure 6.1 Individual tumor growth curves of mice bearing MC38 tumors for key groups in thesis (**A**) Therapeutic study treatment schedule and legend for all figure panels. (**B-I**) Representative tumor growth curves for different treatment groups (**B**) Untreated (**C**) IV ChAdOx1 prime only (**D**) IV SNP prime followed by IV ChAdOx1 boost (**E**) IV SNP given twice (**F**) IV SNP followed by 'empty' ChAdOx1 IV (**G**) IV heterologous prime boost with IFNα receptor inhibition (**H**) IV SNP given twice with IFNα receptor inhibition (**I**) 'Empty' SNP IV followed by IV ChAdOx1 boost